İZMİR KÂTİP ÇELEBİ ÜNİVERSİTESİ
2010
GRADUATE SCHOOL OF NATURAL AND APPLIED SCIENCES

A Comparison of the Performances of Conventional and Low Salinity Water Alternating Gas Injection for Displacement of Oil

Submitted to the Graduate School of Natural and Applied Sciences in partial fulfillment of the requirements for the degree of

Master of Science in Energy Engineering

by

Emmanuel Bucyanayandi

ORCID 0000-0002-4103-0068

Advisor: Prof. Dr. Ibrahim Kocabaş

July, 2022

This is to certify that we have read the thesis **A Comparison of the Performances of Conventional and Low Salinity Water Alternating Gas Injection for Displacement of Oil** submitted by **Emmanuel Bucyanayandi**, and it has been judged to be successful, in scope and in quality, at the defense exam and accepted by our jury as a MASTER'S THESIS.

APPROVED BY:

Advisor: **Prof. Dr. Ibrahim Kocabas**
Izmir Katip Celebi University

Committee Members:

Assoc. Prof. Dr. Sercan Acarer
Izmir Katip Celebi University

Assoc. Prof. Dr. Onur Ertuğrul
Izmir Katip Celebi University

Assist. Prof. Dr. Burak Kulga
Technical University of Istanbul

Date of Defense: July 21, 2022

Declaration of Authorship

I, **Emmanuel Bucyanayandi**, declare that this thesis titled **A Comparison of the Performances of Conventional and Low Salinity Water Alternating Gas Injection for Displacement of Oil** and the work presented in it are my own. I confirm that:

- This work was done wholly or mainly while in candidature for the Master's degree at this university.
- Where any part of this thesis has previously been submitted for a degree or any other qualification at this university or any other institution, this has been clearly stated.
- Where I have consulted the published work of others, this is always clearly attributed.
- Where I have quoted from the work of others, the source is always given. This thesis is entirely my own work, with the exception of such quotations.
- I have acknowledged all major sources of assistance.
- Where the thesis is based on work done by myself jointly with others, I have made clear exactly what was done by others and what I have contributed myself.

Date: 21.07.2022

A Comparison of the Performances of Conventional and Low Salinity Water Alternating Gas Injection for Displacement of Oil

Abstract

The oil and natural gas reside in microscopic pores of subsurface rock layers called a reservoir rock. Besides there always at least two phases exist in oil and gas reservoirs. Therefore, the flow and displacement of oil into the production wells are influenced significantly by capillary forces. Due to the capillary and surface forces, the recovery of oil always remains at low percentages usually between 20 to 40%. In order to increase the recovery factor several secondary and enhanced oil recovery techniques have been developed and implemented. The two secondary recovery methods namely waterflooding and gas flooding immiscibly have increased the recovery factor by approximately 5 to 10%. Applying these two techniques alone has encountered a major problem due to the gravity effect. While water subsides below the oil layer, gas overflow above the oil layer. This phenomenon has caused an immature breakthrough and inefficient sweep especially close to the upper and lower boundaries of the reservoir. In addition, there existed the problem of unfavorable mobility ratio and hence viscous fingering. In order to overcome these problems engineers have developed the water alternating gas injection (WAG) technique. This technique has resolved the problem of heterogeneity and immature breakthrough and hence increased the sweep and displacement efficiencies. Recently a new improved water flooding technique has been under extensive research as it has been observed that low salinity water flooding can improve the microscopic displacement efficiency and hence increase the recovery factor further. However, there is no consensus on the dominant mechanism increasing the efficiency and effectiveness of low salinity water injection in sandstone and carbonate reservoirs and also on the design parameters.

In this work, we will numerically explore the efficiency and effectiveness of low salinity WAG in a sandstone reservoir that is 80 ft thick and 1000 ft long. Fundamentally this study focuses on identifying the crucial physical and chemical factors, such as the initial phase of reservoir fluid, gravity, injection depth, and vertical to horizontal permeability ratio, and injected water salinity to attain an additional oil recovery for a low salinity water alternating gas (LSWAG) injection compared to classical sea waterflooding, gas flooding and WAG injection processes.

The modelling and simulation were carried out by using the CMG-GEM reservoir simulator and its supporting tools like Winprop. The input data were taken from published sources on the Cranfield oil field reservoir. Simulation runs have shown that reservoir thickness, injection depth, horizontal and vertical permeability values have all significant influence. However, the most serious conclusion reached may be stated as the simulation runs showed that there is an increase of oil recovery factor of up to about 6% for WAG injection with low salinity water of 1027ppm to seawater of 51,346 ppm.

Keywords: Waterflooding, CO_2 flooding, Conventional WAG injection, Low salinity WAG injection, Displacement efficiency of WAG Processes

Petrolün Geleneksel Su Gaz Değişimli Ötelenmesi ile Az Tuzlu Su Gaz Değişimli Ötelenmesi Yöntemlerinin Başarımlarının Karşılaştırılması

Öz

Petrol ve doğal gaz reservuar kayaç olarak adlandırılan yeraltı kaya tabakalarının mikroskopik boyuttaki gözenekleri içinde bulunurlar. Bunun yanında petrol ve doğal gaz rezervuarlarının hepsinde en az iki akışkan faz bulunur. Bu iki nedenden dolayı petrolün üretim kuyularına akışı ve ötelenmesi kılcal kuvvetler tarafından önemli ölçüde etkilenir. Kılcal ve yüzey kuvvetlerinden dolayı petrolün kurtarım oranı her zaman %20 ile %40 gibi düşük yüzdelerde kalmıştır. Bu düşük kurtarım katsayısını artırmak için bir seri ikincil ve ileri üretim yöntemi geliştirilmiş ve uygulanmıştır. İki ikincil üretim yöntemi olan su-ötelemesi ve karışımsız gaz ile öteleme yöntemleri kurtarım oranını yaklaşık olarak %5 ile %10 arasında artırmışlardır. Bu iki yöntemin saha uygulamaları yerkürenin gravite kuvvetinin etkisinden dolayı başat bir sorun ile karşı karşıya kalmışlardır. Şöyle ki rezervuar içinde akış sırasında petrolden daha yoğun olan su petrol tabakasının altına doğru akarken çok daha hafif olan gaz ise petrol tabakasının üstüne doğru akmaktadır. Bu olay petrol ötelemesi için basılan akışkanların rezervuar tabakasının özellikle üst ve alt sınırlarında erkenden üretim kuyularına varmalarına ve verimsiz bir süpürme gerçekleşmesine neden olmaktadır. Buna ek olarak, olumsuz hareketlilik oranı ve buna bağlı olarak akmazlık parmakları oluşumu sorunu da bulunmaktadır. Bu problemlerin üstesinden gelebilmek için petrol mühendisleri su gaz değişimli (Water Alternating Gas,WAG) yönetimini geliştirdiler. Bu yöntem, heterojen rezervaur ve erken cephe-yarılımı problemlerini çözmüş ve böylece süpürme ve öteleme etkinliklerini artırmıştır. Yakın geçmişte, az tuzlu su ile ötelemenin mikroskopik öteleme etkenliğini artırdığı ve böylece kurtarım oranını daha da yükseltiğinin gözlemlenmesi dolayısı ile yeni bir geliştirilmiş su ile öteleme yöntemi yaygın araştırmalara konu olagelmiştir. Ancak, bu

konuda çalışan araştırmacılar arasında kumtaşı ve karbonat kayaç rezervuarlarda az tuzlu su ile ötelemede verimliği ve etkenliği artıran baskın mekanizmanın hangisi olduğu ve aynı zamanda tasarım sabitleri üzerinde bir fikirbirliği yoktur.

Biz bu çalışma da, 80 ft kalınlığında ve 1000 ft uzunluğunda bir kumtaşı rezervuarında az tuzlu su ve gaz değişimli öteleme yönteminin verimliliği ve etkenliğini sayısal olarak keşfetmeye çalışacağız. Temel olarak bu çalışma rezervuarda bulunan hidrokarbon faz sayısını, yerküre gravite etkisini, öteleme akışkanının rezervuara basılma noktasının derinliği, dikey geçirgenliğin yatay geçirgenliğe oranı ve öteleme suyunun tuzluluk dercesi gibi hayati fiziksel ve kimyasal etkenlerin yalnızca deniz suyu ötelemesi, yalnızca gaz basımı ile öteleme ve geleneksel tuzlu su gaz değişimli ötelemeye (WAG) göre az tuzlu su gaz değişimli öteleme (LSWAG) yoluyla elde edilecek artı kurtarım oranının belirlenmesi üzerine odaklanmaktadır.

Modelleme ve benzeşimler CMG-GEM simulatörü ve onun destek araçlarından Winprop kullanılarak gerçekleştirilmiştir. Benzeşim yazılımına sağlanan veriler Cranfield petrol rezervuarı üzerine yapılan yayınlardan alınmıştır.

Benzeşim koşturmları rezervuar kalınlığının, öteleme sıvılarının basım noktası derinliklerinin, yatay ve dikey geçirimlilik değerlerinin ciddi etkileri olduğunu göstermiştir. Ancak ulaşılan en ciddi sonuç, benzeşim koşturmaları az tuzlu su (1072 ppm) CO_2 değişimli ötelemenin (LSWAG) deniz suyu (51346 ppm) CO_2 değişimli ötelemeye (WAG) göre %6 daha fazla kurtarım oranı sağladığını göstermiştir.

Anahtar Kelimeler: Su ile öteleme, CO_2 ile öteleme, geleneksel su gaz değişimli öteleme, az tuzlu su ile öteleme, su gaz değişimli öteleme verimliliği

Acknowledgment

First foremost, I would like to acknowledge the advice, encouragement, and motivation from my academic advisor Prof. Dr. Ibrahim Kocabaş. He was always there for me for all kinds of support throughout my master's program. He has provided me commendable guidance to successfully accomplish this work.

I would also like to thank the whole petroleum and natural gas engineering research team at Izmir Katip Celebi University for their advices and cooperation. I want to mention especially Mr. Muhammed Said Ergül for providing me some important resource materials for my work.

The most importantly I want to express my gratitude to the "Yurtdışı Türkler ve Akraba Topluluklar Başkanlığı (YTB)" for providing me a full scholarship for my master's program and funding my living and accommodation expenses.

Table of Contents

List of Tables

List of Figures

List of Abbreviations

CEC	Cation Exchange Capacity
CMG	Computer Modelling Group
COBR	Crude Oil/Brine/Rock
EOR	Enhanced Oil Recovery
CO_2	Carbon Dioxide
EOS	Equation of State
Eqv	Equivalent
Exch	Exchange
FW	Formation Water
IFT	Interfacial Tension
IOR	Improved Oil Recovery
LoSal	Low Salinity Water
MIE	Multi-component Ion Exchange
LSWF	Low Salinity Waterflooding
PDIs	Potential Determining Ions
PPM	Parts Per Million
PR	Peng-Robinson
RF	Recovery Factor
SEM	Scanning Electron Microscope
SW	Sea Water
TDS	Total Dissolved Solids
WAG	Water Alternating Gas
LSWAG	Low Salinity Water Alternating Gas
OOIP	Original Oil in Place

List of Symbols

K	Absolute Permeability
k	Effective Permeability
k_r	Relative Permeability
n	Corey Exponent
Nc	Capillary Number
P, p	Pressure
Q	Volumetric Flow rate
q	Darcy Velocity
S	Saturation
X	Mass fraction
T	Temperature
V	Volume
v	Velocity
μ	Viscosity
ρ	Density
ϕ	Porosity
γ	Transmittivity
λ	Mobility
t	Time
n	Time Level

Chapter 1

Introduction

1.1 Background

The economically feasible production of oil is achieved in three stages namely, primary recovery, secondary recovery, and tertiary or enhanced oil recovery. The primary oil recovery stage refers to the flow of oil from the reservoir into the production wells due to the natural energy/forces that exists in the reservoir. These forces are classified as rock formation drive due to the compressional energy stored in the oil, connate water and porous formation in the reservoir rock, solution gas drive due to the dissolved gas in the oil, gas cap drive due to presence of a gas cap, water drive due to the compressional energy stored in the neighboring large size aquifers, and gravity drive.

The oil recovery factor or the ratio of oil production to initial oil in place in the primary stage ranges from 5% to 30%. Secondary recovery methods, namely immiscible waterflooding and gas flooding are usually applied at some stage of primary recovery to enhance and accelerate the production. The additional oil recovery factor due to secondary recovery methods ranges from 5% to 20%. On the average, the total oil recovery factor after primary and secondary recovery methods is between 15% and 40% [1]. The enhanced oil recovery (EOR) methods are applied to recover a significant amount of oil that usually remains in the reservoir after primary and secondary recovery methods. Figure 1.1 shows the partitions of oil recovery percentage by each type of oil recovery methods. It shows that the additional oil recovery factor of 15% to 25% can be achieved by applying EOR methods.

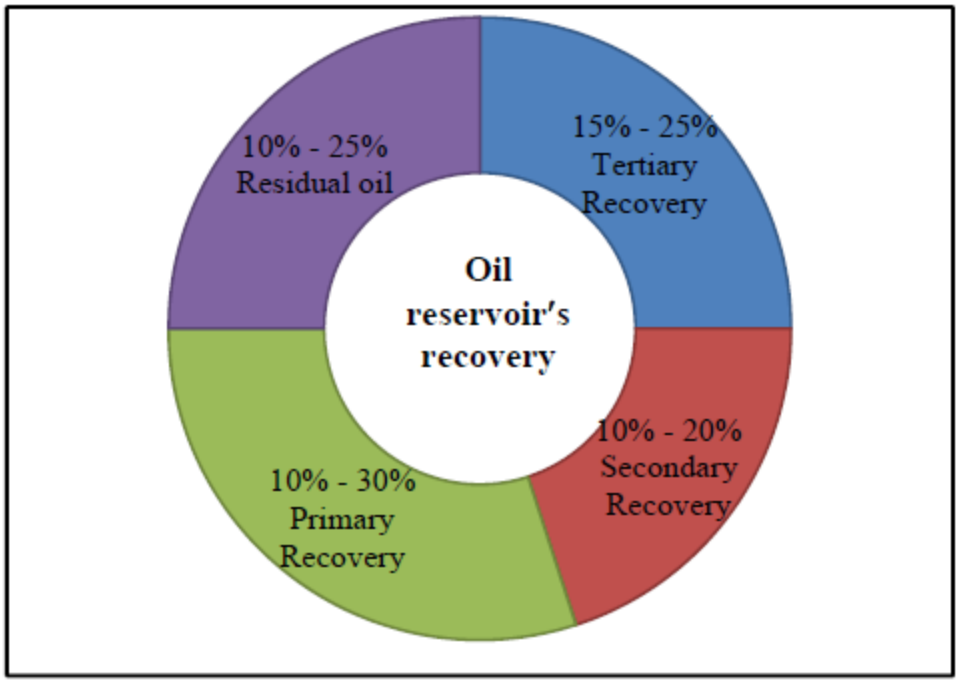

Figure 1.1: Reservoir oil recovery [2,3]

The EOR methods are applied to decrease the viscosity of reservoir fluids, increase capillary forces, and breaking interfacial tensions (IFT) between fluids and rock fractures in reservoirs. EOR methods are classified as chemical, microbial, and thermal. The summary of different classes of EOR methods according to the process or types of injection fluids are shown in figure 1.2 below.

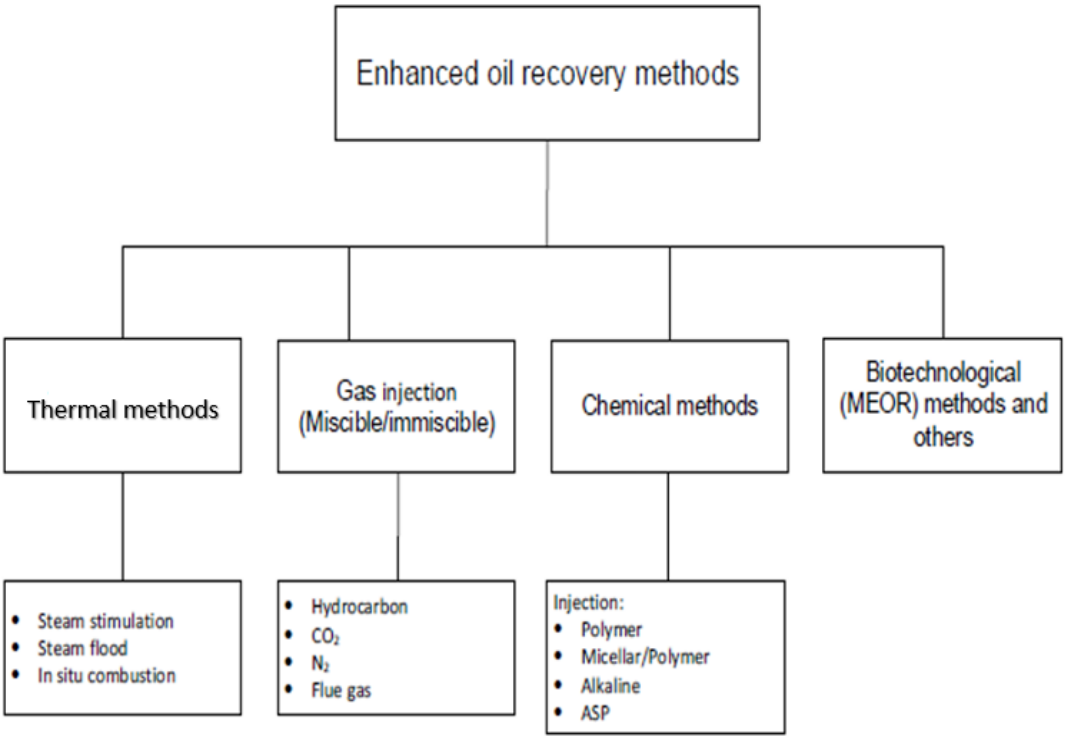

Figure 1.2 EOR methods classification [4]

While water flooding and gas injection are separately considered as secondary oil recovery mechanisms, their combination that is known as water alternating gas (WAG) injection; it is referred as the tertiary or enhanced oil recovery method. Gas has lower viscosity and lower density to crude oil; so, gas injection provides poor macroscopic sweep efficiency and there is early gas breakthrough during continued gas injection [5]. Therefore, WAG injection was initially used in order to improve macroscopic sweep efficiency in gas injection. In fact, WAG injection improves the macroscopic sweep efficiency by water flooding and high displacement efficiency by gas injection [6]. Due to its high-density water sweeps the bottom part of the reservoir and stabilizes the front displacement through maintaining the mobility ratio between water and oil [7].

Although the conventional WAG does improve oil recovery factor, there still remains a substantial amount of oil in reservoir pores due to rock-fluid interfacial tensions (IFT) and wettability conditions. The low salinity water alternating gas (LSWAG) was therefore proposed to break this IFT between rock clay and fluids and hopefully alter oil wetting conditions to water wetting conditions, and hence, further increase oil recovery factor. The

recent researches revealed that low salinity waterflooding (LSWF) alters oil-wet reservoir to water-wet. This wettability alteration is considered as the main mechanism of LSWF to improve oil recovery; however, there are other mechanisms of LSWF. Those include multi-ion exchange (MIE) between rock clay minerals and injected salt water, pH increase, and fines migration, they all target releasing the wetting oil phase from the rock/solid surfaces.

1.2 Objectives

This research is aimed to evaluate and compare the performances of conventional WAG injection and LSWAG in improving the oil recovery factor in an 80 ft thick and 1000 ft long sandstone reservoir. The theoretical and operational design factors considered are the initial phase of reservoir fluid (oil), gravity, injection depth, and vertical to horizontal permeability contrast, and injected water salinity. These factors are selected and adjusted to evaluate the oil sweep efficiencies of sea water WAG and low salinity WAG injection. The influence of these factors sequentially on waterflooding, CO_2 gas injection, and WAG injection is investigated with numerical simulations by using CMG-GEM reservoir simulator.

Chapter 2

Literature Review

2.1 Reviews on WAG Injection

The WAG injection was first implemented in 1957 in Alberta, Canada by Exxon Mobil as the combination of conventional water flooding and gas injection [8,9]. Nowadays, WAG injection is a common technique used in enhanced oil recovery for mature oilfields where the produced gas is re-injected during water flooding [5]. As shown in figure 2.1, WAG injection process is the combination of water flooding (WF) and gas injection (GI) where water and gas are alternately injected in continuous cycles.

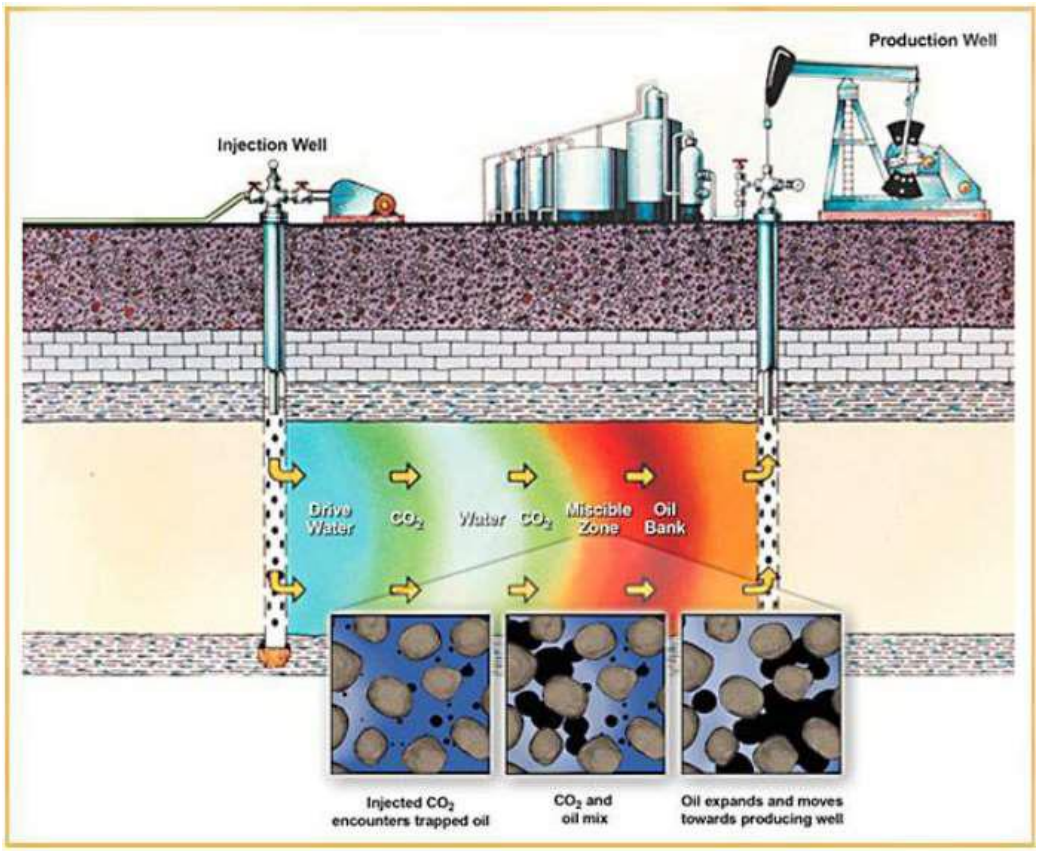

Figure 2.1 Schematic representation of WAG injection [10]

During WAG process, attic oil is produced by gas and the crude at the bottom is produced by water due to the gravity effect [11]. The injection strategies are the main factors that affect WAG injection performance and those include injection well patterns, WAG ratio, number of WAG cycles, volume of each cycle, and injection rate and pressure. The results from various researches on WAG injection indicate that WAG cycles with high Voidage Replacement Ratio (VRR) in gas cycles and WAG ratio of 1:1 have the optimum oil recovery [12].

Kulkarni and Rao conducted core experiment for both immiscible and miscible WAG injection; both scenarios of WAG injection and gas injection (GI) were compared and the results showed that WAG produce the better performance in oil recovery [13]. Performance of WAG injection is high in heterogeneous formations with low permeability [13]. Water flooding in low permeability and heterogeneous formations show poor water injectability, low production ratio, low oil recovery and high water-oil ratio (WOR) [14].

The application of WAG injection in different types of reservoir rock was studied by Christensen, et al., 1998. The results of their study showed that WAG injection is more applicable for sandstone reservoirs among others. Sandstones are considered as water wet and they provide better oil recovery efficiency than other types [9]. The figure 2.2 shows that more WAG projects where run in sandstones with 57% of 59 projects.

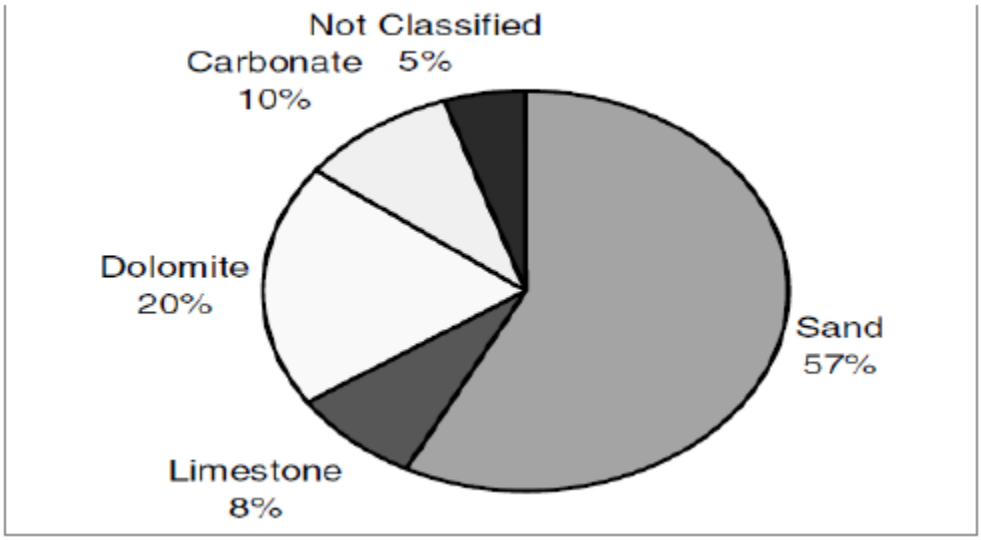

Figure 2.2 WAG injection in different types of rocks [9]

From a number of reports made on the field scale applications, WAG injection was found to be profitable due to the reduction of the volume of gas injected compare to only gas injection [15]. About 80% of WAG injection projects in the US were reported successful and economically fruitful [16]. The study of the 59 WAG field projects by Skauge et al. showed that at least 10% of originally oil in place (OOIP) is recoverable by technique [17]. In addition, WAG injection was applied and found successful in oilfields such as Gullfaks, Stafjord, South Brae, Snorre, and Oseberg Ost in North Sea [11].

As shown by the graph in figure 2.3, the number of WAG projects increased significantly from 1957 to 1996 [9]. In this period, USA had the highest executed WAG injection projects where a total of 37 WAG field projects were conducted. From 1975 to 2005, a number of EOR field projects including WAG injection projects in North Sea were reported by Awan et al. In 1997, a pilot project of WAG injection was conducted in brent reservoir of Statfjord field. This pilot project was successful and it was extended to the whole oilfield. With application of WAG injection water cut of 90% was reduced to 20% in five years and the oil recovery factor was significantly increased [11].

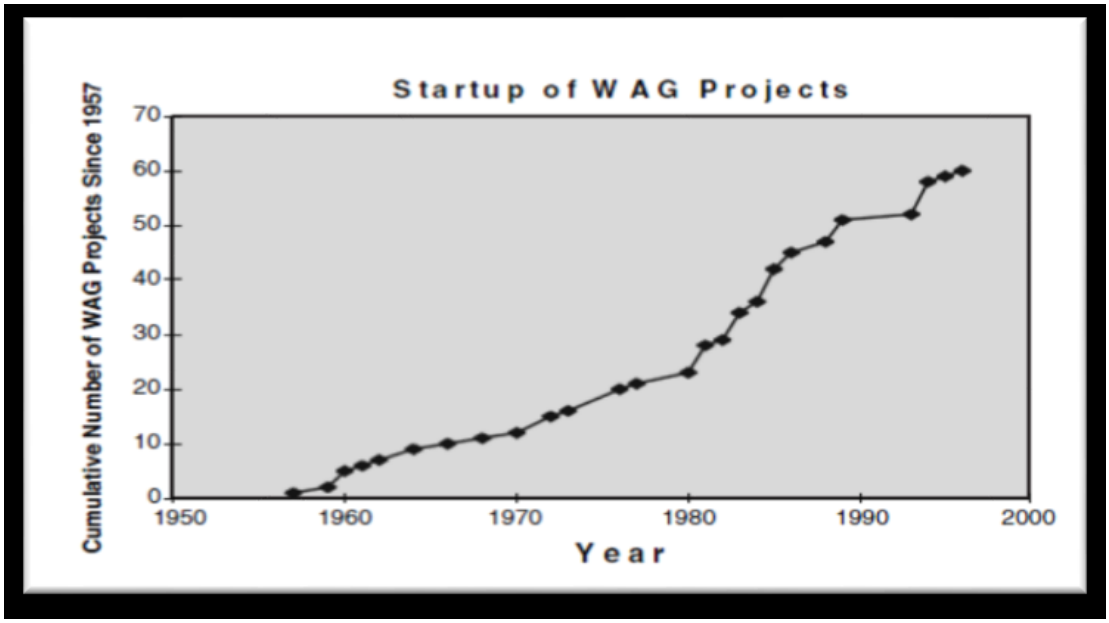

Figure 2.3 Cumulative number of worldwide WAG application from the first project in 1957 to 1996 [9]

For the first time in 2002, immiscible WAG injection test was run at pilot scale in Dulang oilfield. The main objective of this pilot test was to study the contribution of immiscible

WAG injection to the oil recovery. With the use of pilot test, WAG injection can be designed to achieve optimum oil recovery by also minimizing capital and operating costs. The results from the tests indicated that there is high potential of increasing oil recovery factor to 70% and production rate with immiscible WAG injection in Dulang oilfield [18].

In 2003, a WAG project with cycles of 50000 m^3/day of CO_2 and 160 m^3/day of water was examined after 6 months of continuous CO_2 injections in sandstone Ivanic pilot in Croatia oilfield. The pilot project was initially run to evaluate oil recovery with WAG injection (6 months of CO_2 injection and 6 months of water injection) over 19.5 years. However, due to financial reasons, the WAG cycles were abandoned after 2 cycles. The pilot project after 2 cycles showed promising results and a decision to run full field project was made [19,20].

Kulkarni and Rao (2005) conducted laboratory experiments on core samples to study miscible and immiscible WAG process. The experiment was done by flooding 5% NaCl brine and Yates reservoir brine both alternating with CO_2 gas in both cases [21]. As shown in the figure 2.4, oil recovery of 29 cc which is equivalent to 72.5% ROIP for immiscible WAG injection and 38 cc which is equivalent to 89.2% ROIP for miscible WAG injection.

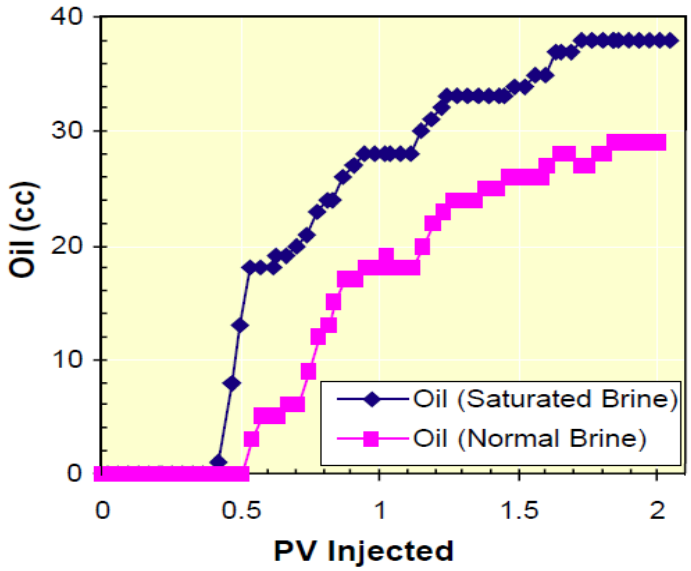

Figure 2.4 Oil recovery during WAG injection with normal brine and with CO_2 saturated brine [21]

In other experiments, Nezhad et al. (2006) studied the implication of WAG (water and CO_2) injection after water flooding and gas injection in secondary recovery. The results of

these experiments showed an increase of oil recovery by 4.08% of OOIP for the sample after waterflooding and 22.24% OOIP after gas injection [22]. Figure 2.5 shows the oil recovery by water alternating gas injection after water flooding.

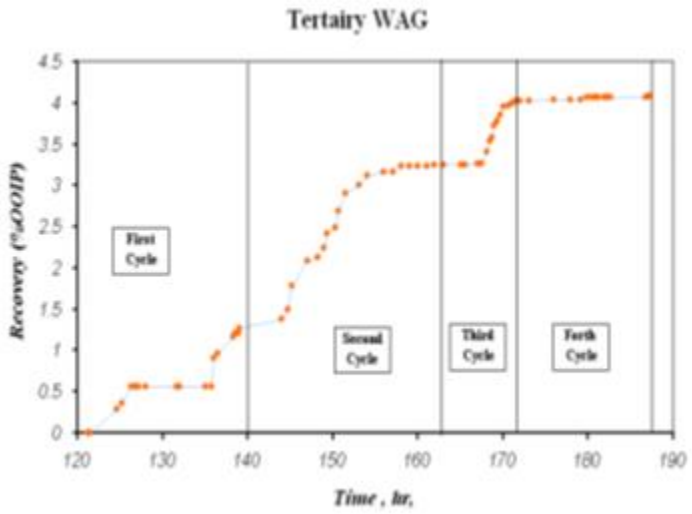

Figure 2.5 Oil recovery vs. time in WAG test after water flooding [22]

A study on the effect of injection spot patterns was done in Iranian oilfields. The results showed that 4 spot patterns (4 producers and 2 injections) produce higher oil recovery than five spot patterns [23]. In others words, not necessarily that increasing the number of wells increases oil recovery.

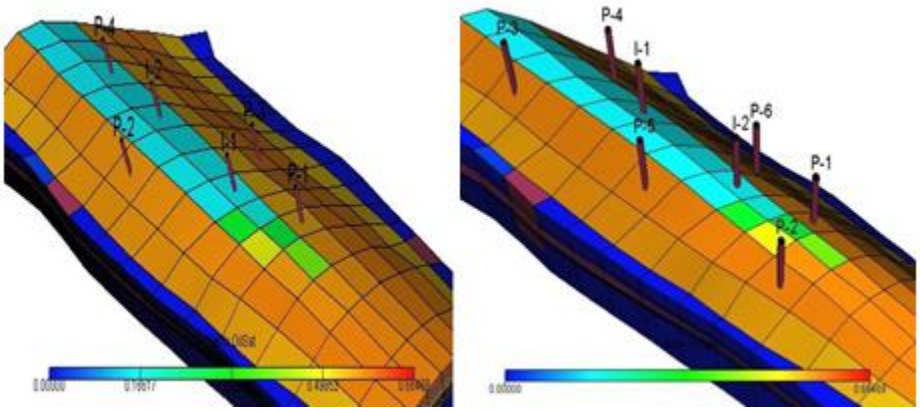

Figure 2.6 Four and five spot injection patterns [23]

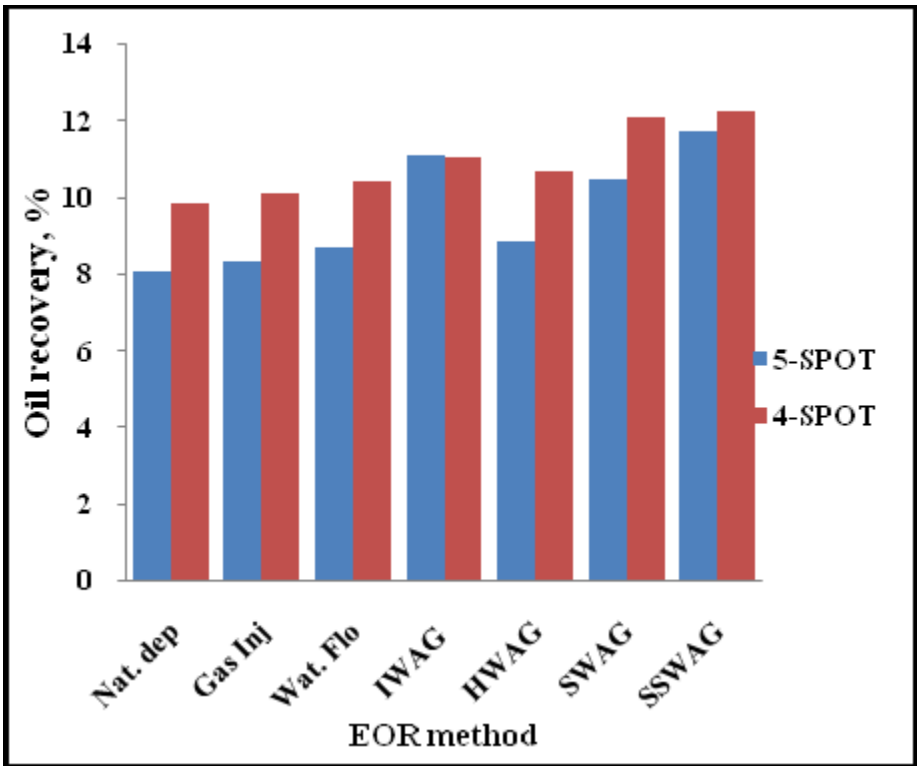

Figure 2.7: Comparison between oil recovery in 4 and 5 spot injection patterns [23]

A comparative study between WAG injection and individual water flooding and gas injection was conducted by Nabil et al, 2004. Their results confirmed the theory that WAG injection improve both microscopic and microscopic sweep efficiencies. The graphs in figure 2.8 show that WAG injection produced highest oil recovery flowed by water flooding and lastly gas injection [24].

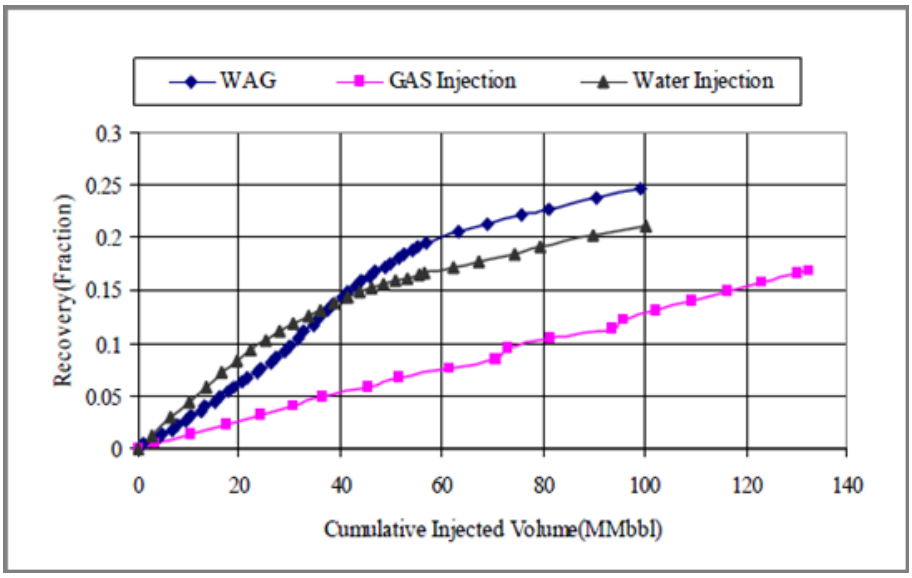

Figure 2.8: Comparison of WAG injection and conventional methods [24]

2.2 Reviews on LSWF

Low salinity waterflooding could increase oil recovery factor from 6 to 12% which takes waterflooding recovery to 8 to 19% OOIP [25]. The increase of oil recovery by low salinity water flooding is attributed to four mechanisms: changing the wettability to water wet due to the clay migration; increasing of pH due to $CaCO_3$ that results in wettability alteration; generation of surfactants and reduction of interfacial tension (IFT); multicomponent ion exchange (MIE) between clay minerals and injected brine [25-27].

Low salinity waterflooding changes the reservoir wettability from oil wet to water wet. In other words, low salinity waterflooding affects the oil wet and it has no effect on water wet sample. It was found that high concentrations of Ca^{+2} and Mg^{+2} ions in brine formation make the sample more oil wet. Low salinity water flooding also changes the composition of rock and its properties. The experiments showed that the low salinity water dissolves anhydride cements in rock formation. As the result, low salinity water flooding increases the permeability of reservoir rock [28].

Low salinity waterflooding causes the pH increase and reduction of IFT. A typical experiment performed for a BP operated North Sea field (BPNS2), pH was increased from

7 to 10 by injecting a diluted brine formation of 15000ppm to between 1500ppm and 150ppm. Figure 2.9 shows the effect of pH increase due to low salinity waterflooding [31].

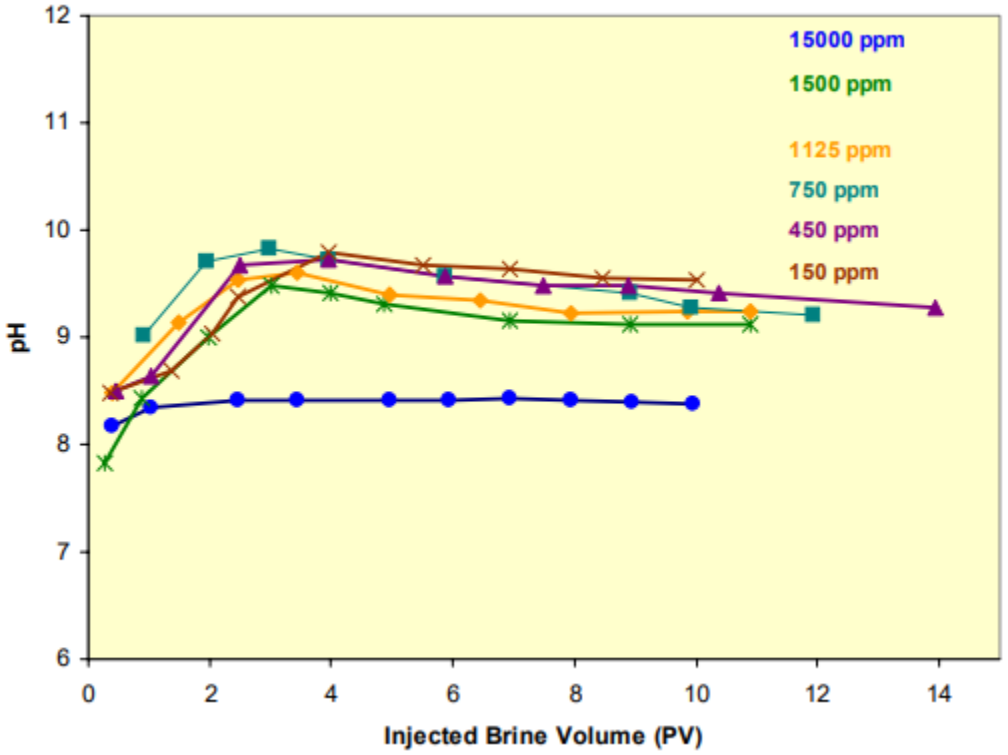

Figure 2.9: Change in effluent pH with injection water salinity in Berea Sandstone/BPNS2 brine system [31]

2.3 Review on Numerical Simulation studies

Yu-Shu et al, 2009 presented a general numerical model to simulate low salinity waterflooding for multi-dimensional porous and fractured reservoirs. This model was formulated by incorporating different mechanisms that result in low salinity waterflooding. These include wettability alteration, reduction of IFT and others. The models for homogenous and fractured reservoirs were run in order to demonstrate the usefulness of the modeling approach in low salinity waterflooding processes.

The governing equations were derived by considering an isothermal system with three phases but with four material components: water, oil, gas, and salt (NaCl). Each material component is treated as single (pseudo component) fluid in flow; and it is assumed that salt

is only transported in aqueous phase. As a result, four material balance equations were derived for each component by applying Darcy's law in multiphase flow. The effects of applied pressure, gravitational forces (density), capillary pressures, rock permeability, and reservoir conditions (temperature), interfacial tension forces, and other flow parameters were analyzed and evaluated in formulating mass balance equations as shown below [29].

For gas
$$\frac{\partial}{\partial t}\left\{\phi\left(S_o\bar{\rho}_{dg} + S_g\rho_g\right)\right\} = -\nabla\left(\bar{\rho}_{dg}\overrightarrow{V_o} + \rho_g\overrightarrow{V_g}\right) + q_g \tag{2.1}$$

For water
$$\frac{\partial}{\partial t}\left(\phi S_w X_w \rho_w\right) = -\nabla\left(X_w\rho_w\overrightarrow{V_w}\right) + q_w \tag{2.2}$$

For oil
$$\frac{\partial}{\partial t}\left(\phi S_o\bar{\rho}_o\right) = -\nabla\left(\bar{\rho}_o\overrightarrow{V_o}\right) + q_o \tag{2.3}$$

For salt component
$$\begin{aligned}\frac{\partial}{\partial t}\left\{\phi S_w X_w\rho_w + (1-\phi)\rho_R\rho_w X_c K_d\right\} \\ = -\nabla\left(X_c\rho_w\overrightarrow{V_w}\right. \\ \left. + \rho_w S_w\phi\tau D_m\nabla X_c\right) + q_c\end{aligned} \tag{2.4}$$

Darcy's Velocity of phase β is defined as:

$$\overrightarrow{V_\beta} = -\frac{kk_{r\beta}}{\mu_\beta}\left(\nabla P_\beta - \rho_\beta g\nabla d\right) \tag{2.5}$$

Where parameters ρ is the density, S is saturation, X is mass fraction, ϕ is effective porosity, μ is viscosity, P is pressure, D_m is molecular diffusion coefficient of salt (NaCl), K_d is the distribution coefficient of salt in water and rock formation, k is the absolute permeability. The subscripts to the notations of parameters: r is for rock formation, o is for oil, w is for water, g is for gas, and c is for salt component. In addition to the above governing equation of low salinity water flooding, the constitutive relations hold:

$$S_w + S_o + S_g = 1 \tag{2.6}$$

$$X_w + X_c = 1 \tag{2.7}$$

Simulation of multiphase flow (with low salinity water flooding) in reservoir was done by numerically solving the above material balance equations. The equations were discretized by using integral finite method. The iterative approach is then used to solve discretized equations. In this case the discrete equations are fully implicit in order to provide stability and large time step size. The discretized equations in the residual form are shown below:

For gas,
$$\begin{aligned} R_i^{g,n+1} = & \left\{ \left[\phi S_o \bar{\rho}_{dg} + \phi S_g \rho_g \right]_i^{n+1} \right. \\ & \left. - \left[\phi S_o \bar{\rho}_{dg} + \phi S_g \rho_g \right]_i^{n} \right\} \frac{V_i}{\Delta t} \\ & - \sum_{j \in \eta_i} \left(\bar{\rho}_{dg} \lambda_o \right)_{ij+\frac{1}{2}\gamma_{ij}}^{n+1} \left[\Psi_{oj}^{n+1} - \Psi_{oi}^{n+1} \right] \\ & - \sum_{j \in \eta_i} \left(\rho_g \lambda_g \right)_{ij+\frac{1}{2}\gamma_{ij}}^{n+1} \left[\Psi_{gj}^{n+1} - \Psi_{gi}^{n+1} \right] \\ & - Q_{gi}^{n+1} \end{aligned} \tag{2.8}$$

For water,
$$\begin{aligned} R_i^{w,n+1} = & \{ [\phi S_w X_w \rho_w]_i^{n+1} - [\phi S_w X_w \rho_w]_i^{n} \} \frac{V_i}{\Delta t} \\ & - \sum_{j \in \eta_i} \left(\rho_w X_w \lambda_w \right)_{ij+\frac{1}{2}\gamma_{ij}}^{n+1} \left[\Psi_{wj}^{n+1} \right. \\ & \left. - \Psi_{wi}^{n+1} \right] - Q_{wi}^{n+1} \end{aligned} \tag{2.9}$$

For oil,

$$R_i^{o,n+1} = \{[\phi S_o \bar{\rho}_o]_i^{n+1} - [\phi S_o \bar{\rho}_o]_i^n\}\frac{V_i}{\Delta t} - \sum_{j\in\eta_i} (\bar{\rho}_o \lambda_o)^{n+1}_{ij+\frac{1}{2}\gamma_{ij}} \left[\Psi_{oj}^{n+1} - \Psi_{oi}^{n+1}\right] - Q_{oi}^{n+1} \quad (2.10)$$

For salt,

$$R_i^{c,n+1} = \{[\phi S_w X_c \rho_w + (1-\phi)\rho_R X_c \rho_w K_d]_i^{n+1} - [\phi S_w X_c \rho_w + (1-\phi)\rho_R X_c \rho_w K_d]_i^n\}\frac{V_i}{\Delta t} - \sum_{j\in\eta_i} (\rho_w X_c \lambda_w)^{n+1}_{ij+\frac{1}{2}\gamma_{ij}} \left[\Psi_{wj}^{n+1} - \Psi_{wi}^{n+1}\right] - \sum_{j\in\eta_i} (S_w \rho_w)^{n+1}_{ij+\frac{1}{2}\gamma_{ij}^D} \left[X_{cj}^{n+1} - X_{ci}^{n+1}\right] - Q_{ci}^{n+1} \quad (2.11)$$

Where:

n: previous time level;

n+1: current time level;

V_i: volume of element;

Δt: time step size,

η_i: set of neighbor element (j) or nodes of element (i) to which element I is connected;

ij+1/2: average at interface between two element I and j;

λ: mobility; so, the mobility of phase β is:

$$\lambda_\beta = \frac{k_{r\beta}}{\mu_\beta} \tag{2.12}$$

γ_{ij}: transmissivity of flow terms

$$\gamma_{ij} = \frac{A_{ij} k_{ij+1/2}}{D_i + D_j} \tag{2.13}$$

$\Psi_{\beta i}^{n+1}$: the potential term

$$\Psi_{\beta i}^{n+1} = P_{\beta i}^{n+1} - \rho_{\beta i j+1/2}^{n+1} g d_i \tag{2.14}$$

The mass balance equations are written in the residual forms where the amount of each component remains (at a particular position (i) and at a given time n+1), is calculated based on the values of input variables at that position and time. The solution is obtained by satisfying initial and boundary conditions. The equations are applicable for multi-phase flow both in fractures and inside the rock matrix.

Yu-Shu et al, 2009 carried out a numerical simulation of low salinity waterflooding for single-phase water and solute transport problem in one dimensional, two-phase (oil and water) flow with different salinities in fractured rock [29]. The numerical solution of this problem was compared to the analytical solution as provided by Javandel et al (1984) and they were in agreement [30].

Yu-Shu et al, 2009 also simulated oil displacement by salty water in a porous medium. This problem considers miscible displacement where oil is displaced by high salinity and low salinity water. In this problem, it was assumed that the flow domain is one dimensional, horizontal, homogenous and isotropic porous medium with 10 m long and a unit section area. Initially the medium contains oil and water with water at residual saturation. The water with two different salinities was injected to study the effect of salinity on oil recovery

rate. It was assumed that there is a linear relationship of residual oil saturation and salt mass fraction. As shown in figures 2.10 and 2.11, the numerical simulations indicate that low salinity water solution has greater effect than high salinity water solution in increasing recovery rates in terms of pore volume injected both at zero capillary pressure and salinity dependent capillary pressure conditions [29].

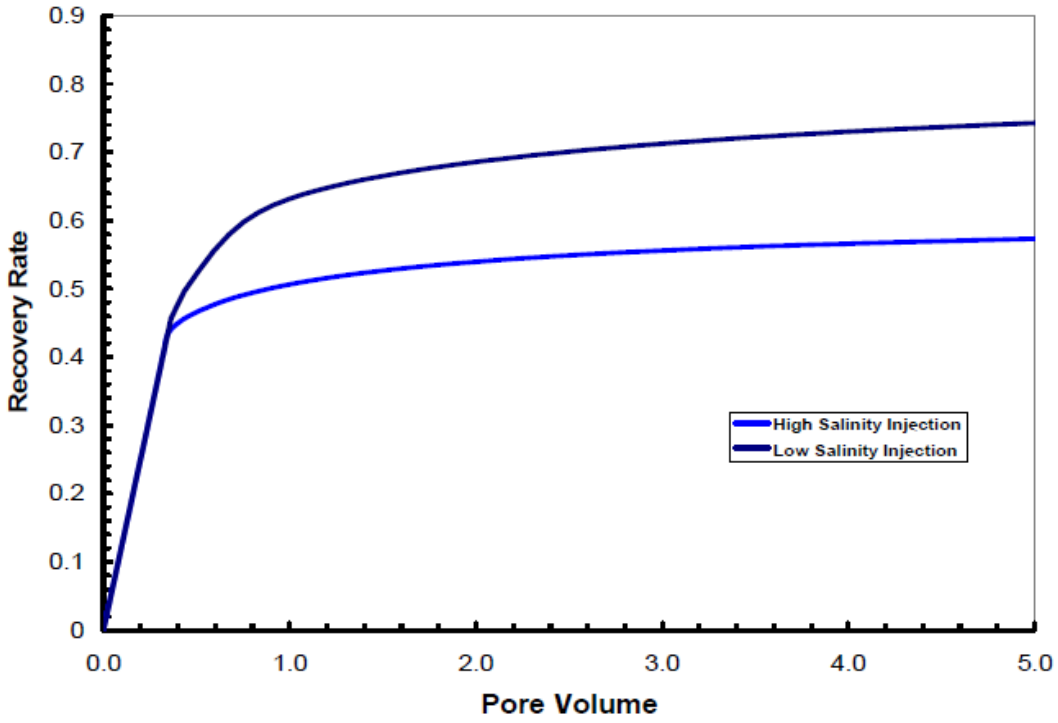

Figure 2.10: Comparison of recovery rates for Low salinity and high salinity waterflooding through 1D of rock column at zero capillary pressure condition [29]

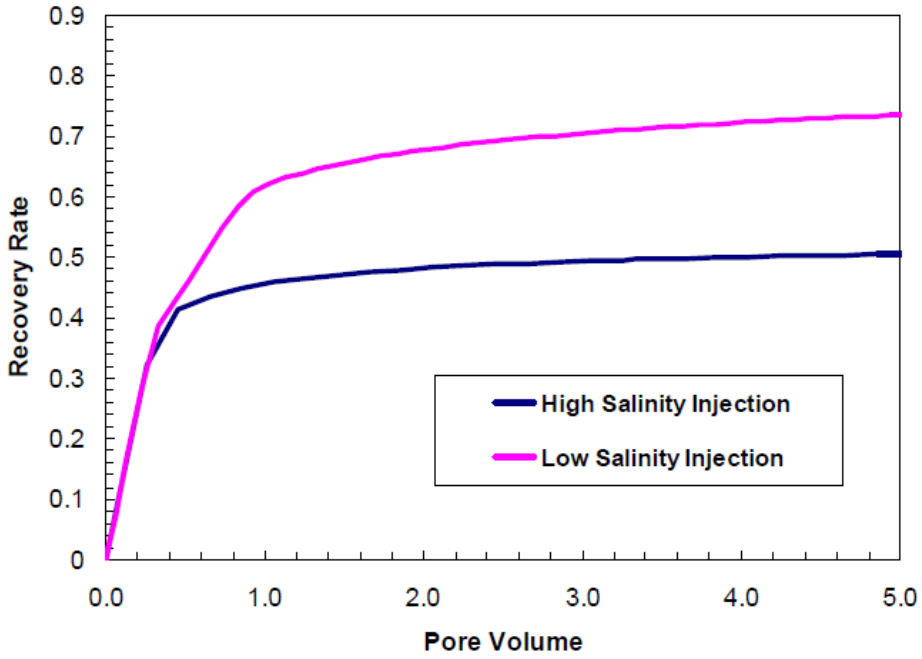

Figure 2.11: Comparison of recovery rates for Low salinity and high salinity waterflooding through 1D rock column at salinity dependent capillary pressure condition [29]

In addition, the model and numerical simulation were applied to the displacement problem in a double porosity fractured medium. This problem considers low salinity water injection in a one dimension, horizontal, uniform, and fractured oil reservoir. The rock is also assumed to be fractured in parallel model. There was no capillary pressure change with low salinity. The simulation of low salinity water flooding in fractured rock showed that there is no significant improvement in oil recoveries in comparison with porous rock [29].

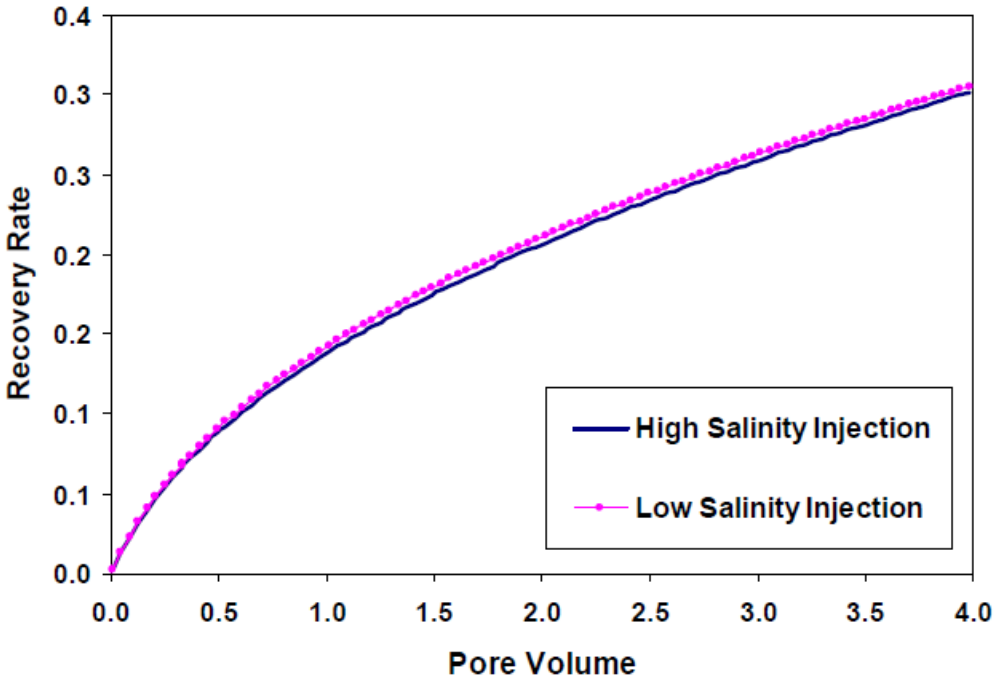

Figure 2.12: Comparison of recovery rates for Low salinity and high salinity waterflooding through 1D double porosity fractured rock column at same capillary pressure condition [29]

Chapter 3

Theory of WAG Processes

3.1 Darcy's Law

The flow of fluids in porous medium is governed by Darcy's law. For multiphase flow in porous medium, Darcy's velocity of individual fluid ($\vec{V_i}$) is proportional to the effective permeability (k_i), and pressure gradient with gravity effect ($\nabla P - \rho g \nabla d$) and inversely proportional to the viscosity μ_i. In oil reservoirs, the velocities of gas, oil, and water are calculated by using the flowing equations as by Darcy's law.

For gas:
$$\overrightarrow{V_g} = -\frac{k_g}{\mu_g}(\nabla P_g - \rho_g g \nabla d) \tag{3.1}$$

For oil:
$$\overrightarrow{V_o} = -\frac{k_o}{\mu_o}(\nabla P_o - \rho_o g \nabla d) \tag{3.2}$$

For water:
$$\overrightarrow{V_w} = -\frac{k_w}{\mu_w}(\nabla P_w - \rho_w g \nabla d) \tag{3.3}$$

3.2 Relative Permeability

The concept of relative permeability was adopted to express the effective permeability to the base permeability (usually effective permeability to oil at irreducible water saturation). Relative permeability to fluid (k_{ri}) is the ability of medium to conduct that fluid in presence of other fluids. Relative permeability depends on microscopic distribution and saturation

of fluid. It is therefore experimentally correlated with saturation of fluid. Brooks-Corey correlation is a power law model proposed for history match both experimental and field data for relative permeability. Relative permeability is correlated with fluid saturation as shown in the following equations [32,80,81].

$$k_{rw} = k_{rw,max}\left(\frac{S_w - S_{wc}}{1 - S_{or} - S_{wc} - S_{gc}}\right)^{n_w} \tag{3.4}$$

$$k_{ro} = k_{ro,max}\left(\frac{S_o - S_{or}}{1 - S_{or} - S_{wc} - S_{gc}}\right)^{n_o} \tag{3.5}$$

$$k_{rg} = k_{rg,max}\left(\frac{S_g - S_{gc}}{1 - S_{or} - S_{wc} - S_{gc}}\right)^{n_g} \tag{3.6}$$

Where:

- S_w: water saturation
- S_{wc}: irreducible water saturation
- S_o: oil saturation
- S_{or}: residual oil saturation
- S_g: gas saturation
- S_{gc}: irreducible gas saturation
- n_w, n_o, and n_g refers to exponents and they range from 1 to 6;
- $k_{rw,max}$, $k_{ro,max}$, and $k_{rg,max}$ are the maximum or end point relative permeabilities

Relative permeabilities are therefore computed from two phase data; the flowing diagrams in figure 3.1 illustrates the relative permeability to oil from oil and water system and oil and gas system.

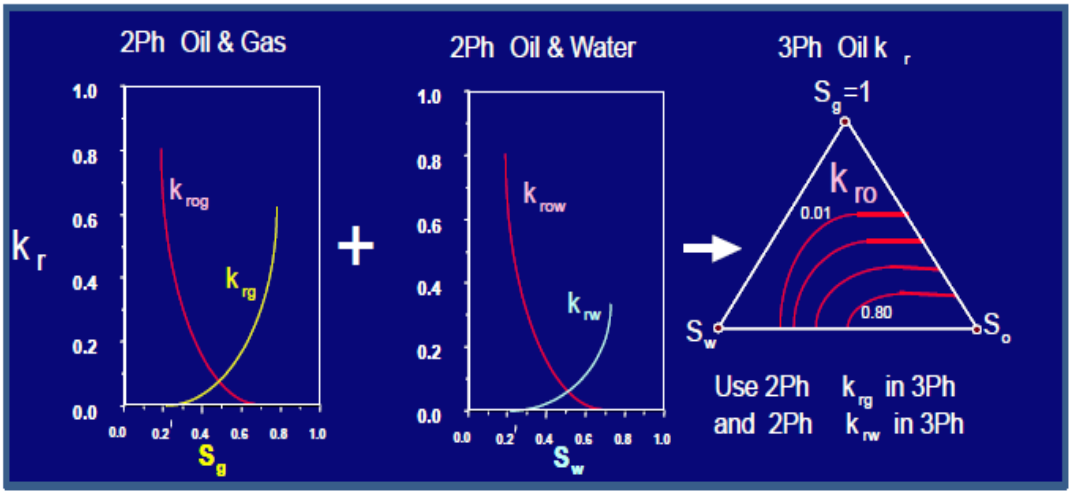

Figure 3.1 Three-phase relative permeability to oil [33]

3.3 Mobility Control

EOR techniques are used to control the movement of both displacing and displaced fluids by maintaining mobility ratio (M) less than 1. Mobility ratio is calculated by dividing the mobility of displacing fluid (water or gas) by that of displaced fluid (oil) [39]. For example: in the case of water injection:

$$\lambda_w = \frac{k_w}{\mu_w} = \frac{k.k_{rw}}{\mu_w} \tag{3.7}$$

$$\lambda_o = \frac{k_o}{\mu_o} = \frac{k.k_{ro}}{\mu_o} \tag{3.8}$$

$$M = \frac{\lambda_w}{\lambda_o} = \frac{\mu_o k_{rw}}{\mu_w k_{ro}} \tag{3.9}$$

Where:

λ_o: Mobility of oil (D/cP)

λ_w: Mobility of water (D/cP)

k_o: Effective permeability to oil (D)

k_w: Effective permeability to water (D)

k_{ro}: Relative permeability to oil (-)

k_{rw}: Relative permeability to water (-)

3.4 Capillary Number

EOR techniques are performed to increase the capillary number N_{ca} to facilitate the flow of reservoir fluids. Capillary number is a function of fluid viscosity (μ), Darcy velocity (v) and interfacial tension (σ) [39].

$$N_{ca} = \frac{v\mu}{\sigma} \tag{3.10}$$

3.5 Microscopic and Macroscopic Sweep Efficiencies

The WAG injection is applied to achieve improved microscopic sweep efficiency and to recovery attic oil that would not be contacted by injected water. Separation of the phases is common with gravity effect especially in high permeable sandstone reservoirs. Injected gas tends to migrate at the top and injected water play a role of piston push at the bottom of the reservoir until breakthrough. As a result, the combination of water and gas injections would increase the oil recovery since the un-swept area reduces in the process. The residual oil reduces more by applying WAG injection than only applying water or gas injection. With combination of water and gas injections, macroscopic and microscopic sweep efficiencies are achieved [34,35]. From figures 3.2, 3.3, and 3.4 below, there is bigger sweep efficiency with WAG injection, than the single injection of water or gas:

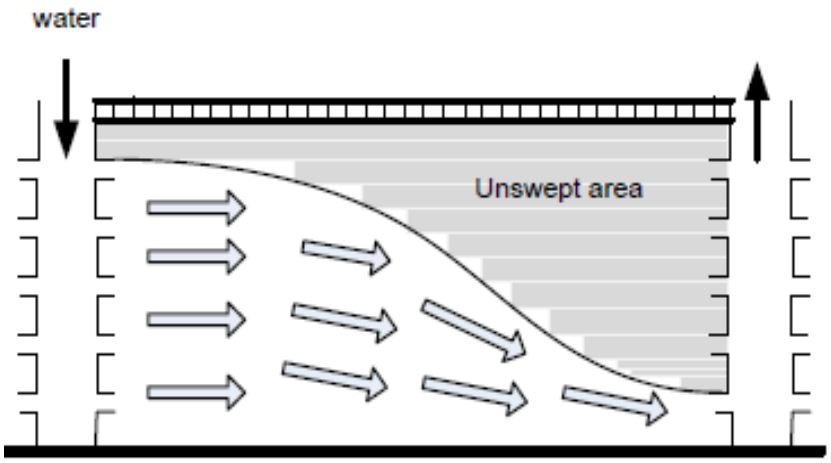

Figure 3.2: Gravity effect during water injection [36]

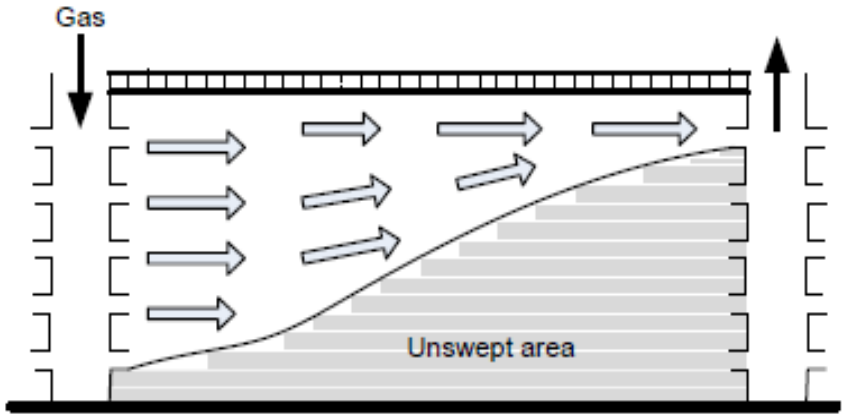

Figure 3.3: Gravity effect during the gas injection [36]

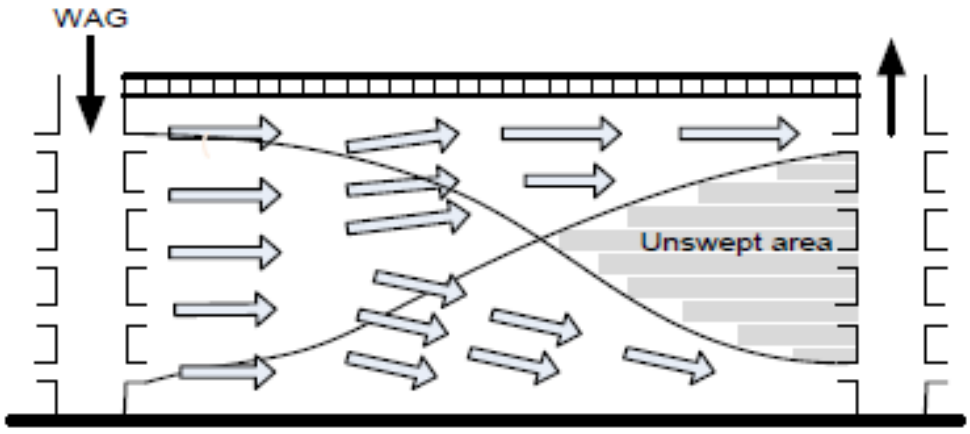

Figure 3.4 Gravity effect during WAG injection [36]

Fraction of oil removed from the swept area by injected fluid indicates the displacement (microscopic) efficiency. On the other hand, volumetric (macroscopic) sweep efficiency is presented by the volume of the reservoir that was contacted by the injected fluid. Displacement efficiency (E_d) and Volumetric efficiency (E_v) are calculated as:

$$E_d = \frac{S_{oi} - S_{or}}{S_{oi}} \tag{3.11}$$

$$E_v = E_A \times E_I, \tag{3.12}$$

Where:

E_d: Displacement efficiency

S_{oi}: Initial oil saturation,

S_{or}: Residual oil saturation

E_v: Volumetric sweep efficiency

E_A: Areal sweep efficiency

E_I,: Vertical sweep efficiency

Total oil recovery efficiency is therefore determined as:

$$E_T = E_d \times E_v \quad (3.13)$$

3.6 Classifications Of WAG Process

Depending on the manner in which water and gas alternate, WAG process can take different forms such as hybrid WAG injection, simultaneous water alternating gas injection (SWAG) and others. In hybrid WAG process, the large volume of gas is first injected and it is followed by smaller volumes of water alternating with gas by maintaining the ratio of 1:1 [9,37]. For SWAG process, water and gas are injected simultaneously. Water and gas are mixed at the surface before they are injected into reservoir. It is a very know technique of WAG operations. SWAG process influences displacement of oil by upward movements of gas and downward movement of water due to gravity differences [34].

In some WAG processes, gas or liquid phase is modified prior to injection in order to increase the sweep efficiency. For example; when gas phase is in the form of foam, the process is referred as foam assistant WAG injection (FAWAG). The foam is used to reduce the mobility of the injected gas and as a result it improves the sweep efficiency and delays breakthrough. The application of foam in controlling the mobility of gas was first introduced by Bond and Holbrook in 1958. The CO_2 foam with surfactants was used to control the mobility of gas phase in WAG process [38]. Foam injections were also used in North Sea to control the mobility of gas phase in WAG process and to reduce the gas oil ratio (GOR) during well production. Liquid phase in WAG process can also contain some additives like low salinity, surfactant, or water-soluble polymers [39].

The WAG processes are however generally classified as miscible and immiscible, depending on the miscibility of injected gas [9,40–42]. The types of gases used in WAG injection are hydrocarbon and non-hydrocarbon gases. Light hydrocarbon gases like methane, ethane, propane, and butane are used while non-hydrocarbon gases that are used in WAG injection include carbon dioxide and nitrogen. If the gas injection takes place

above the minimum miscibility pressure (MMP), the WAG process is referred as miscible and if the gas injection takes place at pressure below MMP, the WAG process is said to be immiscible.

3.6.1 Miscible WAG Injection

Miscible WAG happens when the gas injected is miscible with the reservoir oil. Miscibility is divided into first-contact miscibility and dynamic miscibility. The first contact miscibility is achieved when the injected gas becomes miscible when it contacts with oil. Dynamic or multi-contact miscibility is when the injected gas becomes miscible in oil during the displacement process in the reservoir [42–44]. The partial miscibility can also take place when injected gas is not completely miscible with oil and it retains its free state [43,45]. Miscibility of gas injected reduces the viscosity of reservoir oil and as result its mobility increases and production increases.

3.6.2 Immiscible WAG Injection

In the immiscible WAG process, the injected gas is not miscible with reservoir oil. The front between gas and reservoir oil is maintained during the displacement of oil by injected gas. The gas continues to be in its gaseous state [43,45,46].

3.7 Factors Affecting WAG Injection

There are various factors that affect WAG process and they are categorized as reservoir characteristics (porosity and permeability), fluid properties (density and viscosity), and operational parameters (injection pattern, injection depth, and WAG ratio).

3.7.1 Reservoir Heterogeneity and Stratification

Reservoir heterogeneity and stratification dictate the flow direction of the reservoir fluids. It is very important to understand heterogeneity and stratification of the reservoir in designing WAG injection. In heterogeneous reservoir, the horizontal fluid flow is

influenced by a number of factors like capillary effect, gravity, viscous forces and depression [47]. Vertical flow of fluids in reservoir may increase the sweep area but it would less affect the oil recovery due to the gravity segregation and the decrease in velocity to the production wells. In low permeable layers, heterogeneity causes the loss of front displacement. The effect of heterogeneity is usually observed mainly for WAG and gas injections. Some of the problems encountered during WAG injections due to heterogeneity of the reservoir include loss of miscibility and channeling. As a result, there is early gas breakthrough and low oil recovery.

3.7.2 Reservoir Wettability

As previously mentioned, relative permeability is the measure of ability of porous medium to conduct a fluid in presence of other fluids [48]. Relative permeability is a function of wettability and it controls the initial distribution of the fluids and the displacement of fluids. In a multiphase media like a reservoir, wetting phase occupies smaller pores while the non-wetting phase remains in larger pores. As a result, wetting phase has low relative permeability due to the poor connectivity of smaller pores compare to the non-wetting phase that flow in large pores with high connectivity [49,50]. For example, in figure 3.5, relative permeability of oil is lower in oil wet reservoir comparing in water wet reservoir with equal water/oil saturation.

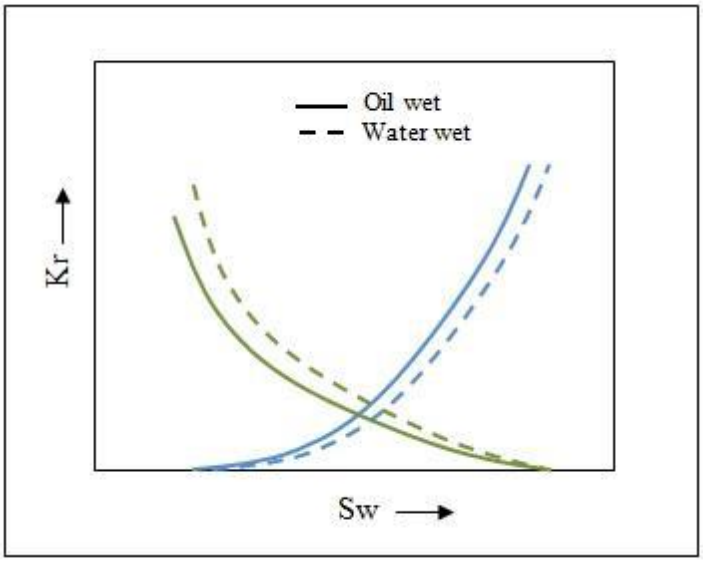

Figure 3.5 Relative permeability for oil wet and water wet conditions

Considering an oil-water phase reservoir, and the reservoir rock is preferentially water wet; during water injection, water would easily displace oil in smaller pores. In a water wet reservoir, the interfacial forces between water and oil are reduced hence oil is more mobile. On the other hand, in the oil wet reservoir, during water injection process water preferably flows through the large pores and as result a significant oil saturation around the pores and in smaller pores remains at water breakthrough. Therefore, water injection is more efficient in water-wet than oil-wet reservoirs [48,49,51,52].

3.7.3 Fluid Properties

Fluid properties can be easily measured in laboratory with different techniques. However, the behaviors of injection fluids in the reservoir changes during the process. Researches on the behavior of injected fluids are needed to understand the changes in fluid properties as the reservoir conditions change during the process. The change of rock-fluid interactions due to the change in reservoir conditions leads to the variation in rock wettability. The change of rock wettability affects the flow parameters such as capillary pressure and relative permeability [53–56].

In WAG process, injected gas invades porous medium and dissolve into oil and decreases its viscosity and hence microscopic sweep efficiency increases. Viscosity is a function of temperature, pressure and specific gravity of a fluid [45]. An experimental study conducted by Kulkani and Roa (2004) showed that low salinity water as injectant water during WAG process increases the solubility of gas, and hence increase the oil recovery.

3.7.4 Injection Pattern

In WAG process, the injection spot pattern is an important factor of displacing reservoir oil to the producing wells. Injection wells and producing wells are distanced with the purpose of minimizing the displacement of flowing fluids but also to prevent undesired breakthroughs. Therefore, increasing the number of injection wells or producing wells not usually increases oil recovery. Orientation of the wells also plays a big role in WAG process. The combination of vertical producing wells and horizontal injection wells show a better recovery [57]. With the use of computer technology and software development, optimum location and orientation of the wells and WAG ratio can be selected through simulation of a number of reservoir models by analyzing frontal propagation and recovery [16,58]

3.7.5 WAG Ratio

WAG ratio is the volume of injected gas divided by the volume of injected water under the reservoir conditions. It is designed by considering the mobility of the fluid. WAG ratio has a big effect on oil recovery. The studies showed that recovery factor decreases as WAG ratio decreases.

However, there are a number of research studies on wettability as the main factor that affects oil recovery during application of high WAG ratios. The results show that high WAG ratios decrease the oil recovery especially in water wet reservoirs. In mixed or oil wet reservoir, high WAG ratios have less impact on WAG performance as a substantial oil recovery is obtained. The WAG ratio of 1:1 was reported as the optimal ratio [37].

3.7.6 Tapering

Tapering is the control of volume of gas injection in later stages of WAG injection. The relative water to gas ratio (WGR) is increased to control flow problems like breakthrough and channeling in WAG injection [59]. The injected gas is reduced especially for economic factors in case it is expensive. CO_2 WAG tapering is used to increase the recovery oil but also to effectively use of the injected gas. The rate of injected gas is high in early cycles of the operation and then reduced at later cycles [47]. Tapering is used to increase the production and also to manage effectively the CO_2 injections [60]. Chevron has used tapering WAG by increasing the ratio of water to gas so as to reduce the production of CO_2 [61]. Khan et al. studied WAG process with tapering technique by shortening the duration of gas injection in WAG cycles. They concluded that tapering WAG techniques has better performance than conventional WAG injection with water gas ratio of 1:1 [62]. Tapering technique reduces the response time of oil bank to the production wells. Therefore, tapering WAG strategy is used both to increase oil recovery and also to effectively manage the injected gas.

Chapter 4

Theory of the Mechanisms of Low Salinity Waterflooding

Low salinity waterflooding is a technique of injecting water with low concentration of salts between (salinity: 1000-2000 ppm). It is a chemical technique that was recently adopted to improve oil production. From different experimental analysis of core flooding, chemical changes of rock and fluids due to low salinity flooding are the main reason of oil recovery improvement. The mechanism of low salinity waterflooding is based on breaking the electric forces exhibited by high salinity formation water to oil to rock surface. Hence, certain conditions that include the presence of clay minerals like calcite and dolomite and the polarity of oil, they are the key conditions for effectiveness of low salinity waterflooding [26, 31]. The following are the main mechanisms by which low salinity waterflooding improve the oil displacement in the reservoir:

4.1.1 Multicomponent Ion Exchange (MIE)

In the reservoir, oil is attached to rock surface by bonding to multivalent cations. By injecting the low salinity water, K^+ and Na^+ ions replace these multivalent ions like Ca^{2+} and Mg^{2+}. As a result, the oil is released from rock surface in the form of calcium or magnesium carboxy complex. Unlike for high salinity water that strengthen the oil bonding to clay, injection of low salinity water weakens these bonding for ion exchange to occur. The effectiveness of low salinity water flooding therefore depends on composition of water formation and injection brine.

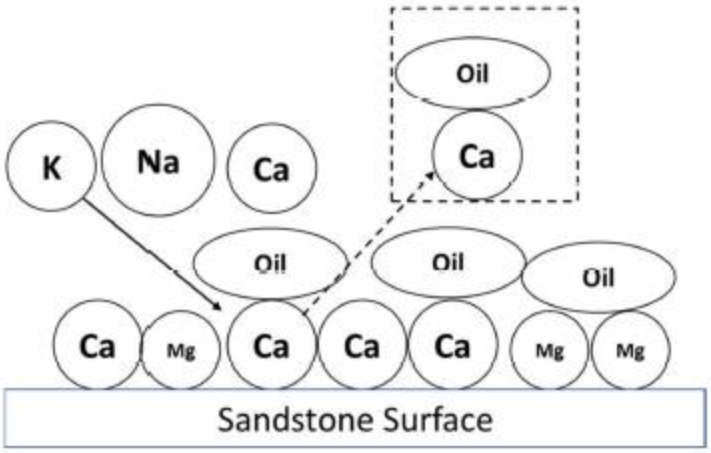

Figure 4.1: Low salinity mechanisms of multiple ions exchange (MIE) with potassium replacing calcium and liberation of oil in the form of calcium carboxylate complex, modified after [63]

4.1.2 Wettability Alteration

According to different researches, low salinity water injection changes the wettability. The low salinity waterflooding alters the reservoir from oil wet to water wet. It was obtained that low salinity waterflooding affect the oil wet and it has no effect on water wet sample. It was found that high concentrations of Ca^{2+} and Mg^{2+} ions in brine formation make the sample more oil wet [31].

The effect of reservoir rock mineralogy on the application of low salinity water was also reviewed. Low salinity water flooding changes the composition of rock and its properties. The experiments showed that the low salinity water dissolves anhydride cements in rock formation. As the result, low salinity water flooding increases the permeability of reservoir rock [31].

4.1.3 Fines Migration

Tang and Morrow expressed that low salinity water allows mixed-wet clay particles carrying oil to migrate from pore walls. The fines migration exposes pore surface to water wetting and as results of the oil displacement is increased [31].

4.1.4 Increased pH Effect and Reduced Interfacial Tension (IFT)

Low salinity water flooding leads to generation of hydroxyl ions to reactions with rock minerals. This causes the pH increase from 7 to 8 and even to 9. In fact, low salinity flooding like alkaline flooding reduces the interfacial tensions between oil and rock and increases pH. The IFT are the forces that hold oil into pore spaces. The increase of pH and reduction of interfacial tensions between reservoir rock and fluids alter the rock to more water wettability and hence improve oil recovery. In addition, Oil with its chemical structure, the increase of pH facilitates the in-situ surfactant generation by saponification reactions [25]. In this case, low salinity water flooding acts like surfactant flooding and cause oil dispersion into water. On the other hand, it is shown in figure 4.2 that with high salinity, the generated surfactant would precipitate and prevent the oil recovery.

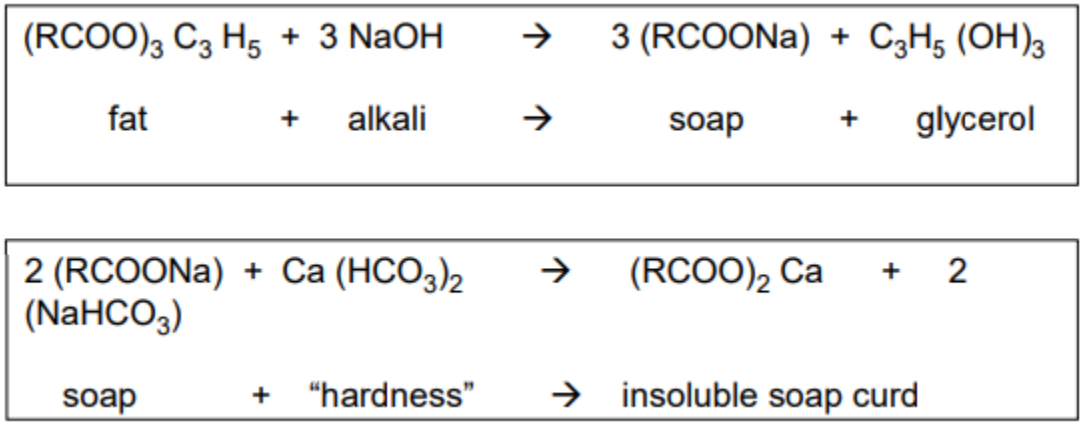

Figure 4.2: Saponification mechanism of an elevated pH for removal of harmful multivalent cations due to low salinity water injection [25].

Chapter 5

Simulations of Injection into a Sandstone Reservoir

This chapter presents a series of simulations that have been carried out for the purpose of comparing the efficiency and effectiveness of the classical immiscible waterflooding, immiscible gas flooding, and seawater WAG processes to low salinity water flooding in a sandstone reservoir. For the comparison purposes a number of operating and/or design parameters/variables have also been investigated. The following subsections presents the details of the numerical simulator, reservoir and fluid modelling, and modelling of each process including sea waterflooding, CO_2 gas flooding, conventional WAG modelling, LSWF and its related models such as geochemical reactions modelling and wettability alteration modelling and finally LSWAG modelling which are implemented in this work.

5.1 Reservoir Simulator

The CMG-GEM one of the reservoir simulators developed by Computer Modeling Group (CMG) was used to simulate different scenarios of waterflooding, gas injection, and WAG injection. CMG is a software company that provides dynamic reservoir and production technologies to the oil and gas industry. The main reservoir simulators developed by CMG include IMEX, GEM, and STARS. The IMEX stand for implicitly explicitly black oil simulator and it is used for conventional and unconventional reservoirs. The IMEX is used mainly for history matching and forecasting primary, secondary and enhanced oil recovery processes where fluid composition and reservoir temperature are not changed in the process. The GEM is a Generalized Equation of State Model reservoir simulator, i.e., it is an equation of state compositional simulator for multi-component reservoir fluids. The GEM is used to simulate all the processes involving chemical change in the reservoir but at a constant temperature. The STARS on the other hand stands for Steam, Thermal and

Advanced processes Reservoir Simulator, it is therefore a thermal compositional reservoir simulator (CMG, 2020).

The supporting tools of CMG simulators include WINPROP, builder, RESULTS, and others. The WINPROP software is used to model the reservoir fluids. The builder tool is the main modelling and simulation interface for all CMG simulators, it is used to enter and process the input data. The RESULTS tool is launched to produce three results output files; an output restart file (RST), an output simulation results file (SRF), and an output file. Figure 5.1 shows all CMG simulators and tools as released in mid-2020.

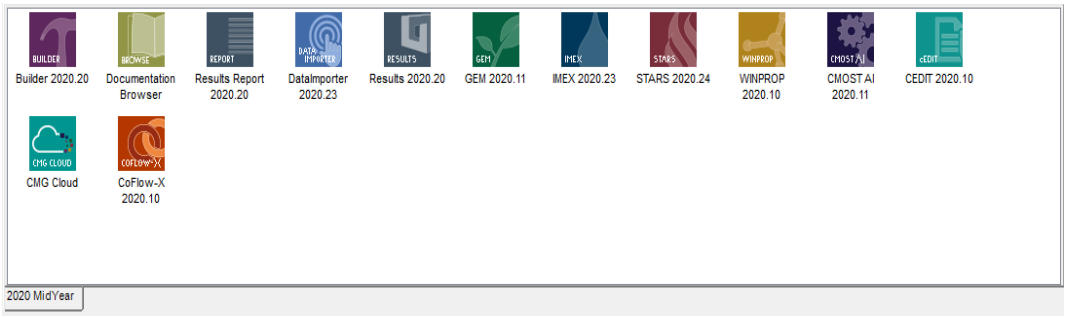

Figure 5.1 CMG Technologies Launcher 2020.11

5.2 Reservoir and Fluids Modelling

The actual data from the Cranfield oil field reservoir and some assumptions were considered to model a reservoir and formation fluids. As published in the Mississippi oil and gas board (MOGB) publication in 1966, Cranfield oil field was discovered in 1943, its reservoir has a geological dome with gas cap, oil ring and water at different depths [64]. Until 1966, the total oil and gas production was at least 37mmbbl and 672 bscf respectively, then the reservoir was subjected to secondary oil recovery by water drive in 2005, and with enhanced oil recovery by CO_2 flooding in 2008 at some part of the field [65]. A CO_2 sequestration test was also carried out in Cranfield pilot size of 9400 ft x 8400ft with net pay of 80ft [66,67]. In this study, the reservoir model in table 5.1 was built by using the data published on Cranfield oil field reservoir.

Table 5.1: Reservoir model

Parameter	Value
Reservoir size (ft)	1000 x 100x 80
Number of grid blocks	20x1x8
Reservoir depth (ft)	9950
Reservoir Temperature (°F)	257
Initial oil saturation	0.6
Initial Pressure (psi)	4650
Salinity, TDS (ppm)	150,000

By using GEM builder and Winprop, a reservoir model was built by inputting the data to be processed by CMG-GEM. The dimension of the reservoir model is 1000 ft x 100ft x 80ft. In fact, as shown in figure 5.2 the two-dimensional (2D) reservoir model was considered with single injection well and producer well pattern.

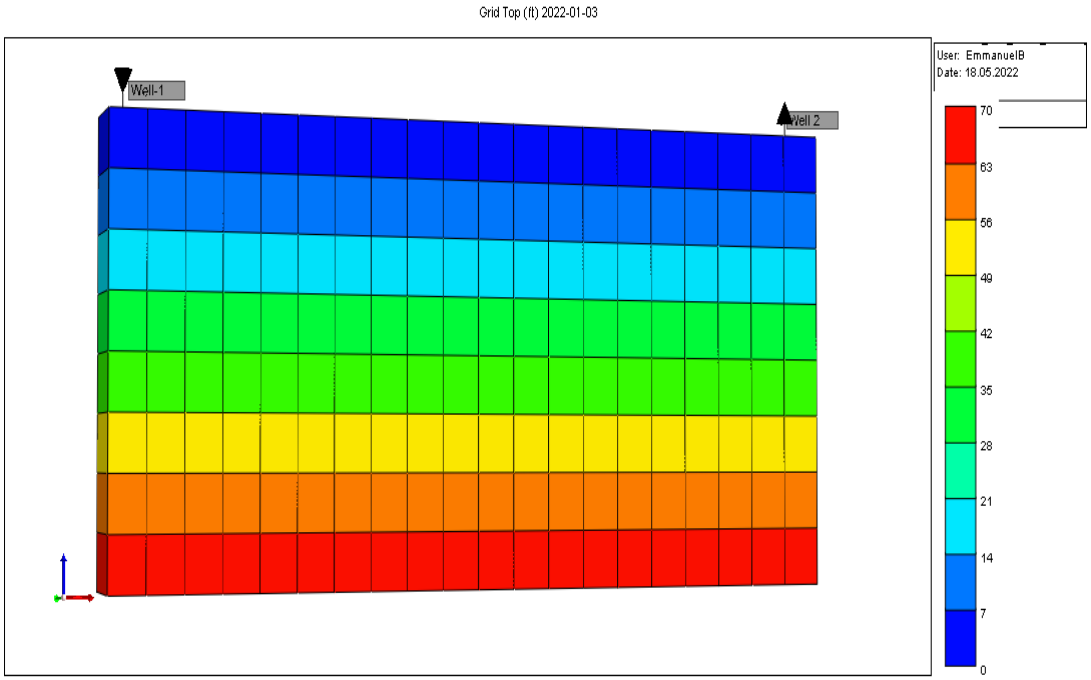

Figure 5.2: Reservoir model with single injector and producer wells

Reservoir fluids model was built by using the data of composition of reservoir fluids as also published in MOGB publication, 1966 [64]. The composition of reservoir fluid is shown in table 5.2. The two-phase envelope in figure 5.3 shows that the crude oil is in two phases (liquid and gas) at initial conditions of 4650psi and 257°F

Table 5.2:Reservoir Fluid Composition [64].

Component	Composition (Mol Fraction)
CO_2	0.0184
CH_4	0.5376
C_2H_6	0.0717
C_3H_8	0.0334
IC_4	0.0104
NC_4	0.0158
IC_5	0.0123
NC_5	0.0095
NC_6	0.0248
C_{7+}	0.2661

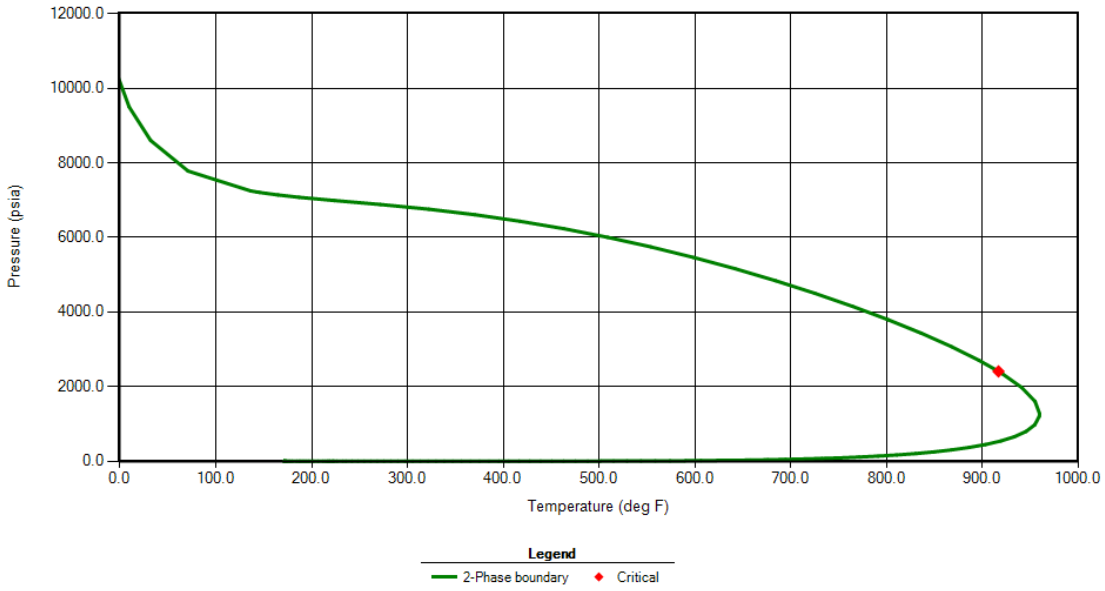

Figure 5.3: The two-phase envelope for crude oil initially in two phases using Peng-Robinson EOS

The initial liquid state of reservoir fluid was also created by assuming the composition of methane as 33.76% and that of C_{7+} as 46.661% instead of 53.76% and 26.661% respectively. The two-phase envelope with reservoir fluid (crude oil) initially in liquid phase is shown in figure 5.4 below.

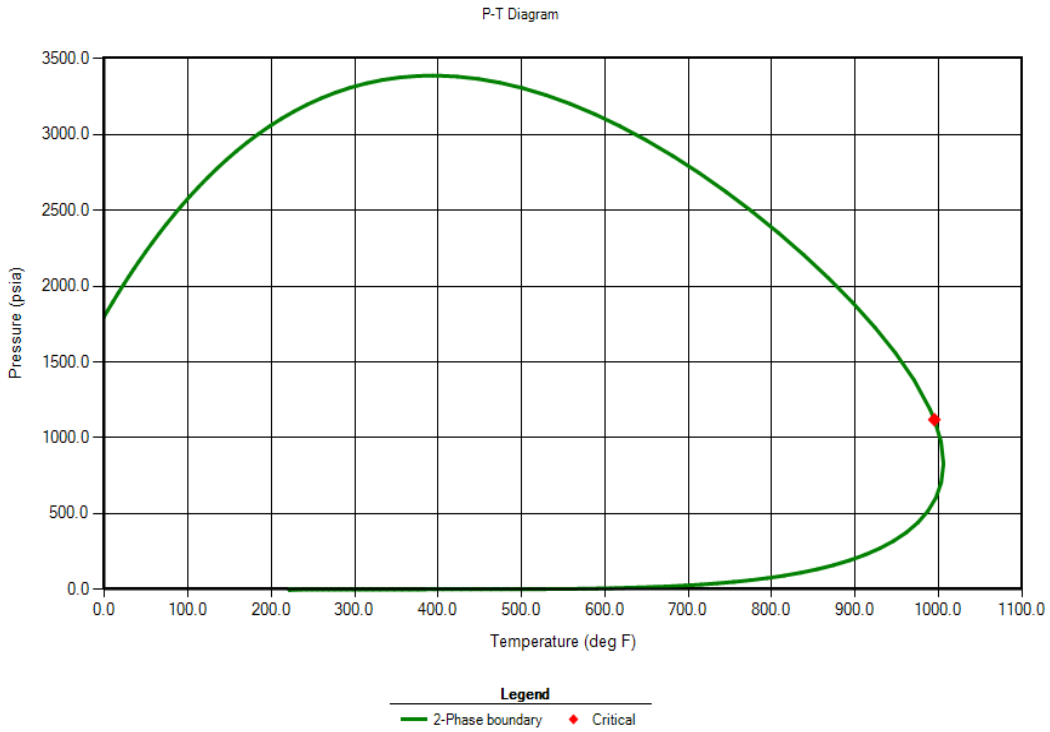

Figure 5.4: The two-phase envelope of crude oil initially in liquid phase using Peng-Robinson EOS

The relative permeability data in table 5.3 were assumed for high salinity waterflooding. Brooks-Corey correlation was applied to model and produce the oil-water and liquid-gas relative permeability curves as shown in figure 5.5 and 5.6 respectively.

Table 5.3: Rock and fluid parameters for relative permeability curves of the base case [66,67].

Rock-fluid parameters	Values
$\boldsymbol{k_{rwo}^0}$: $\boldsymbol{k_{rw}}$ at irreducible oil	0.5
$\boldsymbol{k_{row}^o}$: $\boldsymbol{k_{ro}}$ at connate water	0.65
$\boldsymbol{k_{rgw}^0 = k_{rgo}^0}$: $\boldsymbol{k_{rg}}$ at connate liquid	0.8
$\boldsymbol{S_{org}}$: endpoint saturation (residual oil for gas liquid table)	0.15
$\boldsymbol{S_{wrg} = S_{wro}}$: endpoint saturation (connate water)	4.0
$\boldsymbol{S_{orw}}$, endpoint saturation (residual oil for water oil table)	0.2
$\boldsymbol{S_{grw} = S_{gro}}$: endpoint saturation (connate gas)	0.075
$\boldsymbol{n_{1wo}}$: exponent for calculating $\boldsymbol{k_{rw}}$	4.0
$\boldsymbol{n_{1wg} = C_{1og}}$: exponent for calculating $\boldsymbol{k_{rog}}$	4.0
$\boldsymbol{n_{1ow}}$: exponent for calculating $\boldsymbol{k_{row}}$	2.38
$\boldsymbol{n_{1gw} = C_{1go}}$: exponent for calculating $\boldsymbol{k_{rg}}$	2.2

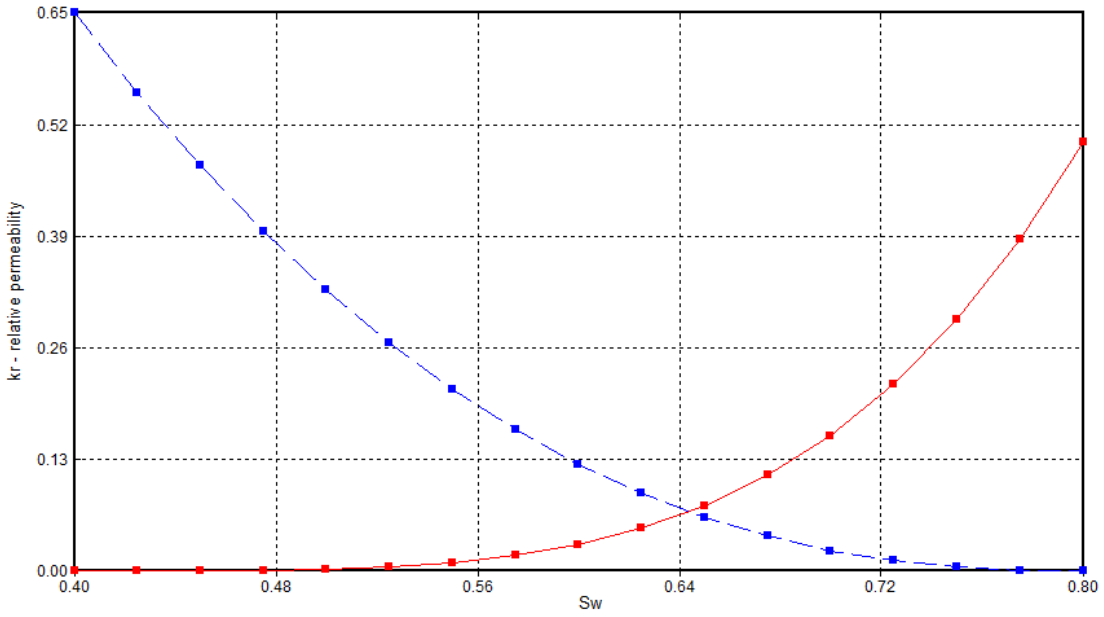

Figure 5.5: Relative permeability curves for water-oil system

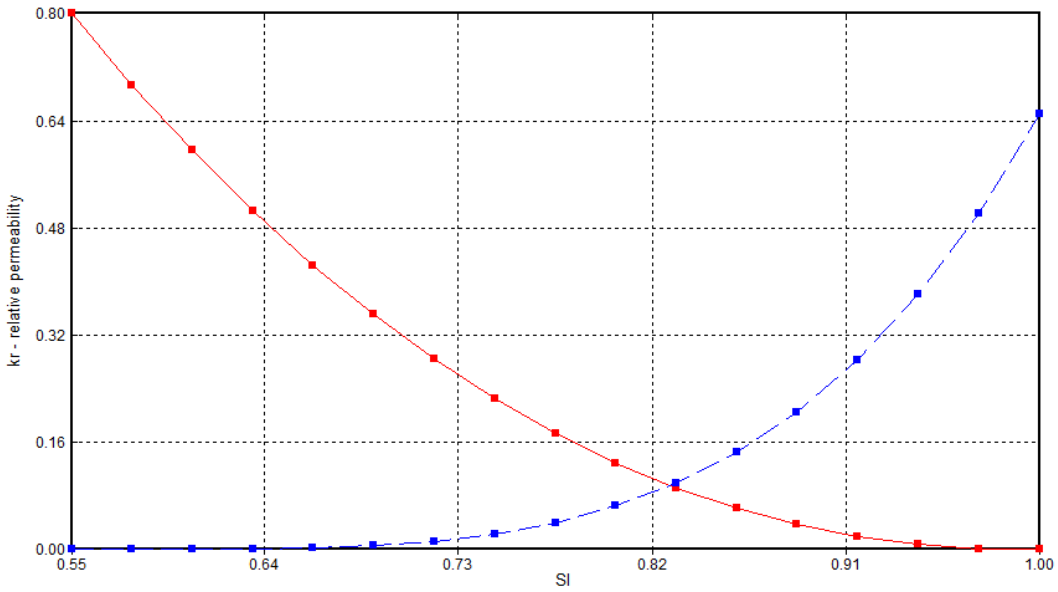

Figure 5.6: Relative permeability for gas-liquid system

5.3 Waterflooding Modelling

Waterflooding was modelled by using Process Wizard interface in builder that was provided for modelling the processes that involve geochemical changes. The maximum bottom hole pressure of 5500 psi and the maximum surface water rate (SWR) of 100bbl/day were set as the injector well constraints. The producer well constraints were the minimum bottom hole pressure of 4060 psi and the surface oil rate (STO) of 200bbl/day. The simulations were run for 6 years continuously.

Firstly, two waterflooding scenarios with oil initially in single phase and two phase were simulated and compared. Secondary, two simulations of waterflooding were run with injecting water through the whole zones and upper zones of reservoir. Thirdly, the two scenarios of waterflooding were simulated with different vertical to horizontal permeability ratios. Five simulation runs of waterflooding with different salinity of injected water were also performed.

The geochemical reactions and wettability alteration were modelled by using the data taken from different literatures. The Cranfield oil reservoir is a Lower Tuscaloosa Formation (LTF) that is locally referred as “D-E sand”. The reservoir of up to 80ft thick is made of

porous and permeable fluvial sandstones and conglomerates. It is light green due to presence of abundant chlorite [68]. The X-ray diffraction (XRD), and scanning electron microscopy (SEM) mineralogy analysis was carried out for the LTF core and brine samples. The results showed that the LTF is mainly composed of quartz (79.4%), chlorite (chamosite) (11.8%), kaolinite (3.1%), and illite (1.3%). There is also the presence of soluble and active minerals like calcite (1.1%), dolomite (0.4%), and albite (0.2%). On the other hand, the Tuscaloosa formation brine is a Na-Ca-Cl water type. The average salinity of the formation water is measured as 150000ppm (Total Dissolved Solids, TDS) and its pH is 5.7 [69, 70]. Table 5.4 shows the elemental composition of the formation brine used.

Table 5.4: Mineral composition of Lower Tuscaloosa Formation brine [70]

Ions	Concentration (ppm)
Ca^{2+}	11798
Mg^{2+}	1035
Na^{+}	43743
SO_4^{2-}	238
Cl^{-}	92223

The data for synthetic sea water were taken from experimental research by Teklu et al., 2017 [71]. Low salinity water was hence modelled by diluting sea water 2 times, 4 times and 5 times. The ions concentration of injected sea water and low salinity water are illustrated in table 5.5.

Table 5.5: Concentration of ions of brine and low salinity water used for simulation

Ions	Sea Water (ppm)	LoSal1 (ppm)	Losal2(ppm)	LoSal3(ppm)
Ca^{2+}	691.5	346	173	13.7
Mg^{2+}	3459.0	1729.5	864.9	69.2
Na^{+}	1286.1	6495.1	3247.6	259.8
SO_4^{2-}	4098.8	2049.8	1024.9	82.1
Cl^{-}	30110.6	15058.7	7529.7	602.1
TDS	51346	25679.1	12840.1	1026.9

5.3.1 Geochemical Reactions Modelling

The injection of water with different salinity content to formation brine affects the rock-brine-oil system interfaces equilibrium and causes chemical change in the reservoir. Software packages like WOLERY and PHREEQC were programed for this geochemistry. These databases were therefore used through Process Wizard interface provided in GEM simulator to model the aqueous, mineral, and ion exchange reactions. These chemical reactions are reversible according to ions concentration in injected water.

Aqueous Reactions:

$$CO_2 + H_2O \leftrightarrow H^+ + {HCO_3}^-$$

$$H^+ + OH^- \leftrightarrow H_2O$$

$$CaSO_4 \leftrightarrow Ca^{2+} + {SO_4}^{2-}$$

$$MgSO_4 \leftrightarrow Mg^{2+} + {SO_4}^{2-}$$

$$NaCl \leftrightarrow Na^+ + Cl^-$$

Mineral Reactions:

$$CaCO_3 + H^+ \leftrightarrow Ca^{2+} + {HCO_3}^-$$

$$CaMg(CO_3)_2 + 2H^+ \leftrightarrow Ca^{2+} + Mg^{2+} + {HCO_3}^-$$

Ion Exchange Reactions:

$$\frac{1}{2}Ca - X_2 + Na^+ \leftrightarrow \frac{1}{2}Ca^{2+} + Na - X$$

$$\frac{1}{2}Mg - X_2 + Na^+ \leftrightarrow \frac{1}{2}Mg^{2+} + Na - X$$

In these ion exchange reactions, Na^+ is taken up by the exchanger X on the clay surface. In case of low salinity water injection, multivalent ions like Ca^{2+} and Mg^{2+} dissolute with

carboxylate group from the clay surface and exchange with mono-valent ions like Na^+ and K^+.

For these ion exchange reactions on clay surface are measured by equivalent fractions $\zeta(Na-X)$, $\zeta(Ca-X_2)$, and $\zeta(Mg-X_2)$. Therefore, ion exchanges are modelled by selectivity coefficients which are operational variables [72-76]

$$K'_{Na/Ca} = \frac{\zeta(Na-X)[m(\mathrm{Ca}^{2+})]^{0.5}}{[\zeta(Ca-X_2)]^{0.5} m(Na^+)} \times \frac{[\gamma(Ca^{2+})]^{0.5}}{\gamma(Na^+)} \tag{5.1}$$

$$K'_{Na/Mg} = \frac{\zeta(Na-X)[m(Mg^{2+})]^{0.5}}{[\zeta(Mg-X_2)]^{0.5} m(Na^+)} \times \frac{[\gamma(Mg^{2+})]^{0.5}}{\gamma(Na^+)} \tag{5.2}$$

Where m is the ion concentration and γ is the activity coefficient. In GEM, a parameter Cation Exchange Capacity (CEC) was introduced to measure the number of ions adsorbed on clay surface by ion exchange. Hence, the total number of moles of $Na-X$, $Ca-X_2$, and $Mg-X_2$ are calculated for total grid bulk volume (V) as:

$$V\varphi(CEC) = VN_{Na-X} + 2VN_{Ca-X_2} + 2VN_{Mg-X_2} \tag{5.3}$$

The number of moles of $Na-X$, $Ca-X_2$, and $Mg-X_2$ per grid block are therefore calculated by dividing the bulk volume:

$$\varphi(CEC) = N_{Na-X} + 2N_{Ca-X_2} + 2N_{Mg-X_2} \tag{5.4}$$

Consequently, equivalent fractions:

$$\zeta(Na-X) = \frac{N_{Na-X}}{\varphi(CEC)} \tag{5.5}$$

$$\zeta(Ca - X_2) = \frac{N_{Ca-X_2}}{\varphi(CEC)} \tag{5.6}$$

$$\zeta(Mg - X_2) = \frac{N_{Mg-X_2}}{\varphi(CEC)} \tag{5.7}$$

5.3.2 Wettability Alteration Model

Wettability alteration due to LSWF is modelled by shifting relative permeability curves to water wetting conditions. Normally relative permeability data for simulation are measured through core analysis experiments. However, in this study, relative permeability data are assumed for formation brine and the rock is considered oil wet. Therefore, relative permeability curves for LSWF were obtained by reducing S_{or} from 0.2 to 0.14 but the curvature was not changed as shown in the figure 5.7.

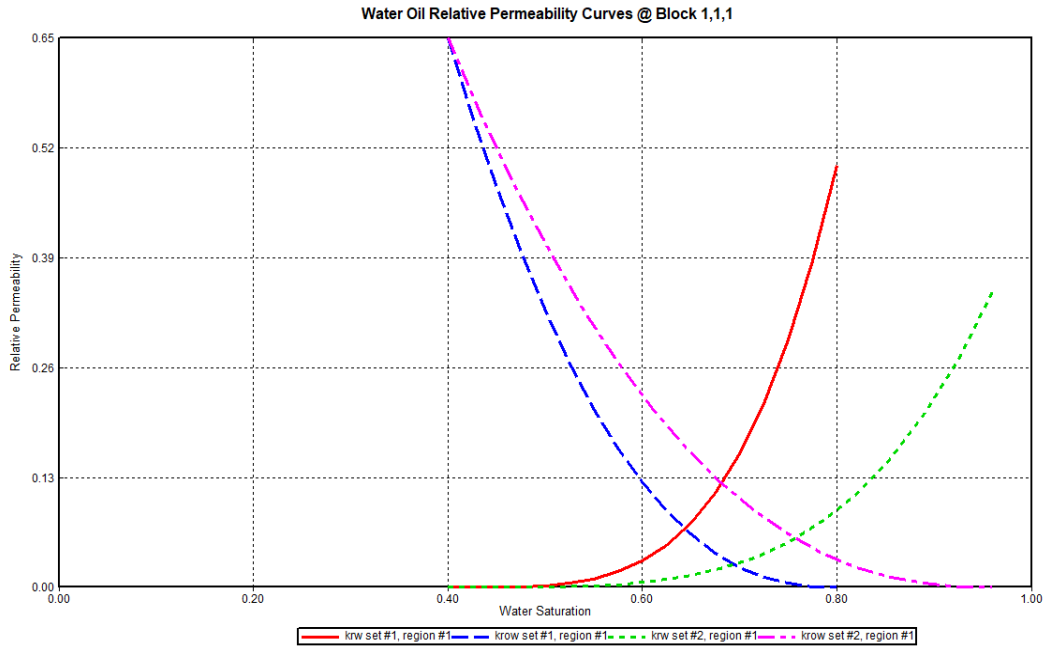

Figure 5.7: Wettability alteration modeling by shifting relative permeability curves from oil wet to water wet behavior

From these two sets of relative permeability curves, it is required to perform an interpolation for oil-water relative permeability for different salinity water injections.

Relative permeability changes because the adsorption, dissolution, or precipitation that take place during salty water injection. GEM provides three options of oil water relative permeability curves interpolations:

1. Ion exchange equivalent fraction of an ion on the rock surface ($\zeta(Na-X)$, $\zeta(Ca-X_2)$, and $\zeta(Mg-X_2)$)
2. Aqueous ion concentration (Ca^{2+}, SO_4^{2-} or Na^{+})
3. Porosity fraction change due to mineral deposition

The first option which was used in this study is the most preferred because it includes ion exchange as the main mechanism of low salinity waterflooding. It was assumed in this study that if the initial equivalent fraction $\zeta(Ca-X_2)$, is greater than 0.4, the relative permeability curves for high salinity is used and if it is less than 0.19, then those for low salinity are used. The initial equivalent fraction $\zeta(Ca-X_2)$, between 0.4 and 0.19, the interpolation is performed.

The interpolant for ion exchange is calculated as proposed in [77-79].

$$\omega = \frac{\zeta(Ca-X_2) - \zeta(Ca-X_2)^{HSW}}{\zeta(Ca-X_2)^{\,LSW} - \zeta(Ca-X_2)^{\,HSW}} \tag{5.8}$$

Relative permeability values can then be calculated by linear interpolation as shown in the following equations.

$$K_{rw} = \omega K_{rw}^{LSW} + (1-\omega)K_{rw}^{HSW} \tag{5.9}$$

$$K_{ro} = \omega K_{ro}^{LSW} + (1-\omega)K_{ro}^{HSW} \tag{5.10}$$

Where K_{rw} and K_{ro} are water and oil relative permeability for injected brine respectively, K_{rw}^{HSW} and K_{ro}^{HSW} are water and oil relative permeability for formation brine respectively, K_{rw}^{LSW} and K_{ro}^{LSW} are water and oil relative permeability of low salinity water respectively.

5.4 CO_2 Gas Flooding Modelling

The CO_2 gas that was already modelled in the components section was selected as the injected fluid. Like for waterflooding, CO_2 gas flooding was simulated for 6 years continuously. The injector well constraint set was the maximum bottom hole pressure of 5500 psi and surface gas rate of 100000 ft^3/day. The producer well constraints set were the minimum bottom hole pressure of 4060 psi and surface oil rate (STO) of 200bbl/day. The CO_2 gas injection were also simulated in different scenarios where initial phase of oil, injection depth, vertical to horizontal permeability ratios were taken into considerations.

5.5 Conventional WAG and LSWAG Modelling

The typical WAG injection was modelled by injecting both water and CO_2 gas at the same injector well. The injector well was open and shut-in alternately after each six month for 6 years. The figure 5.8 is the graphical illustration of the WAG model created. The maximum bottom hole pressure of 5500 psi and maximum surface water rate (SWR) of 100bbl/day were the constraints for water flooding. The maximum bottom hole pressure of 5500 psi and surface gas rate of 100000 ft^3/day for CO_2 gas injection were also used. The minimum bottom hole pressure of 4060 psi and maximum surface oil rate (STO) of 200bbl/day were applied as constraints for producer well. In addition, simulations with maximum surface oil rate of 500bbl/day were also carried out to evaluate the salinity effect in injected water. Different scenarios of waterflooding and CO_2 gas injection stated in above sections were replicated for simulation of WAG injection.

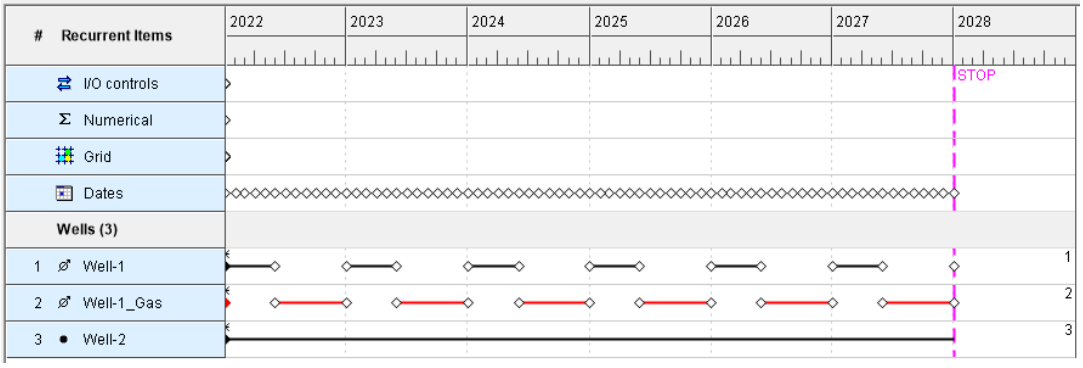

Figure 5.8: Graphic Model of WAG injection

Chapter 6

Results and Discussion

In this chapter, simulation results of different scenarios of water, gas, conventional WAG and LSWAG injections are discussed in detail. First, the effect of the stated physical factors (operating/design variables/factors) such as initial phase of oil, gravity, injection depth, and vertical permeability on oil recovery efficiency through sweep efficiency by classical waterflooding and CO_2 gas injections are investigated separately. Then after taking into account of the physical factors effect, the simulation results of conventional WAG injection are analyzed comparing with sea waterflooding and gas flooding operations. In addition, the effect of water salinity is evaluated via simulation results on waterflooding with different ion concentration in injected water which is called as low salinity waterflooding and sometimes as engineered waterflooding as it tries to identifies the salinity value to attain the highest displacement efficiency. Finally, the comparison of the performances of sea water and low salinity water in WAG injection is presented. The results are illustrated and displayed through plots of time series parameters and property profiles.

6.1 Effect of Physical Factors during waterflooding and Gas injection

6.1.1 Effect of initial phase of reservoir fluid

The effect of initial phase of crude oil was evaluated by simulation of waterflooding and CO_2 gas injection separately. Due to high mole fraction of methane compared to those of other components, oil was initially found to exist in two phases (liquid and gas) as shown in figure 5.3 in chapter 5. Mole fraction of oil components was therefore adjusted to create

initial single liquid phase by increasing mole fraction of C_{7+} to 0.4661 and decreasing mole fraction of methane to 0.3376.

Figures 6.1 and 6.2 show the oil recovery factors comparison with oil initially in single phase and two-phases during sea waterflooding and CO_2 gas injection respectively. The oil recovery factor difference may be attributed to the fact that gas oil ratio is high for oil initially in two phases during production. In fact, the high gas production with oil initially in two phases influenced the relative permeabilities and caused to obtain less oil recovery percentage.

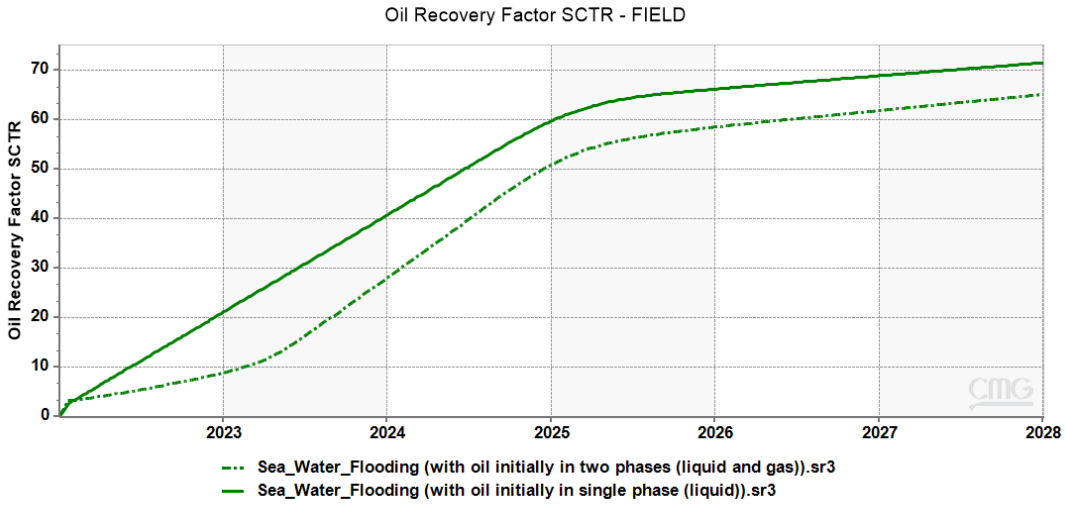

Figure 6.1. Effect of initial phase of crude oil on oil recovery factor during waterflooding

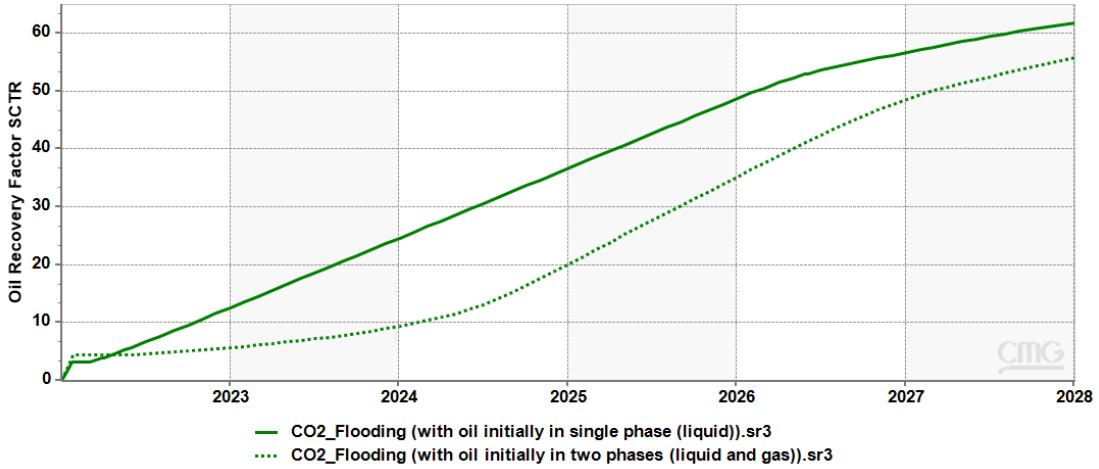

Figure 6.2. Effect of initial phase of crude oil on oil recovery factor during CO_2 injection

6.1.2 Gravity Effect

The figures 6.3 and 6.4 display the water and gas saturation on the course of continuing waterflooding and CO_2 gas injection respectively. During waterflooding, water displaces oil from side-bottom of the reservoir from injector to the producer well. In fact, due to gravity effect, water flow down at the lower zones of the reservoir because it is denser than oil. The pressure difference also causes water saturation to increase going forward from the injection well to the producing well. In the case of continued CO_2 gas injection, gravity effect also causes the gas to move at the upper zones of the reservoir from injection well to the producer well.

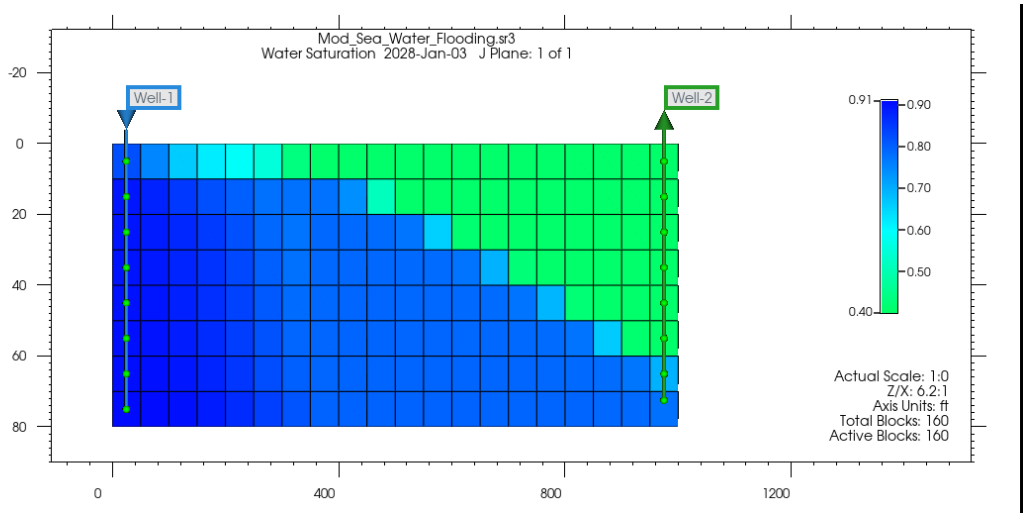

Figure 6.3: Water saturation during waterflooding

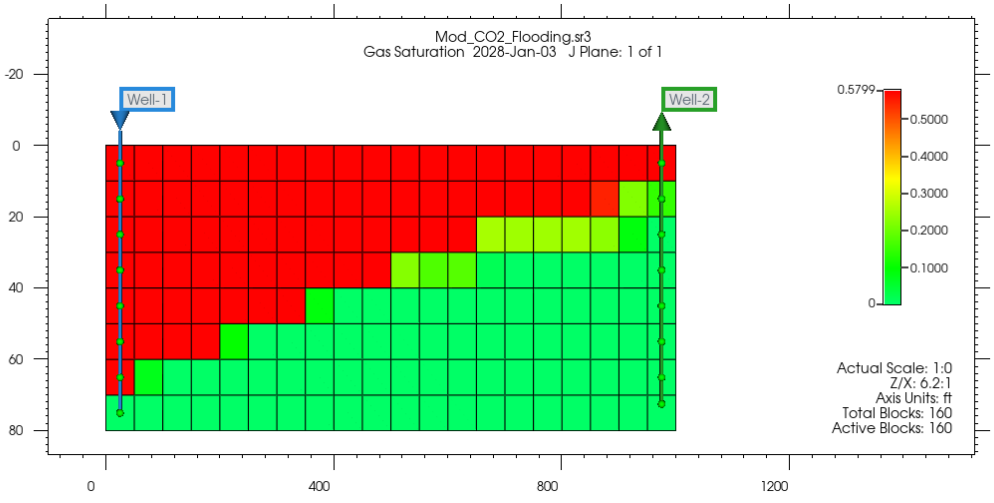

Figure 6.4 : Gas saturation during CO_2 gas flooding

6.1.3 Injection Depth Effect

To control the water and gas early breakthrough from lower and upper zones of reservoir respectively, and improve the sweep efficiencies, the adjustment on the injection depth was applied by perforating upper zones for waterflooding and lower zones for gas injection. It was deemed to be of importance to inject water from upper zones to increase the volumetric sweep efficiency by retarding the water breakthrough while favoring the horizontal front displacement of water in upper zones of the reservoir. The graph 6.5 is the comparison between front displacement of water when injected from upper zones and when injected from all zones.

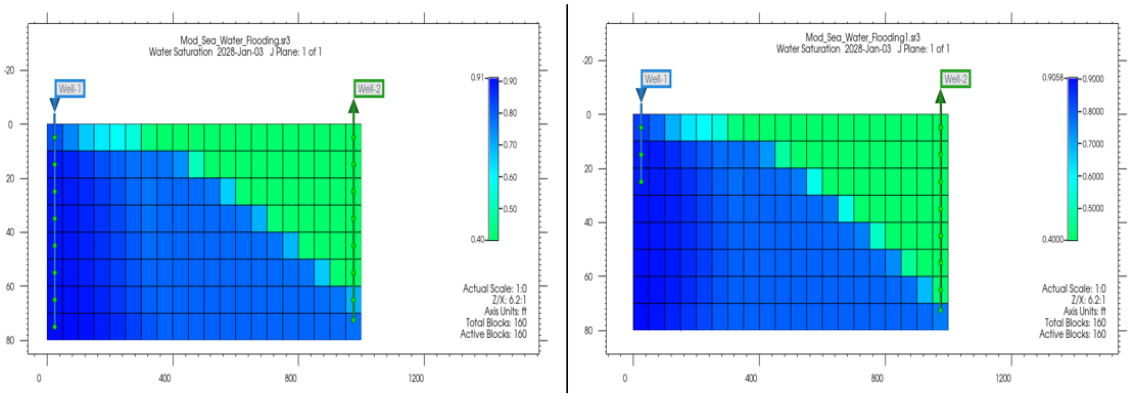

(a) (b)

Figure 6.5: Water saturation profile during waterflooding from (a) all zones, (b) upper zones

On the other hand gas was injected from lower zones of the reservoir to allow gas to contact with oil at the lower and middle zones of the reservoir and eventually prevent early gas breakthrough at the upper zones of the reservoir. The graph 6.6 below shows the positive impact of injecting gas through perforations in the lower zones; there is an increased region contacted with gas and hence increased the oil sweep efficiency.

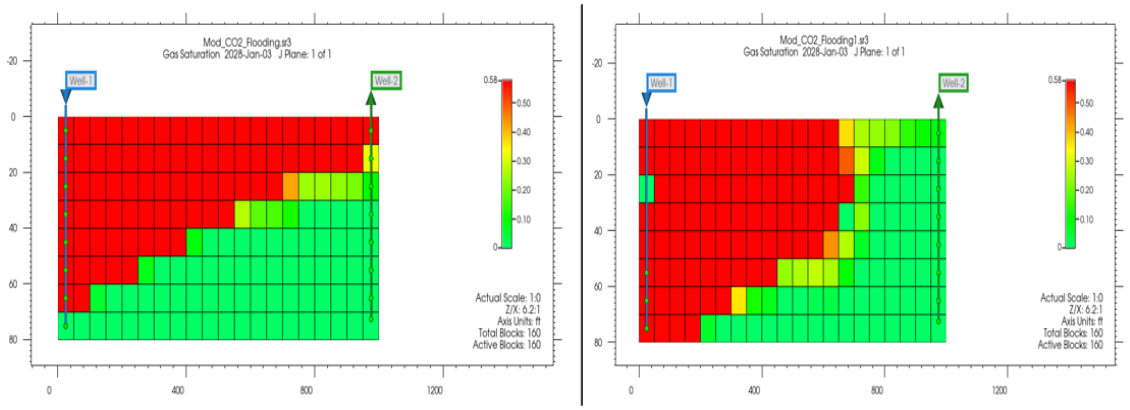

(a) (b)

Figure 6.6: Gas saturation profile during CO_2 gas injection from (a) all zones, (b) lower zones

6.1.4 Effect of Vertical to Horizontal Permeability Ratio

Vertical permeability controls vertical flow of reservoir fluids as well as the injected fluid. The ratio of vertical permeability to horizontal permeability was therefore also evaluated

through simulation results. The simulation results of waterflooding and CO_2 gas injection with constant horizontal permeability (50md) and different vertical permeability (50 md and 10 md) are reported through water and gas saturation profiles. From figure 6.7, with low vertical permeability there is an increase of volumetric sweep efficiency of water displacing oil during waterflooding. In fact, volumetric sweep efficiency is increased with low vertical to horizontal permeability ratio because water injected from the upper zones can relatively flow horizontally. In figure 6.8, lowering the vertical permeability increases the frontal displacement of oil by gas injection in lower and middle zones of the reservoir while also controlling the early gas break through from the upper zones of the reservoir.

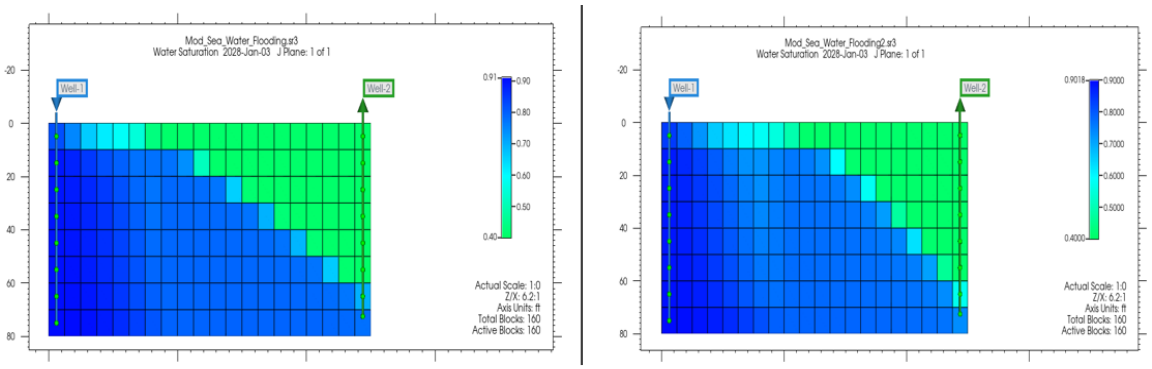

(a) (b)

Figure 6.7: Water saturation during waterflooding with vertical permeability of (a) 50 md and (b) 10 md

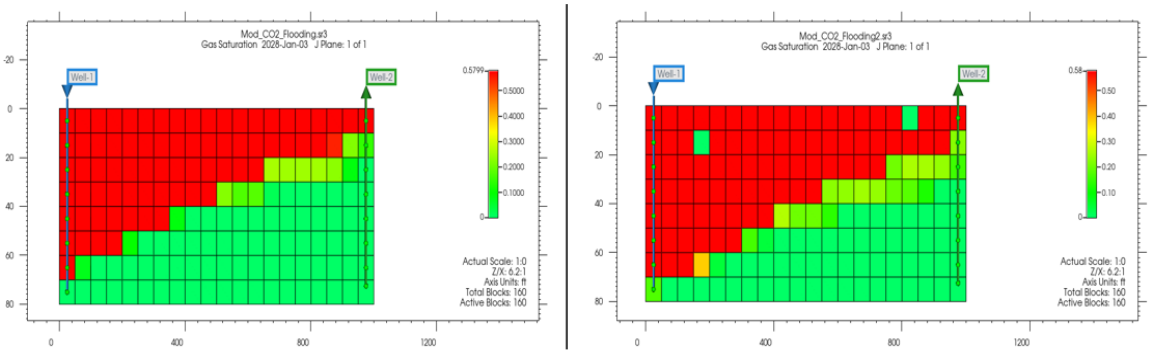

(a) (b)

Figure 6.8 Gas saturation during CO_2 gas injection with vertical permeability of (a) 50 md and (b)10 md

6.2 Conventional WAG injection

In both cases of separate waterflooding and gas injection, there are water and gas breakthrough from lower and upper zones of the reservoir respectively while there remains a sizable region un-swept. It is therefore for this reason that the combination of water and gas was proposed and applied to produce the attic oil that remains in the case of only waterflooding and oil in lower zones in the case of only gas injection. The initial single phase of oil was considered for WAG injection as it produced higher oil recovery percentage. The gravity effect during WAG injection is the most obvious because of density differences between water, oil, and gas. The waterflooding from the upper zones of the reservoir while gas is injected from the lower zones also prevented the early breakthrough of injected fluids and increased sweep efficiency in the process. The vertical permeability was also adjusted to further retarding vertical flow of injected fluids and as a result oil was displaced in the middle zones of the reservoir. It is shown in figure 6.9 that the combination of water and gas is more efficient for increasing the sweep area.

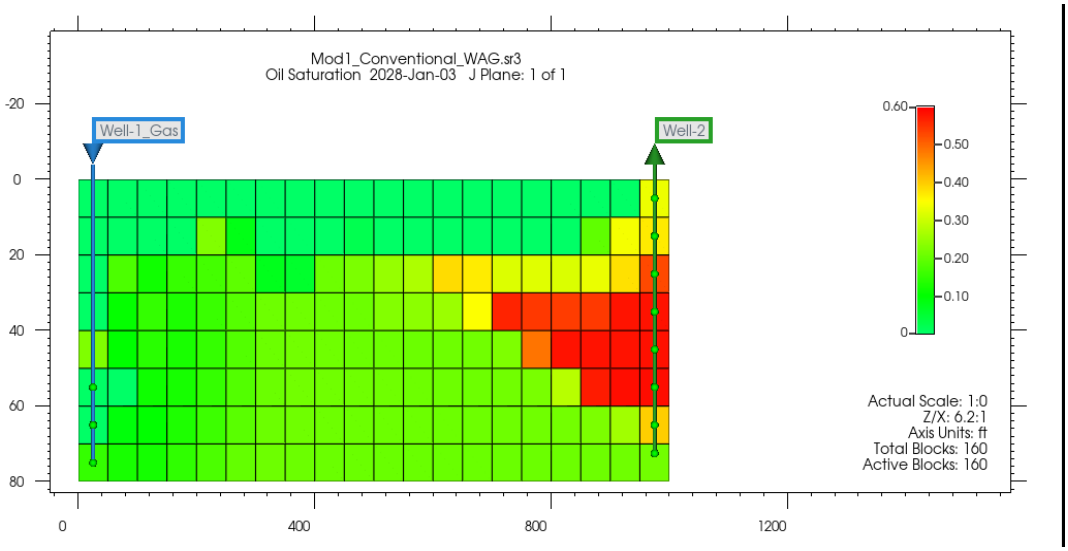

Figure.6.9: Frontal displacement of oil during WAG injection

The water and gas saturation curves indicate clearly the gravity effect in controlling fluids displacement in the reservoir. In figure 6.10, gas saturation is increasing with time in the upper zones. In figure 6.11, water saturation is increasing with time especially in the lower zones.

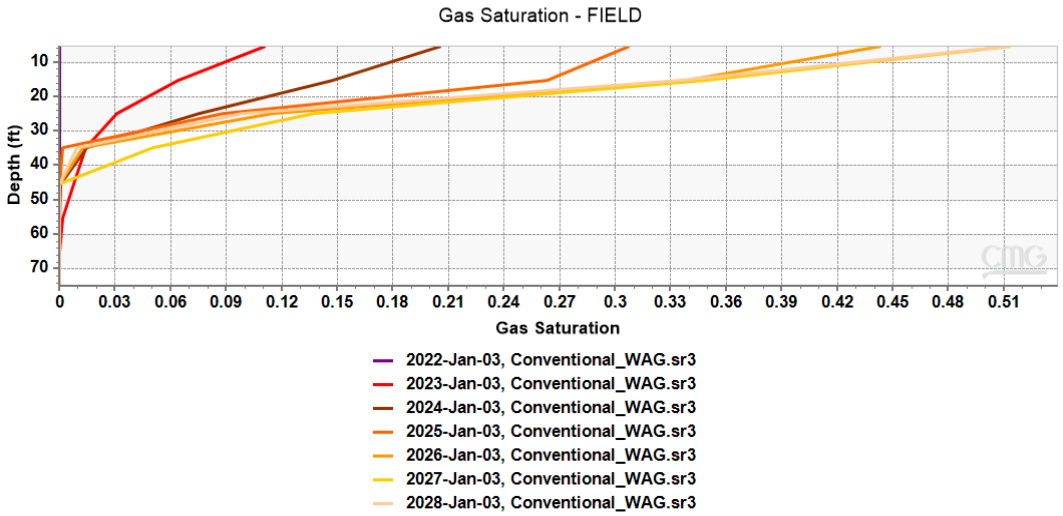

Figure 6.10: Gas saturation profiles during WAG injection with time

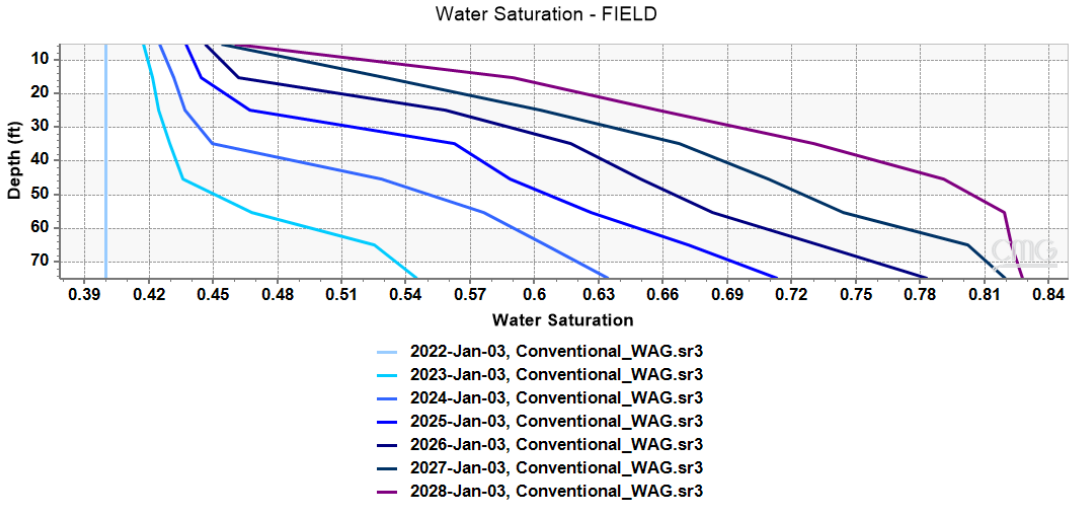

Figure.6.11: Water saturation profiles during WAG injection with time

The shape oil saturation curves in figure 6.12 indicates that oil is more swept both in the upper and lower zones during WAG injection because neither gas or water is a piston like displacer of oil. In fact, the residual oil saturation decreases more during WAG injection to individual waterflooding or gas injection.

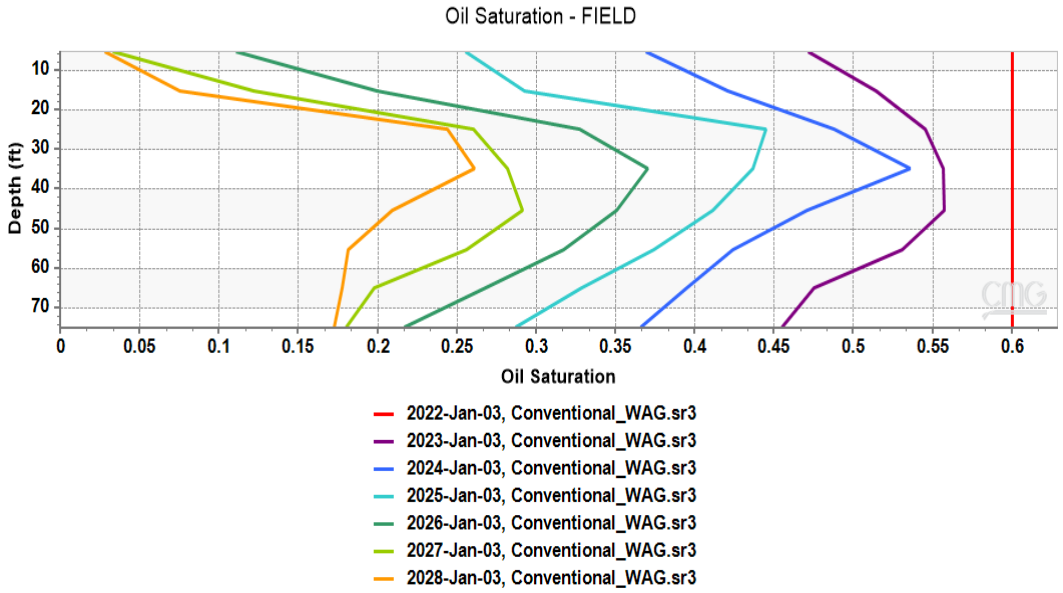

Figure 6.12: Oil saturation profiles during WAG injection with time

The figure 6.13 shows the comparison of oil recovery factor for waterflooding, CO_2 gas injection and conventional WAG injection. The WAG injection increased oil recovery factor by about 10% from individual waterflooding and CO_2 gas injection. This result is explained by the fact that the combination of water and gas improved both macroscopic oil sweep and oil displacement efficiencies. In fact, water displace oil from side-bottom and hence improve the macroscopic oil sweep efficiency. On the other hand, the CO_2 gas increases oil mobility by reducing its viscosity and hence it improves the oil displacement efficiency.

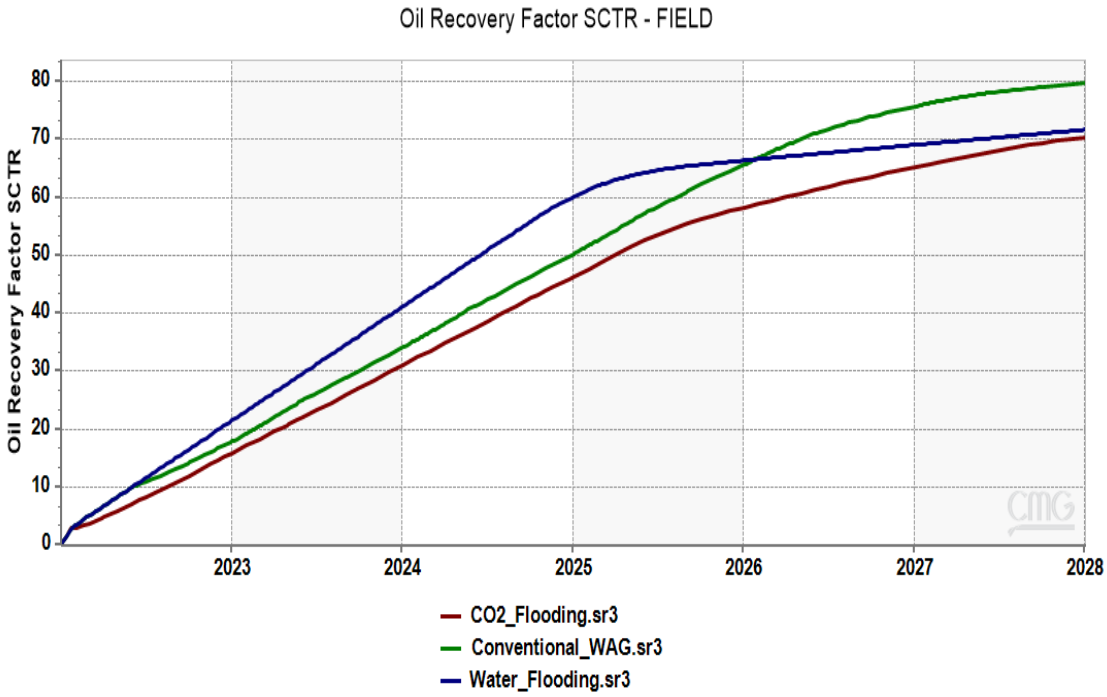

Figure.6.13: Advantage of WAG injection over continued waterflooding and CO_2 gas injection

6.3 Low Salinity Waterflooding (LSWF)

The effect of salinity of injected water was evaluated through the results from a series of waterflooding by tunning its salinity. From the simulation results of different waterflooding scenarios as shown in figure 6.14, there is an increase of about 8% of oil recovery factor from simulation with sea water of 51346ppm to simulation with low salinity of 1026.9ppm. In addition, the results show that low salinity and deionized waterflooding provide the same oil recovery factor. It means that the necessary dissolution of clay minerals for optimum oil recovery is achieved with low salinity of 1026.9ppm.

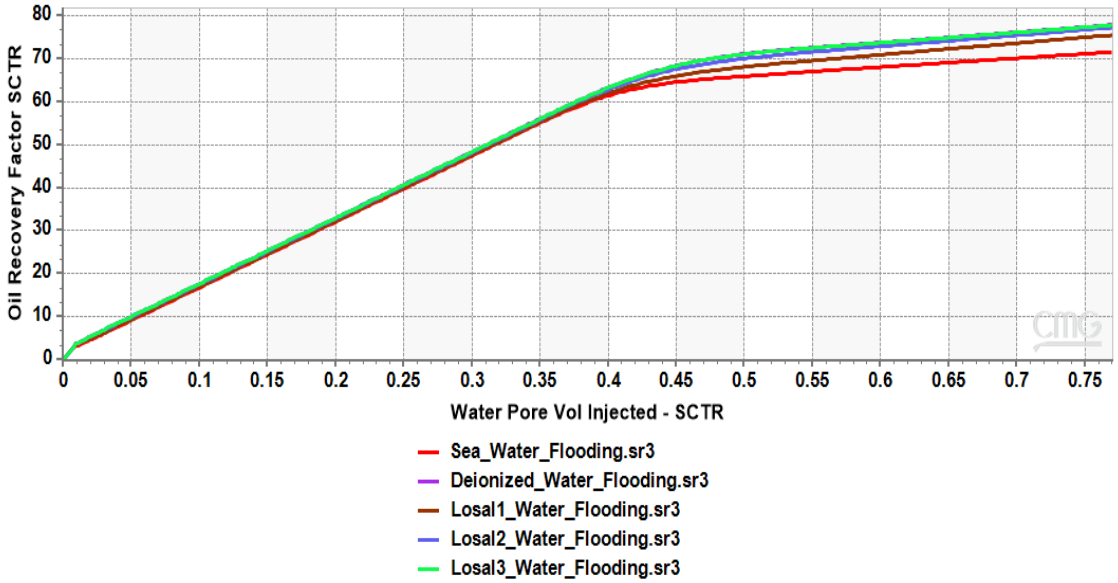

Figure 6.14: Oil recovery factor from different simulation scenarios of low salinity waterflooding

This increase of oil recovery factor is attributed to the multi-ion exchange and mineral reactions that take place when low salinity water is injected into the rock containing clay minerals. As a result, there is wettability alternation from oil wet to preferred water wet when low salinity water is injected. In fact, the multi-ion exchange and wettability alteration are the two main mechanisms that oil is freed from pores and displaced by water in the case of LSWF. In addition, low salinity waterflooding increases oil recovery by breaking the rock-brine-oil interfacial tension. There is dissolution of rock minerals like calcite and dolomite which respectively release Ca^{2+} and Mg^{2+} with carboxyl complex in a multi-ion exchange during low salinity waterflooding.

On contrary, high salinity waterflooding results no wettability change instead there is more of ion adsorption. The adsorption of divalent ions like Ca^{2+} on clay surface creates a strong interfacial tension between oil and clay surface.

6.3.1 Ion Exchange During LSWF

The initial chemical equilibrium of crude oil-brine-rock (CORB) system is destabilized when injected water has different salinity and composition to the connate water. Therefore,

the pre-adsorbed ions like Ca^{2+} and Mg^{2+} on mineral surface are dissolved and exchanged with monovalent ions like Na^{+} and H^{+}. As explained in chapter 4, the ion exchange alters the wettability to water wet as the oil is released with divalent ions. The amount of ion exchanged on clay surface is indicated by ion equivalent fraction. In the figures below, the graphs show that ion equivalent exchange of Ca^{2+} and Mg^{2+} increased on the course of water flooding with low salinities to the connate water. In fact, the graphs confirm the fact that Ca^{2+} and Mg^{2+} ions are released from rock surface and exchanged with monovalent ions from injected water. In fact, Figures 6.15 and 6.16 indicate that the effluent concentrations of Ca^{2+} and Mg^{2+} ions increase with time respectively. In contrast, the ion equivalent exchange of Na^{+} and H^{+} decreased. Figure 6.17 indicates the decrease of effluent concentration of Na^{+} due to ion exchange that take place at the clay surface. In figure 6.18, the adsorption of H^{+} caused the reduction of effluent concentration of H^{+} and as a result the pH increased.

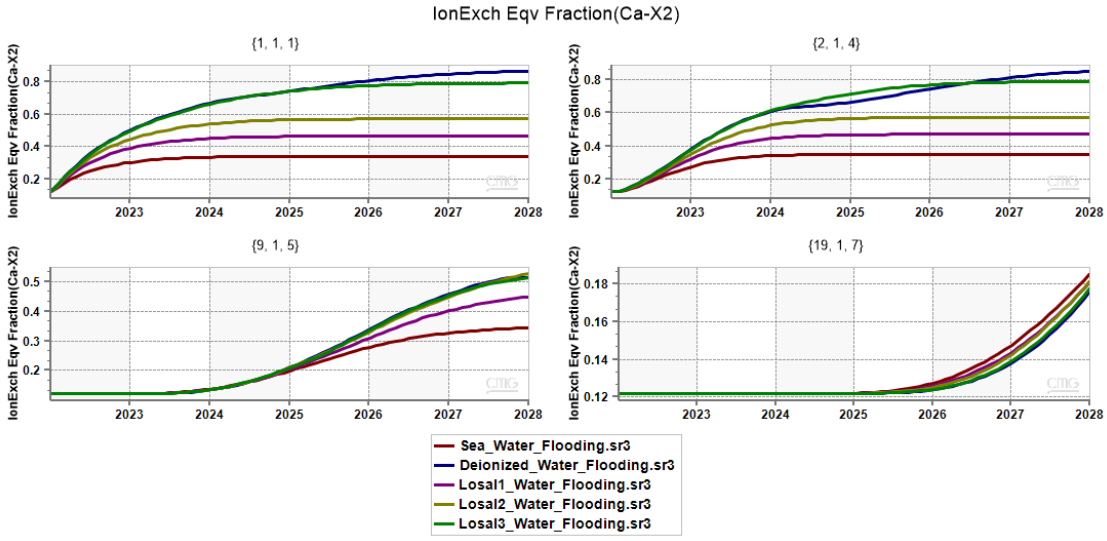

Figure.6.15: Ion exchange equivalent fraction of $\boldsymbol{Ca^{2+}}$in different blocks

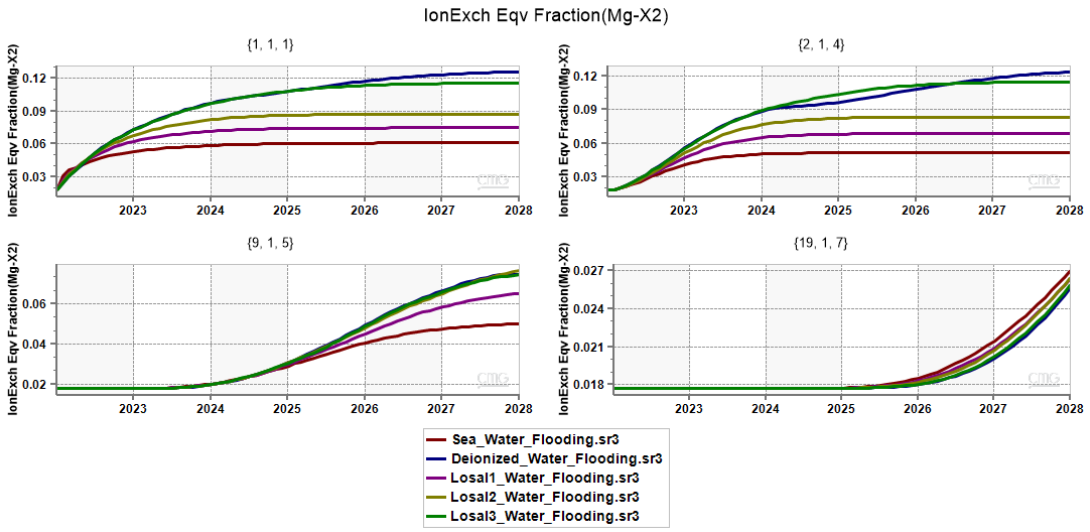

Figure 6.16: Ion exchange equivalent fraction of $\boldsymbol{Mg^{2+}}$ in different blocks

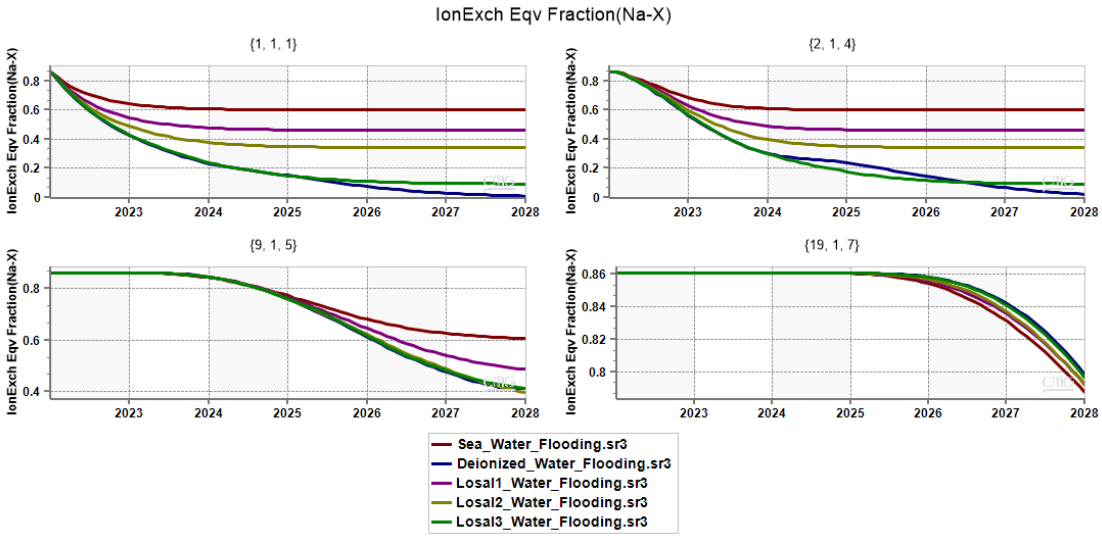

Figure.6.17: Ion exchange equivalent fraction of $\boldsymbol{Na^{+}}$ in different blocks

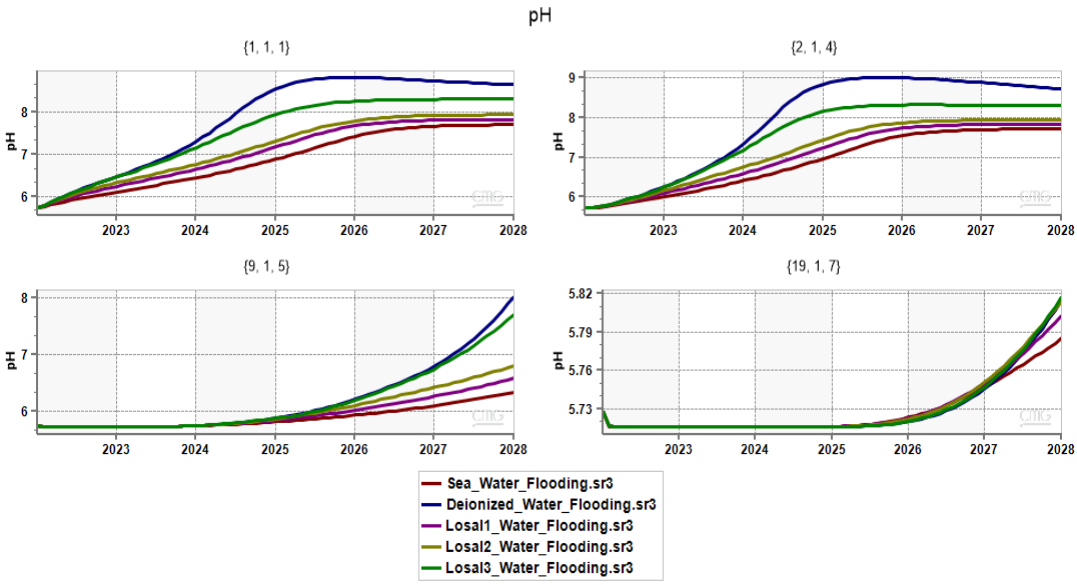

Figure 6.18: The change in pH during low salinity waterflooding

6.4 Conventional WAG vs LSWAG

In this section, the combination of waterflooding and gas injection while focusing on the effect of salinity content in injected water is evaluated and the performances of conventional WAG and LSWAG injections are compared. The simulations results of conventional and LSWAG injections showed that the combination of waterflooding from upper zones and CO_2 gas injection from lower zones of the reservoir, and reducing vertical to horizontal permeability ratio improves significantly the total sweep efficiency. The contribution of CO_2 gas injection in improving the oil displacement was observed for both conventional WAG and LSWAG injections. The waterflooding contributed on improving the volumetric sweep efficiency in both cases but low salinity content in LSWAG injection particularly increases microscopic sweep efficiency due to multi-ion exchange that release oil from pores in the form of calcium/magnesium carboxylate complex. In other words, the increase of oil recovery factor by LSWAG injection is mainly attributed to multi-ion exchange and wettability alteration processes that take place during low salinity waterflooding. From the graphs in figure 6.19, LSWAG injection produced oil recovery factor of up to 6% more than conventional WAG after 6 years running.

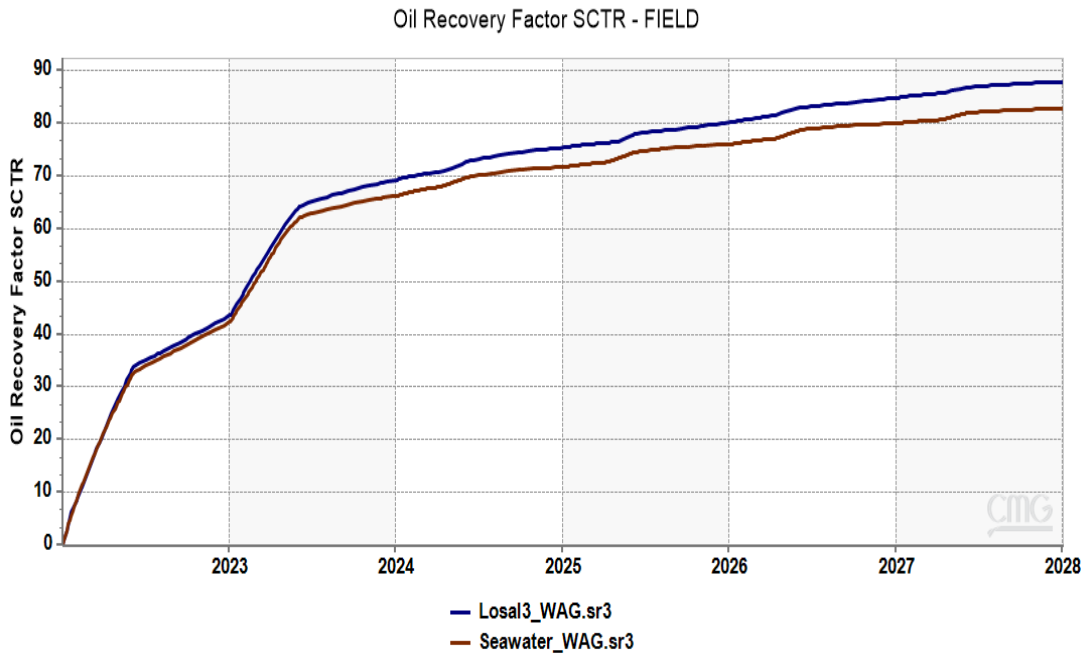

Figure 6.19: Comparisons of oil recovery factor from conventional WAG and LSWAG with maximum oil flow rate of 500bbl/day

The simulation results of sea water WAG and LSWAG with setting the maximum oil flow rate of 500bbl/day showed a significant effect of low salinity water. As shown in figure 6.19 above, high oil flow rate in early years leads to sudden increase of oil recovery factor and gradual decrease of oil flow rate leads to gradual increase of oil recovery factor. The graphs show that as the breakthrough of injected fluids takes place the effect of salinity content is more significant. In fact, low salinity water effect is effective and efficient after there is minimal influence of strong physical factors such as gravity.

Chapter 7

Conclusion

In this study, different ideas and aspects of conventional WAG and LSWAG injections were reviewed. The effect of initial phase of crude oil, gravity, injection depth, and vertical permeability were considered and adjusted to minimize water and gas breakthrough while improving oil recovery factor during WAG injection. The application of conventional WAG injection and LSWF individually was a success in improving oil recovery. However, this study showed that the combination or hybrid of the two methods improve further oil recovery for a typical sandstone reservoir. The effect of LSWF on releasing and displacing oil from pore surfaces is described through different mechanisms. The mechanisms of LSWF include fine migration, increase of pH and reduction of rock-oil IFT, multi-ion exchange, and wettability alternation.

A series of simulation runs of different scenarios of waterflooding, CO_2 gas flooding, and WAG injection were performed by using CMG-GEM simulator. After the results were discussed and analyzed; the flowing conclusions were drawn:

1. The conventional WAG injection is the combination mechanism of waterflooding and gas injection that was invented to improve individual method of oil recovery. During WAG process, the oil sweep efficiency increases, and as a result the oil recovery factor also increases. From the simulation results in this study, there is an increase of about 10% of oil recovery factor by conventional WAG injection to continued classical waterflooding and CO_2 gas injection.
2. The effect of initial phase of reservoir fluid was analyzed and the results showed that the oil recovery factor is higher with oil initially in single phase (liquid) than in two phases (liquid-gas). In fact, comparing with oil initially in single liquid phase, the oil initially in two phases (liquid-gas) produces higher gas to oil ratio (GOR) and as a result, the oil recovery factor is lower.

3. The simulation results also showed that waterflooding from upper zones and gas injection from lower zones of reservoir increase oil sweep efficiency by improving front displacement in the middle zones and hence prevent early breakthrough of injected fluids.
4. The lower vertical to horizontal permeability ratio is also favorable for both waterflooding and CO_2 gas injection. The volumetric sweep efficiency is increased with low vertical to horizontal permeability ratio as horizontal displacment is improved in the middle zones of the reservoir. Low vertical permeability also delays the breakthrough of injected fluids.
5. Water salinity effect was observed while comparing oil recovery factors from simulations of conventional WAG and LSWAG. There is up to about 6% increase of oil recovery factor from conventional WAG with sea water of 51,346 ppm of salinity to LSWAG with diluted sea water to 1027ppm of salinity.
6. Multi- ion exchange reactions between divalent ions like Ca^{2+} and Mg^{2+} adsorbed on clay surface and monovalent ions like Na^{+} and H^{+} are the cause of wettability alteration from oil wet or mixed wet to water wet. Initially, pre-adsorbed divalent ions on clay surface bridge carboxylate group to the negative ions of clay surface and oil wet system is created in the reservoir. Therefore, wettability alteration is considered as the main mechanism by which oil recovery is improved with low salinity waterflooding.

Chapter 8

Recommendations

This study was performed by using the Cranfield oil field data as published in different research papers; however, some assumptions were made in order to focus on the main purpose of this project. It is therefore recommended that actual data from field project on LSWF be used in future work. It should be noted that the assumptions on the relative permeability data for both high salinity water and low salinity water injections were made to carry out the GEM simulations. This leaves a gap to bridge the actual field projects results with simulation results. It is therefore very interesting to carry out a history matching of field results and GEM simulation results to ensure the successfulness and certainty.

In addition, the optimization analysis is recommended in the future work. An advanced research study on the comparison of conventional and LSWAG injections is required focusing on evaluation of technical, environmental, and economic conditions for optimum oil recovery factor. The CMOST-AI software that is an intelligent optimization and analysis included in CMG package is recommended for the optimization and sensitivity analysis as wells as history matching.

References

[1] Bonder P. EOR-the time is now: Its contribution of world energy supply. Society of Petroleum Engineers. 2010;

[2] Muggeridge A, Cockin A, Webb K, Frampton H, Collins I, Moulds T, et al. Recovery rates, enhanced oil recovery and technological limits. Vol. 372, Philosophical Transactions of the Royal Society A: Mathematical, Physical and Engineering Sciences. Royal Society; 2014.

[3] Zitha P, Felder R, Zornes D, Brown K, Mohanty K. Increasing Hydrocarbon Recovery Factors. Society of Petroleum Engineers. 2011;

[4] Lake WL, Walsh PM. Enhanced oil recovery (EOR). Department of Petroleum and Geosystems Engineering, University of Texas at Austin. 2008;

[5] Hustad OS, Holt T. Gravity Stable Displacement of Oil by Hydrocarbon Gas After Waterflooding. In: Eighth Symposium on Enhanced Oil Recovery. Tulsa: Society of Petroleum Engineers (SPE); 1992.

[6] Touray ST. EFFECT OF WATER ALTERNATING GAS INJECTION ON ULTIMATE OIL RECOVERY. In 2013.

[7] Knappskog OA. Evaluation of WAG injection at Ekofisk [Internet]. University of Stavanger, Norway. 2012 [cited 2022 Jun 12]. Available from: https://uis.brage.unit.no/uis-xmlui/handle/11250/183466

[8] Surguchev LM, Korbol R, Haugen S, Krakstad OS. Screening of WAG Injection Strategies for Heterogeneous Reservoirs. In: European Petroleum Conference. Cannes, France: Society of Petroleum Engineers; 1992. p. 565–76.

[9] Christensen JR, Stenby EH, Skauge A. Review of WAG Field Experience. Proceedings of the SPE International Petroleum Conference & Exhibition of Mexico. 1998 Mar 3;357–70.

[10] U.S Department of Energy. 2013.

[11] Awan AR, Teigland R, Kleppe J. A Survey of North Sea Enhanced-Oil-Recovery Projects Initiated During the Years 1975 to 2005. SPE Reservoir Evaluation & Engineering [Internet]. 2008 Jun 19 [cited 2022 Jun 9];11(03):497–512. Available

from: https://onepetro.org/REE/article/11/03/497/197431/A-Survey-of-North-Sea-Enhanced-Oil-Recovery

[12] Panda MN, Ambrose JG, Beuhler GG, McGuire PL. Optimized EOR design for the Eileen West End Area, greater Prudhoe Bay. SPE Reservoir Evaluation and Engineering. 2009;12(1):25–32.

[13] Kulkarni MM, Rao DN. Experimental Investigation of Various Methods of Tertiary Gas Injection. SPE Annual Technical Conference Proceedings. 2004 Sep 26;

[14] Liao CL, Liao XW, Zhao XL, Lu N, Ding HN, Wang H, et al. Study on enhanced oil recovery technology in low permeability heterogeneous reservoir by water-alternate-gas of CO2 flooding. Society of Petroleum Engineers - SPE Asia Pacific Oil and Gas Conference and Exhibition, APOGCE 2013: Maximising the Mature, Elevating the Young. 2013;2:1201–12.

[15] Pariani GJ, McColloch KA, Warden SL, Edens DR. An Approach To Optimize Economics in a West Texas CO2 Flood. Journal of Petroleum Technology [Internet]. 1992 Sep 1 [cited 2022 Jun 9];44(09):984–1025. Available from: https://onepetro.org/JPT/article/44/09/984/70669/An-Approach-To-Optimize-Economics-in-a-West-Texas

[16] Néstor L. Management of Water Alternating Gas (WAG) Injection Projects. In: SPE Latin American and Caribbean Petroleum Engineering Conference Proceedings. Caracas, Venezuela: Society of Petroleum Engineers; 1999.

[17] Skauge A, Stensen J. Review of WAG Field Experience. In: 1st International conference and exhibition, modern challenges in oil recovery. 2003.

[18] Nadeson G, Anua NAB, Singhal A, Ibrahim RB. Water-Alternating-Gas (WAG) Pilot Implementation, A First EOR Development Project in Dulang Field, Offshore Peninsular Malaysia. SPE Asia Pacific Oil and Gas Conference and Exhibition, APOGCE. 2004 Oct 18;391–9.

[19] Novosel D. Initial results of WAG CO2 IOR pilot project implementation in Croatia. IIORC 05 - 2005 SPE International Improved Oil Recovery Conference in Asia Pacific, Proceedings. 2005;275–81.

[20] Novosel D. Thermodynamic criteria and final results of WAG CO2 injection in a pilot project in Croatia. SPE Middle East Oil and Gas Show and Conference, MEOS, Proceedings. 2009;1:318–32.

[21] Kulkarni MM, Rao DN. Experimental investigation of miscible and immiscible Water-Alternating-Gas (WAG) process performance. Journal of Petroleum Science and Engineering [Internet]. 2005 Jul 30 [cited 2022 Jun 10];1–2(48):1–20. Available from: https://www.infona.pl//resource/bwmeta1.element.elsevier-763d22d1-41bc-3871-871c-4663af10d0a2

[22] Nezhad SAT, Mojarad MRR, Paitakhti SJ, Moghadas JS, Farahmand DR. Experimental study on applicability of water-alternating-CO2 injection in the secondary and tertiary recovery. Society of Petroleum Engineers - 1st International Oil Conference and Exhibition in Mexico 2006, IOCEM 2006. 2006;574–7.

[23] Darvishnezhad MJ, Moradi B, Zargar G, Jannatrostami A, Montazeri GH. Study of various water alternating gas injection methods in 4- and 5-spot injection patterns in an iranian fractured reservoir. In: Society of Petroleum Engineers - Trinidad and Tobago Energy Resources Conference 2010, SPE TT 2010. Society of Petroleum Engineers; 2010. p. 588–95.

[24] Drid N, Tiab D. The Performance of WAG in a Stratified Reservoir, Hassi-Messaoud Field, Algeria. SPE Asia Pacific Oil and Gas Conference and Exhibition, APOGCE. 2004 Oct 18;293–302.

[25] McGuire PL, Chatham JR, Paskvan FK, Sommer DM, Carini FH. Low salinity oil recovery: An exciting new EOR opportunity for Alaska's north slope. SPE Western Regional Meeting, Proceedings. 2005;439–53.

[26] Bernard GG. Effect of Floodwater Salinity on Recovery Of Oil from Cores Containing Clays. In: 38th Annual Calfornia Regional Meeting of the Society of Petroleum Engineeers [Internet]. California, USA: Society of Petroleum Engineers; 1967 [cited 2022 Jun 10]. Available from: http://onepetro.org/SPEWRM/proceedings-pdf/67CRM/All-67CRM/SPE-1725-MS/2087847/spe-1725-ms.pdf

[27] Buckley JS, Takamura K, Morrow NR. Influence of Electrical Surface Charges on the Wetting Properties of Crude Oils. SPE Reservoir Engineering [Internet]. 1989

Aug 1 [cited 2022 Jun 10];4(03):332–40. Available from: https://onepetro.org/RE/article/4/03/332/76525/Influence-of-Electrical-Surface-Charges-on-the

[28] Hamouda AA, Valderhaug OM. Investigating Enhanced Oil Recovery from Sandstone by Low-Salinity Water and Fluid/Rock Interaction. Energy and Fuels [Internet]. 2014 Feb 20 [cited 2022 Jun 10];28(2):898–908. Available from: https://pubs.acs.org/doi/abs/10.1021/ef4020857

[29] Wu YS, Bai B. Efficient Simulation for Low Salinity Waterflooding in Porous and Fractured Reservoirs. Proceedings of the SPE Reservoir Simulation Symposium (2009, The Woodlands, TX) [Internet]. 2009 Feb 1 [cited 2022 Jun 10];1:126. Available from: https://scholarsmine.mst.edu/geosci_geo_peteng_facwork/160

[30] Javandel I, Doughty C, Tsang C. Groundwater Transport: Handbook of Mathematical Models. Water Resources Monograph Series [Internet]. 1984 [cited 2022 Jun 10];10:228. Available from: http://dx.doi.org/10.1029/WM010

[31] Tang GQ, Morrow NR. Influence of brine composition and fines migration on crude oil/brine/rock interactions and oil recovery. Journal of Petroleum Science and Engineering. 1999 Dec 1;24(2–4):99–111.

[32] Brooks RH, Corey AT. Hydraulic properties of porous media. Hydrology Papers . 1964;3:1–37.

[33] Sohrabi M, Fatemi M, Ireland S. Enhanced Oil Recovery by Water Alternating Gas (WAG) Injection: The Opportunity and the Challenge. In: DEVEX Conference. 2014.

[34] Caudle BH, Dyes AB. Improving Miscible Displacement by Gas-Water Injection. In: 32nd Annual Fall Meeting of Society of Petroleum Engineers Oct 6–9, 1957 [Internet]. Dallas, Tex.: Transactions of the AIME; 1958 [cited 2022 Jun 10]. p. 281–3. Available from: https://onepetro.org/TRANS/article/213/01/281/161053/Improving-Miscible-Displacement-by-Gas-Wate r

[35] Jaturakhanawanit S, Wannakomol A. Water Alternating Gas Injection for Enhanced oil Recovery in the Phitsanulok Basin. Suranaree J Sci Technol. 2011;18(4):267–72.

[36] Samba MA, Elsharafi MO. Literature review of Water Alternating Gas. J Earth Energy Eng. 2018 Oct 31;7(2):33–45.

[37] Claridge EL. CO2 Flooding Strategy in a Communicating Layered Reservoir. Journal of Petroleum Technology [Internet]. 1982 Dec 1 [cited 2022 Jun 10];34(12):2746–56. Available from: https://onepetro.org/JPT/article/34/12/2746/69172/CO2-Flooding-Strategy-in-a-Communicating-Layered

[38] Aarra MG, Skauge A, Martinsen HA. FAWAG: A Breakthrough for EOR in the North Sea. In: SPE Annual Technical Conference and Exhibition. San Antonio, Texas: SPE Annual Technical Conference and Exhibition; 2002.

[39] Don W Green, G Paul Willhite. Enhanced oil recovery [Internet]. Vol. 4, Enhanced Oil Recovery. Richardson, TX : Henry L. Doherty Memorial Fund of AIME, Society of Petroleum Engineers,; 1998 [cited 2022 Jun 10]. 2252–2256 p. Available from: http://energy.gov/fe/science-innovation/oil-gas-research/enhanced-oil-recovery

[40] Jensen TB, Harpole KJ, Osthus A. EOR Screening for Ekofisk. In: Proceedings of the European Petroleum Conference. Paris, France: OnePetro; 2000. p. 151–61.

[41] Wang J, McVay DA, Ayers WB. Compositional simulation and optimization of secondary and tertiary recovery strategies in monument butte field, utah. In: Society of Petroleum Engineers - SPE Eastern Regional/AAPG Eastern Section Joint Meeting 2008. Society of Petroleum Engineers; 2008. p. 470–88.

[42] Clifford KH, Stephen WWebb. Gas transport in porous media [Internet]. Vol. 418, Journal of Fluid Mechanics. Dordrecht ;;[London]: Springer; 2006 [cited 2022 Jun 10]. 376–376 p. Available from: www.springer.com

[43] Willhite GP. Enhanced oil recovery. Richardson, TX : Society of Petroleum Engineers,; 1986. 326 p.

[44] Al-Shuraiqi HS, Muggeridge AH, Grattoni CA. Laboratory Investigations Of First Contact Miscible Wag Displacement: The Effects Of Wag Ratio And Flow Rate. In: SPE International Improved Oil Recovery Conference in Asia Pacific. Kuala Lumpur, Malaysia: Society of Petroleum Engineers; 2003.

[45] Latil M. Enhanced oil recovery. Houston : Gulf Pub. Co.,; 1980. 236 p.

[46] Fanchi JR. Principles of applied reservoir simulation. Gulf Professional Pub; 2006. 511 p.

[47] Rogers JD, Grigg RB. A Literature Analysis of the WAG Injectivity Abnormalities in the CO2 Process. In: SPE - DOE Improved Oil Recovery Symposium Proceedings. OnePetro; 2000.

[48] Craig FF. The reservoir engineering aspects of waterflooding. Society of Petroleum Engineers; 1971. 134 p.

[49] Anderson WG. Wettability Literature Survey- Part 1: Rock/Oil/Brine Interactions and the Effects of Core Handling on Wettability. Journal of Petroleum Technology [Internet]. 1986 Oct 1 [cited 2022 Jun 10];38(10):1125–44. Available from: https://onepetro.org/JPT/article/38/10/1125/73751/Wettability-Literature-Survey-Part-1-Rock-Oil

[50] Ahmed TH. Reservoir engineering handbook. Elsevier/Gulf Professional; 2006. 1360 p.

[51] Donaldson EC, Thomas RD. Microscopic Observations of Oil Displacement in Water-Wet and Oil-Wet Systems. In: Fall Meeting of the Society of Petroleum Engineers of AIME. New Orleans, Louisiana: OnePetro; 1971.

[52] Satter Abdus, Iqbal GM, Buchwalter JL. Practical enhanced reservoir engineering: assisted with simulation software. PennWell Corporation; 2008. 688 p.

[53] Zahoor MK, Derahman MN, Yunan MH. Wag process design—an updated review. Brazilian Journal of Peteroleum and Gas. 2011 Jun 24;5(2):109–21.

[54] Schembre JM, Tang GQ, Kovscek AR. Interrelationship of Temperature and Wettability on the Relative Permeability of Heavy Oil in Diatomaceous Rocks. SPE Reservoir Evaluation & Engineering [Internet]. 2006 Jun 19 [cited 2022 Jun 12];9(03):239–50. Available from: https://onepetro.org/REE/article/9/03/239/196352/Interrelationship-of-Temperature-and-Wettability

[55] Shahabi Nejad K, Danesh A. Visual Investigation of Oil Depressurisation in Pores with Different Wettability Characteristics and Saturation Histories. In: SPE Europec/EAGE Annual Conference [Internet]. Madrid, Spain: Society of petroleum Engineers; 2005 [cited 2022 Jun 12]. Available from:

https://onepetro.org/SPEEURO/proceedings/05EURO/All-05EURO/Madrid,%20Spain/74596

[56] Jackson MD, Valvatne PH, Blunt MJ. Prediction of wettability variation within an oil/water transition zone and its impact on production. SPE Journal. 2005;10(2):184–95.

[57] Redman RS. Horizontal Miscible Water Alternating Gas Development of the Alpine Field, Alaska. In: SPE Western Regional/AAPG Pacific Section Joint Meeting. Anchorage, Alaska: Society of petroleum Engineers; 2002.

[58] Chase CA, Todd MR. Numerical Simulation of CO2 Flood Performance. Society of Petroleum Engineers Journal [Internet]. 1984 Dec 1 [cited 2022 Jun 12];24(06):597–605. Available from: https://onepetro.org/spejournal/article/24/06/597/72398/Numerical-Simulation-of-CO2-Flood-Performance

[59] Shahverdi H. Characterization of Three-phase Flow and WAG Injection in Oil Reservoirs. [Edinburgh, Scotland]: Heriot-Watt University; 2012.

[60] Masoner LO, Abidi HR, Hild GP. Diagnosing CO2 Flood Performance Using Actual Performance Data. In: SPE/DOE Improved Oil Recovery Symposium. Tulsa, Oklahoma: Society of Petroleum Engineers; 1996.

[61] Hadlow RE. Update of Industry Experience With CO2 Injection. In: SPE Annual Technical Conference and Exhibition. Washington, D.C.: Society of Petroleum Engineers; 1992. p. 24–9.

[62] Khan MY, Kohata A, Patel H, Syed FI, al Sowaidi AK. Water Alternating Gas WAG Optimization Using Tapered WAG Technique for a Giant Offshore Middle East Oil Field. In: Society of Petroleum Engineers - Abu Dhabi International Petroleum Exhibition and Conference 2016. Abu Dhabi, UAE: Society of Petroleum Engineers; 2016.

[63] Srisuriyachai F, Muchalintamolee N. Cation interference in low salinity water injection in sandstone formation. In: 76th European Association of Geoscientists and Engineers Conference and Exhibition 2014: Experience the Energy - Incorporating SPE EUROPEC 2014 [Internet]. European Association of Geoscientists & Engineers (EAGE) Publishing BV; 2014 [cited 2022 Jun 12]. p.

3565–9. Available from: https://www.earthdoc.org/content/papers/10.3997/2214-4609.20141012

[64] Mississippi Oil and Gas Board. Cranfield Field, Cranfield Unit, basal Tuscaloosa reservoir, Adams and Franklin Counties. In Mississippi Oil and Gas Board Publication, Jackson Mississippi; 1966. 42-58.

[65] Hovorka SD, Choi JW, Meckel TA, Trevino RH, Zeng H, Kordi M, et al. Comparing carbon sequestration in an oil reservoir to sequestration in a brine formation—field study. In: 9th International Conference on Greenhouse Gas Control Technologies (GHGT-9). Washington, D.C.: GCCC Digital Publication Series; 2008.

[66] Hosseini SA, Lashgari H, Choi JW, Nicot JP, Lu J, Hovorka SD. Static and dynamic reservoir modeling for geological CO2 sequestration at Cranfield, Mississippi, U.S.A. International Journal of Greenhouse Gas Control. 2013 Oct 1;18:449–62.

[67] Delshad M, Kong X, Tavakoli R, Hosseini SA, Wheeler MF. Modeling and simulation of carbon sequestration at Cranfield incorporating new physical models. International Journal of Greenhouse Gas Control. 2013 Oct 1;18:463–73.

[68] Stancliffe JR, Adams RE. Lower Tuscaloosa Fluvial Channel Styles at Liberty Field, Amite County, Mississippi. Gulf Coast Association of Geological Societies Transactions. 1986;36:305–13.

[69] Lu J, Kharaka YK, Thordsen JJ, Horita J, Karamalidis A, Griffith C, et al. CO2–rock–brine interactions in Lower Tuscaloosa Formation at Cranfield CO2 sequestration site, Mississippi, U.S.A. Chemical Geology. 2012 Jan 6;291:269–77.

[70] Soong Y, Howard BH, Dilmore RM, Haljasmaa I, Crandall DM, Zhang L, et al. CO2/brine/rock interactions in Lower Tuscaloosa formation. Greenhouse Gases: Science and Technology. 2016 Dec 1;6(6):824–37.

[71] Teklu TW, Alameri W, Kazemi H, Graves RM, AlSumaiti AM. Low salinity water–Surfactant–CO2 EOR. Petroleum. 2017 Sep 1;3(3):309–20.

[72] Gaines GL, Thomas HC. Adsorption studies on clay minerals. II. A formulation of the thermodynamics of exchange adsorption. The Journal of Chemical Physics. 1953;21(4):714–8.

[73] Modelling of Low Salinity Water Flooding using STARS and GEM | Computer Modelling Group Ltd. [Internet]. [cited 2022 Jun 24]. Available from: https://www.cmgl.ca/training/modelling-low-salinity-water-flood

[74] Dang CTQ, Nghiem LX, Chen Z, Nguyen QP. Modeling low salinity waterflooding: Ion exchange, geochemistry and wettability alteration. In: Proceedings - SPE Annual Technical Conference and Exhibition. Society of Petroleum Engineers (SPE); 2013. p. 4302–23.

[75] Dang C, Nghiem L, Nguyen N, Chen Z, Nguyen Q. Modeling and optimization of low salinity waterflood. Society of Petroleum Engineers - SPE Reservoir Simulation Symposium 2015. 2015;1:55–73.

[76] Dang C, Nghiem L, Nguyen N, Chen Z, Nguyen Q. Mechanistic modeling of low salinity water flooding. Journal of Petroleum Science and Engineering. 2016 Oct 1;146:191–209

[77] Qiao C, Li L, Johns RT, Xu J. A mechanistic model for wettability alteration by chemically tuned waterflooding in carbonate reservoirs. SPE Journal. 2015 Aug 1;20(4):767–83.

[78] Jerauld GR, Lin CY, Webb KJ, Seccombe JC. Modeling Low-Salinity Waterflooding. SPE Reservoir Evaluation & Engineering [Internet]. 2008 Dec 29 [cited 2022 Jan 24];11(06):1000–12. Available from: https://onepetro.org/REE/article/11/06/1000/197778/Modeling-Low-Salinity-Waterflooding

[79] Egbe DIO, Jahanbani Ghahfarokhi A, Nait Amar M, Torsæter O. Application of Low-Salinity Waterflooding in Carbonate Cores: A Geochemical Modeling Study. Natural Resources Research [Internet]. 2021 Feb 1 [cited 2022 Jan 24];30(1):519–42. Available from: https://link.springer.com/article/10.1007/s11053-020-09712-5

[80] Behrenbruch P, Goda H M. Two-phase relative permeability prediction: A comparison of the modified Brooks-Corey methodology with a new Carman-Kozeny based flow formulation, SPE Journal [Internet]. 2006. Avalable from: https://doi.org/10.2118/101150-MS.

[81] Alpak F O, Lake L W, Embid S M. Validation of a modified Carman-Kozeny equation to model two-phase relative permeabilities, SPE Journal [Internet]. 1999. Available from: https://doi.org/10.2118/56479-MS.

Appendices

Appendix A

GEM Data File

```
INUNIT FIELD

WSRF WELL 1

WSRF GRID TIME

OUTSRF GRID ACTIV 'Ca++' ACTIV 'Mg++' ACTIVCOEF 'Ca++' ADS 'Ca++' ADS
'Mg++' EQVFRIEX 'Ca-X2' EQVFRIEX 'Mg-X2' EQVFRIEX 'Na-X' EQVFRIEXN 'Ca-
X2' EQVFRIEXN 'Mg-X2' EQVFRIEXN 'Na-X'

KRG KRINTER KRO KRW MINERAL 'Calcite' MINERAL 'Dolomite' MOLALITY
'Ca++' MOLALITY 'Mg++' MOLALITY 'Na+' PH PRES

SALIN SG SO SW TEMP TGIP

OUTSRF RES ALL

WPRN GRID 0

OUTPRN GRID NONE

OUTPRN RES NONE

**  Distance units: ft

RESULTS XOFFSET         0.0000

RESULTS YOFFSET         0.0000

RESULTS ROTATION          0.0000  **  (DEGREES)

RESULTS AXES-DIRECTIONS 1.0 -1.0 1.0

**
**********************************************************************
***

** Definition of fundamental cartesian grid

**
**********************************************************************
***
```

GRID VARI 20 1 8

KDIR DOWN

DI IVAR

20*50

DJ JVAR

100

DK ALL

160*10

DTOP

20*0

** 0 = null block, 1 = active block

NULL CON 1

PERMI CON 50

POR CON 0.2

PERMJ CON 50

PERMK CON 50

** 0 = pinched block, 1 = active block

PINCHOUTARRAY CON 1

PRPOR 4630

CPOR 0.000004

END-GRID

TRPOR 257

** Model and number of components

** Model and number of components

** Model and number of components

** Model and number of components

** Model and number of components

** Model and number of components

** Model and number of components

** Model and number of components

** Model and number of components

** Model and number of components

** Model and number of components

** Model and number of components

** Model and number of components

** Model and number of components

** Model and number of components

** Model and number of components

** Model and number of components

** Model and number of components

MODEL PR

**=-=-=Component Selection/Properties

**REM

NC 10 10

COMPNAME 'CO2' 'CH4' 'C2H6' 'C3H8' 'IC4' 'NC4' 'IC5' 'NC5' 'NC6' 'C7+'

HCFLAG

0 1 1 1 1 1 1 1 1 1

TRES 257

VISCOR HZYT

MIXVC 1.0

PVC3 1.2

VISCOEFF

0.1023 0.023364 0.058533 -0.040758 0.0093324

MW

44.01 16.043 30.07 44.097 58.124 58.124 72.151 72.151 86.178 274.0

AC

0.225 0.008 0.098 0.152 0.176 0.193 0.227 0.251 0.296 0.780251

PCRIT

72.8 45.4 48.2 41.9 36.0 37.5 33.4 33.3 29.3 15.4487687094

VCRIT

0.094 0.099 0.148 0.203 0.263 0.255 0.306 0.304 0.37 1.00567942595

TCRIT

304.2 190.6 305.4 369.8 408.1 425.2 460.4 469.6 507.4 844.703219076

PCHOR

78 77 108 150.3 181.5 189.9 225 231.5 271 708.453

SG

0.818 0.3 0.356 0.507 0.563 0.584 0.625 0.631 0.664 0.92

TB

-164.578 -433.498 -197.626 -46.642 51.206 88.142 179.834 206.402 312.35 1321.78

OMEGA

0.457236 0.457236 0.457236 0.457236 0.457236 0.457236 0.457236 0.457236 0.457236 0.457236

OMEGB

0.0777961 0.0777961 0.0777961 0.0777961 0.0777961 0.0777961 0.0777961 0.0777961 0.0777961 0.0777961

VSHIFT

0 0 0 0 0 0 0 0 0 0

VSHIF1

0 0 0 0 0 0 0 0 0 0

TREFVS

140 140 140 140 140 140 140 140 140 140

HEATING_VALUES

0 0.800232 1.40131 1.99531 2.57004 2.57004 3.17866 3.17866 3.76844 0

VISVC

0.094 0.099 0.148 0.203 0.263 0.255 0.306 0.304 0.37 1.00567942595

BIN

0.103

0.13 0

0.135 0 0

0.13 0 0 0

0.13 0 0 0 0

0.125 0 0 0 0 0

0.125 0 0 0 0 0 0

0.125 0 0 0 0 0 0 0

0 0 0 0 0 0 0 0 0

CW 2.19253e-05

REFPW 645.418

SOLUBILITY HENRY

EQUIL-REACT-RATE ON

CHEM-EQUIL-SET ON

CRDAMP-ALL 0.1

** Grid upscale factor=0.00131033

MRDAMP-ALL 0.00131033

YAQU-RATE-CUTOFF

1.0e-8 1.0 1.0 1.0 1.0 1.0 1.0 1.0 1.0 1.0

ACTIVITY-MODEL B-DOT

SALINITY-CALC ON

RF_EXPONENT 3.0

RFCALC POWER

HENRY-MOD1-CO2

BIN-TDEP-CO2

GEOCHEM_V2

NC-AQUEOUS 12

COMPNAME-AQUEOUS

'H+' 'Ca++' 'Mg++' 'Na+' 'SO4--' 'Al+++' 'SiO2' 'Cl-' 'HCO3-' 'OH-' 'CaSO4' 'MgSO4'

MW-AQUEOUS

1.0079 40.08 24.305 22.9898 96.0576 26.9815 60.0843 35.453 61.0171 17.0073 136.138 120.363

ION-SIZE-AQUEOUS

9 6 8 4 4 9 -0.5 3 4.5 3.5 4 4

CHARGE-AQUEOUS

1 2 2 1 -2 3 0 -1 -1 -1 0 0

NC-MINERAL 3

COMPNAME-MINERAL

'Calcite' 'Dolomite' 'Kaolini*'

MW-MINERAL

100.089 184.403 258.16

MASSDENSITY-MINERAL

2709.95 2864.96 2594.05

REACTION-CHEM 'CO2' + 'H2O' = 'H+' + 'HCO3-'

LOG-CHEM-EQUIL-COEFS

-6.54924 0.00900174 -0.000102115 2.76188e-07 -3.56142e-10

REACTION-CHEM 'H+' + 'OH-' = 'H2O'

LOG-CHEM-EQUIL-COEFS

14.9282 -0.0418762 0.000197367 -5.54951e-07 7.58109e-10

REACTION-CHEM 'CaSO4' = 'Ca++' + 'SO4--'

LOG-CHEM-EQUIL-COEFS

-2.2673 -0.000966685 -7.21167e-05 4.52585e-07 -1.14535e-09

REACTION-CHEM 'MgSO4' = 'Mg++' + 'SO4--'

LOG-CHEM-EQUIL-COEFS

-2.17055 -0.00148402 -4.6643e-05 2.61102e-07 -6.82724e-10

REACTION-RATE-TST 'H+' + 'Calcite' = 'Ca++' + 'HCO3-'

LOG-CHEM-EQUIL-COEFS

2.06889 -0.0142668 -6.06096e-06 1.45921e-07 -4.18928e-10

REACTIVE-SURFACE-AREA 2989.25

ACTIVATION-ENERGY 23500

LOG-TST-RATE-CONSTANT -5.81

REF-TEMP-RATE-CONST 25

REACTION-RATE-TST 2 'H+' + 'Dolomite' = 'Ca++' + 'Mg++' + 2 'HCO3-'

LOG-CHEM-EQUIL-COEFS

3.39441 -0.0355985 1.32613e-05 2.41057e-07 -8.14935e-10

REACTIVE-SURFACE-AREA 2584.4

ACTIVATION-ENERGY 52200

LOG-TST-RATE-CONSTANT -7.53

REF-TEMP-RATE-CONST 25

REACTION-RATE-TST 6 'H+' + 'Kaolini*' = 5 'H2O' + 2 'Al+++' + 2 'SiO2'

LOG-CHEM-EQUIL-COEFS

9.72954 -0.0988976 0.000291558 -3.27028e-07 -3.31101e-10

REACTIVE-SURFACE-AREA 28262

ACTIVATION-ENERGY 22200

LOG-TST-RATE-CONSTANT -13.1798

REF-TEMP-RATE-CONST 25

NC-IEX 4

COMPNAME-IEX

'Na-X' 'Ca-X2' 'Mg-X2' 'H-X'

AQIONS-IEX

'Na+' 'Ca++' 'Mg++' 'H+'

REACTION-IEX 'Na+' + 0.5 'Ca-X2' = 0.5 'Ca++' + 'Na-X'

**Selectivity cofficents for ion-exchanger 1

SCOEFF-IEX

25 0.01

90 0.4

REACTION-IEX 'Na+' + 0.5 'Mg-X2' = 0.5 'Mg++' + 'Na-X'

**Selectivity cofficents for ion-exchanger 2

SCOEFF-IEX

25 0.01

90 0.5

REACTION-IEX 'H-X' + 'Na+' = 'Na-X' + 'H+'

**Selectivity cofficents for ion-exchanger 3

SCOEFF-IEX

25 0.01

90 0.4

COMPNAME-SAL 'Na+'

AQUEOUS-VISCOSITY KESTIN

*WINPROP 2020.10

ROCKFLUID

INTERP_SCAL ON

RPT 1

INTCOMP EQVFRIEX 'Ca-X2'

KRINTRP 1

INTCOMP_VAL 0.19

** Sw krw krow

SWT

0.4 0 0.65

0.425 7.62939e-06 0.557449

0.45 0.00012207 0.473034

0.475 0.000617981 0.396545

0.5 0.00195312 0.327762

0.525 0.00476837 0.266454

0.55 0.0098877 0.212377

0.575 0.0183182 0.165274

0.6 0.03125 0.124871

0.625 0.0500565 0.0908743

0.65 0.0762939 0.0629662

0.675 0.111702 0.0407996

0.7 0.158203 0.0239889

0.725 0.217903 0.0120964

0.75 0.293091 0.0046085

0.775 0.386238 0.000885335

0.8 0.5 0

** Sl krg krog

SLT

0.55 0.8 0

0.578125 0.694108 9.91821e-06

0.60625 0.596359 0.000158691

0.634375 0.506642 0.000803375

0.6625 0.424839 0.00253906

0.690625 0.350825 0.00619888

0.71875 0.284463 0.012854

0.746875 0.225611 0.0238136

0.775 0.17411 0.040625

0.803125 0.12979 0.0650734

0.83125 0.092461 0.0991821

0.859375 0.0619099 0.145213

0.8875 0.0378929 0.205664

0.915625 0.020123 0.283274

0.94375 0.00824692 0.381018

0.971875 0.00179484 0.50211

1 0 0.65

KRINTRP 2

INTCOMP_VAL 0.4

** Sw krw krow

SWT

0.4 0 0.65

0.425 7.62939e-06 0.557449

0.45 0.00012207 0.473034

0.475 0.000617981 0.396545

0.5 0.00195312 0.327762

0.525 0.00476837 0.266454

0.55 0.0098877 0.212377

0.575 0.0183182 0.165274

0.6 0.03125 0.124871

0.625 0.0500565 0.0908743

0.65 0.0762939 0.0629662

0.675 0.111702 0.0407996

0.7 0.158203 0.0239889

0.725 0.217903 0.0120964

0.75 0.293091 0.0046085

0.775 0.386238 0.000885335

0.8 0.5 0

** Sl krg krog

SLT

0.55 0.8 0

0.578125 0.694108 9.91821e-06

0.60625 0.596359 0.000158691

0.634375 0.506642 0.000803375

0.6625 0.424839 0.00253906

0.690625 0.350825 0.00619888

0.71875 0.284463 0.012854

0.746875 0.225611 0.0238136

0.775 0.17411 0.040625

0.803125 0.12979 0.0650734

0.83125 0.092461 0.0991821

0.859375 0.0619099 0.145213

0.8875 0.0378929 0.205664

0.915625 0.020123 0.283274

0.94375 0.00824692 0.381018

0.971875 0.00179484 0.50211

1 0 0.65

TSOIRW 0.04

TSORW 0.04

TKRWIRO 0.35

RTYPE CON 1

CEC-IEX CON 50

INITIAL

VERTICAL BLOCK_CENTER WATER_OIL

REFPRES

4650

REFDEPTH

0

DWOC

80

MOLALITY-AQUEOUS

1.99731e-06 0.297876 0.042628 1.98975 0.00243661 3.70625e-05 0.000798916 2.86554 1e-10 1e-10 1e-10 1e-10

VOLUMEFRACTION-MINERAL

0.011 0.004 0.031

ZGLOBALC 'NC6' CON 0.0248

ZGLOBALC 'NC5' CON 0.0095

ZGLOBALC 'NC4' CON 0.0158

ZGLOBALC 'IC5' CON 0.0123

ZGLOBALC 'IC4' CON 0.0104

ZGLOBALC 'CO2' CON 0.0184

ZGLOBALC 'CH4' CON 0.5376

ZGLOBALC 'C7+' CON 0.2661

ZGLOBALC 'C3H8' CON 0.0334

ZGLOBALC 'C2H6' CON 0.0717

NUMERICAL

RUN

DATE 2022 1 3

**

WELL 'Well-1'

INJECTOR 'Well-1'

```
INCOMP  AQUEOUS  0.0  0.0  0.0  0.0  0.0  0.0  0.0  0.0  0.0  0.0  1.04582129e-11
0.0181868142  0.149988431  0.595436849  0.0449774209  3.90684398e-13  1.7545358e-
13  0.895279369  1.72759815e-13  0.0  0.0  0.0

OPERATE  MAX  BHP  5500.0  CONT

OPERATE  MAX  STW  100.0  CONT

**        rad  geofac  wfrac  skin

GEOMETRY  K  0.25  0.37  1.0  0.0

PERF     GEOA  'Well-1'

** UBA           ff        Status  Connection

1 1 1       1.0  OPEN    FLOW-FROM  'SURFACE'  REFLAYER

1 1 2       1.0  OPEN    FLOW-FROM  1

1 1 3       1.0  OPEN    FLOW-FROM  2

1 1 4       1.0  OPEN    FLOW-FROM  3

1 1 5       1.0  OPEN    FLOW-FROM  4

1 1 6       1.0  OPEN    FLOW-FROM  5

1 1 7       1.0  OPEN    FLOW-FROM  6

1 1 8       1.0  OPEN    FLOW-FROM  7

LAYERXYZ  'Well-1'

** perf geometric data: UBA, block entry(x,y,z) block exit(x,y,z), length

1 1 1  25.000000  50.000000  0.000000  25.000000  50.000000  10.000000  10.000000

1 1 2  25.000000  50.000000  10.000000  25.000000  50.000000  20.000000  10.000000

1 1 3  25.000000  50.000000  20.000000  25.000000  50.000000  30.000000  10.000000

1 1 4  25.000000  50.000000  30.000000  25.000000  50.000000  40.000000  10.000000

1 1 5  25.000000  50.000000  40.000000  25.000000  50.000000  50.000000  10.000000

1 1 6  25.000000  50.000000  50.000000  25.000000  50.000000  60.000000  10.000000

1 1 7  25.000000  50.000000  60.000000  25.000000  50.000000  70.000000  10.000000
```

```
1 1 8  25.000000  50.000000  70.000000  25.000000  50.000000  75.000000  5.000000
OPEN 'Well-1'
**
WELL  'Well-2'
PRODUCER 'Well-2'
OPERATE  MAX  STO  200.0  CONT
OPERATE  MIN  BHP  4060.0  CONT
**         rad  geofac  wfrac  skin
GEOMETRY  K  0.25  0.37  1.0  0.0
PERF      GEOA  'Well-2'
** UBA             ff        Status  Connection
20 1 1        1.0  OPEN    FLOW-TO  'SURFACE'  REFLAYER
20 1 2        1.0  OPEN    FLOW-TO  1
20 1 3        1.0  OPEN    FLOW-TO  2
20 1 4        1.0  OPEN    FLOW-TO  3
20 1 5        1.0  OPEN    FLOW-TO  4
20 1 6        1.0  OPEN    FLOW-TO  5
20 1 7        1.0  OPEN    FLOW-TO  6
20 1 8        1.0  OPEN    FLOW-TO  7
LAYERXYZ  'Well-2'
** perf geometric data: UBA, block entry(x,y,z) block exit(x,y,z), length
20 1 1  975.000000  50.000000  0.000000  975.000000  50.000000  10.000000  10.000000
20 1 2  975.000000  50.000000  10.000000  975.000000  50.000000  20.000000  10.000000
20 1 3  975.000000  50.000000  20.000000  975.000000  50.000000  30.000000  10.000000
20 1 4  975.000000  50.000000  30.000000  975.000000  50.000000  40.000000  10.000000
```

```
20 1 5  975.000000  50.000000  40.000000  975.000000  50.000000  50.000000  10.000000
20 1 6  975.000000  50.000000  50.000000  975.000000  50.000000  60.000000  10.000000
20 1 7  975.000000  50.000000  60.000000  975.000000  50.000000  70.000000  10.000000
20 1 8  975.000000  50.000000  70.000000  975.000000  50.000000  75.000000  5.000000
**
WELL  'Well-1_Gas'
INJECTOR 'Well-1_Gas'
INCOMP  SOLVENT  1.0  0.0  0.0  0.0  0.0  0.0  0.0  0.0  0.0  0.0
OPERATE  MAX  BHP  5500.0  CONT
OPERATE  MAX  STG  100000.0  CONT
**         rad  geofac  wfrac  skin
GEOMETRY  K  0.25  0.37  1.0  0.0
PERF      GEOA  'Well-1_Gas'
** UBA             ff         Status  Connection
1 1 1        1.0  OPEN    FLOW-FROM  'SURFACE'  REFLAYER
1 1 2        1.0  OPEN    FLOW-FROM  1
1 1 3        1.0  OPEN    FLOW-FROM  2
1 1 4        1.0  OPEN    FLOW-FROM  3
1 1 5        1.0  OPEN    FLOW-FROM  4
1 1 6        1.0  OPEN    FLOW-FROM  5
1 1 7        1.0  OPEN    FLOW-FROM  6
1 1 8        1.0  OPEN    FLOW-FROM  7
LAYERXYZ  'Well-1_Gas'
** perf geometric data: UBA, block entry(x,y,z) block exit(x,y,z), length
1 1 1  25.000000  50.000000  0.000000  25.000000  50.000000  10.000000  10.000000
```

1 1 2 25.000000 50.000000 10.000000 25.000000 50.000000 20.000000 10.000000

1 1 3 25.000000 50.000000 20.000000 25.000000 50.000000 30.000000 10.000000

1 1 4 25.000000 50.000000 30.000000 25.000000 50.000000 40.000000 10.000000

1 1 5 25.000000 50.000000 40.000000 25.000000 50.000000 50.000000 10.000000

1 1 6 25.000000 50.000000 50.000000 25.000000 50.000000 60.000000 10.000000

1 1 7 25.000000 50.000000 60.000000 25.000000 50.000000 70.000000 10.000000

1 1 8 25.000000 50.000000 70.000000 25.000000 50.000000 75.000000 5.000000

SHUTIN 'Well-1_Gas'

DATE 2022 2 3.00000

DATE 2022 3 3.00000

DATE 2022 4 3.00000

DATE 2022 5 3.00000

DATE 2022 6 3.00000

SHUTIN 'Well-1'

OPEN 'Well-1_Gas'

DATE 2022 7 3.00000

DATE 2022 8 3.00000

DATE 2022 9 3.00000

DATE 2022 10 3.00000

DATE 2022 11 3.00000

DATE 2022 12 3.00000

DATE 2023 1 3.00000

OPEN 'Well-1'

SHUTIN 'Well-1_Gas'

DATE 2023 2 3.00000

DATE 2023 3 3.00000

DATE 2023 4 3.00000

DATE 2023 5 3.00000

DATE 2023 6 3.00000

SHUTIN 'Well-1'

OPEN 'Well-1_Gas'

DATE 2023 7 3.00000

DATE 2023 8 3.00000

DATE 2023 9 3.00000

DATE 2023 10 3.00000

DATE 2023 11 3.00000

DATE 2023 12 3.00000

DATE 2024 1 3.00000

OPEN 'Well-1'

SHUTIN 'Well-1_Gas'

DATE 2024 2 3.00000

DATE 2024 3 3.00000

DATE 2024 4 3.00000

DATE 2024 5 3.00000

DATE 2024 6 3.00000

SHUTIN 'Well-1'

OPEN 'Well-1_Gas'

DATE 2024 7 3.00000

DATE 2024 8 3.00000

DATE 2024 9 3.00000

DATE 2024 10 3.00000

DATE 2024 11 3.00000

DATE 2024 12 3.00000

DATE 2025 1 3.00000

OPEN 'Well-1'

SHUTIN 'Well-1_Gas'

DATE 2025 2 3.00000

DATE 2025 3 3.00000

DATE 2025 4 3.00000

DATE 2025 5 3.00000

DATE 2025 6 3.00000

SHUTIN 'Well-1'

OPEN 'Well-1_Gas'

DATE 2025 7 3.00000

DATE 2025 8 3.00000

DATE 2025 9 3.00000

DATE 2025 10 3.00000

DATE 2025 11 3.00000

DATE 2025 12 3.00000

DATE 2026 1 3.00000

STOP

OPEN 'Well-1'

SHUTIN 'Well-1_Gas'

DATE 2026 2 3.00000

DATE 2026 3 3.00000

DATE 2026 4 3.00000

DATE 2026 5 3.00000

DATE 2026 6 3.00000

SHUTIN 'Well-1'

OPEN 'Well-1_Gas'

DATE 2026 7 3.00000

DATE 2026 8 3.00000

DATE 2026 9 3.00000

DATE 2026 10 3.00000

DATE 2026 11 3.00000

DATE 2026 12 3.00000

DATE 2027 1 3.00000

OPEN 'Well-1'

SHUTIN 'Well-1_Gas'

DATE 2027 2 3.00000

DATE 2027 3 3.00000

DATE 2027 4 3.00000

DATE 2027 5 3.00000

DATE 2027 6 3.00000

SHUTIN 'Well-1'

OPEN 'Well-1_Gas'

DATE 2027 7 3.00000

DATE 2027 8 3.00000

DATE 2027 9 3.00000

DATE 2027 10 3.00000

DATE 2027 11 3.00000

DATE 2027 12 3.00000

DATE 2028 1 3.00000

OPEN 'Well-1'

SHUTIN 'Well-1_Gas'

RESULTS PROCESSWIZ PROCESS

Appendix B

Publication from the Thesis

İZMİR KÂTİP ÇELEBİ UNIVERSITY

6th International Students Science Congress
20-21 May 2022, İzmir – Türkiye

İZMİR Uluslararası Misafir Öğrenci Derneği

A Comparison of the Performances of Conventional and Low Salinity Water Alternating Gas Injection for Displacement of Oil

Emmanuel Bucyanayandi, Muhammed Said Ergül and Ibrahim Kocabaş*
İzmir Kâtip Çelebi University, Department of Energy Engineering, Çiğli Main Campus, İzmir, Türkiye
**Correspondent author: bucyaemmanuel@gmail.com*

Keywords: waterflooding, CO_2 flooding, conventional WAG injection, low salinity WAG injection, displacement efficiency of WAG processes
Discipline: Petroleum Engineering

Abstract

This study focuses on identifying the crucial physical and chemical factors, such as gravity, injection depth, and vertical permeability, and salinity of connate and injected water for improving oil recovery percentage during water alternating gas (WAG) injection. The Conventional WAG injection attracts interest from oil and gas industry and it has become one of the most reliable enhanced oil recoveries (EOR) techniques. The WAG injection is applied essentially for controlling the mobility of reservoir fluids. During WAG injection, water acts as side-bottom push due to its high density to oil, hence it improves the macroscopic oil sweep efficiency. Gas injection on the other hand reduces oil viscosity and improves oil displacement efficiency. Also, with appropriate injection depth, and low vertical permeability, WAG injection has an advantage of preventing the early breakthrough of injected fluids during production.

Although the conventional WAG does improve oil recovery factor, there still remains a substantial amount of oil in reservoir pores due to rock-fluid interfacial tensions (IFT). The Low salinity waterflooding (LSWF) is therefore proposed in this study to break this IFT between rock clay and fluids, and further increase oil recovery factor. Recent researches revealed that LSWF alters oil-wet reservoir to water-wet behavior. This wettability alteration is believed to be the main mechanism of LSWF to improve oil recovery; however other mechanisms of LSWF were also proposed. Those include multi-ion exchange (MIE) between rock clay minerals and injected salt water, pH increase, and fines migration.

In this study, a comprehensive literature review was performed on both conventional WAG and LSWF also known as smart waterflooding studies on experimental core analysis and field projects. Therefore, different scenarios -involving both physical and chemical factors- of WAG injection were numerically simulated by using CMG-GEM software simulator. GEM, which stands for, Generalized Equation-of-State Model, a compositional simulator for multi-components reservoir fluids. GEM is the preferred simulator because low salinity water flooding involves the chemical change at a constant temperature. The modified Cranfield oil field data were used as the input data for WAG injection simulations which is available in the published literature. The ion equivalent fraction of Ca^{2+} that indicates the adsorption of Ca^{2+} on clay surface was selected as the interpolant for relative permeability curves. Therefore, LSWF was modelled by shifting the water and oil relative permeability curves for initially oil-wet conditions to water-wet. The simulation results showed that there is an increase of oil recovery factor of about 5% for WAG injection with low salinity water of 1027ppm to brine of 51,346 ppm. The presence of Ca^{2+} and Mg^{2+} ions in the connate water also proved to be the key for successful ion exchange with Na^{+} ions in injected water.

Curriculum Vitae

Name Surname : Emmanuel Bucyanayandi

E-mail (1) : bucyaemmanuel@gmail.com

E-mail (2) : emmanuel.bucyanayandi@aun.edu.ng

Education:

2019–2022	Izmir Katip Celebi University, Dept. of Energy Eng.
2012–2016	American University of Nigeria, Dept. of Petroleum Chem.

Work Experience:

June – Sept. 2018	Rwanda Mines, Petroleum and Gas Board (RMB), Rwanda
June – Dec. 2016	Intels Nigeria Ltd, Nigeria

Publications:

1. A Comparison of the Performances of Conventional and Low Salinity Water Alternating Gas Injection for Displacement of Oil: presented at International Students Science Congress, on May 20, 2022 at Izmir Katip Çelebi University, Turkey.
2. Waste Plastics to Fuel Oils Using Waste-Derived Catalysts: presented at International Students Science Congress, on May 3, 2019 at Izmir Katip Çelebi University, Turkey.